

# Nulling data analysis and how to interpret results

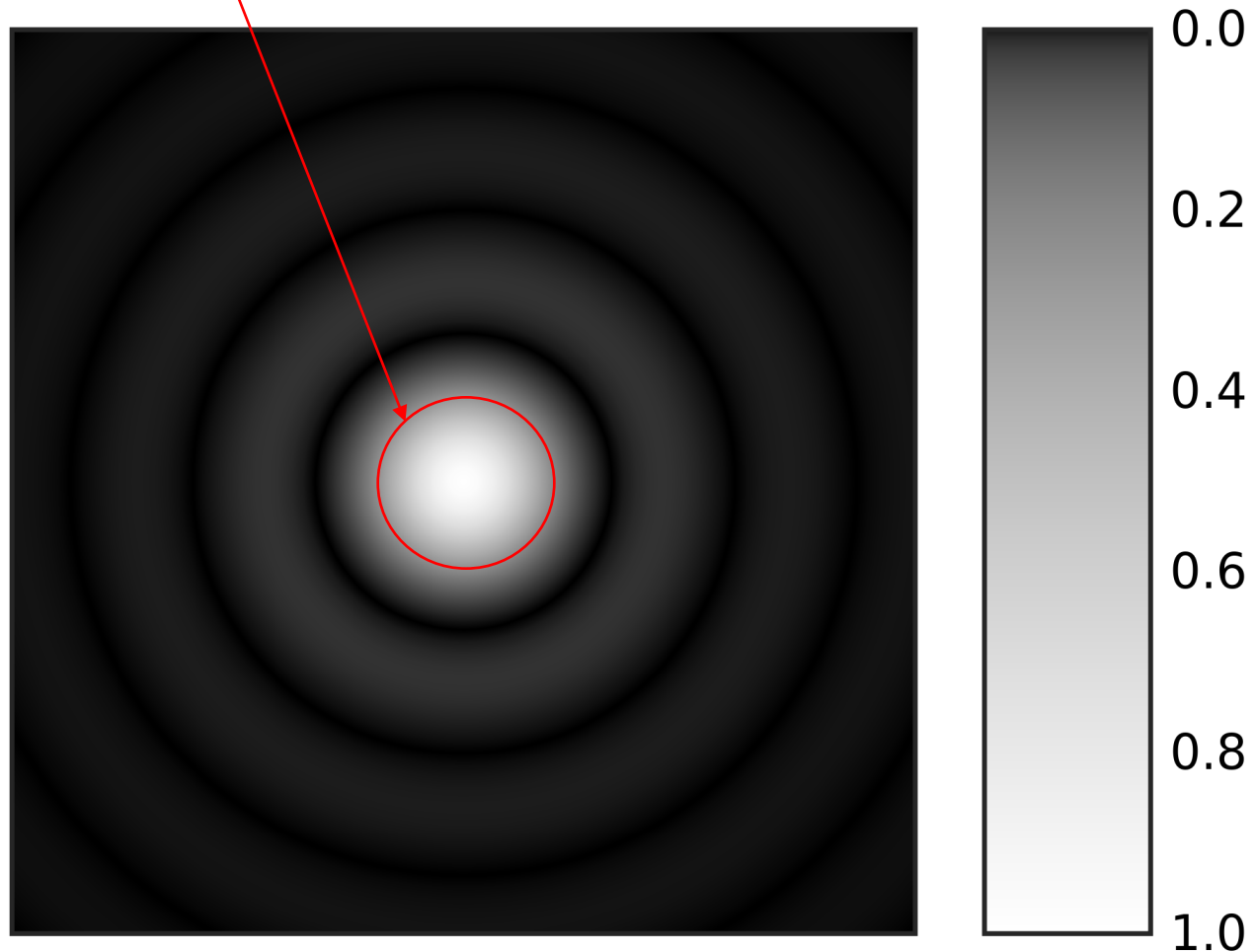
D. Defrère  
University of Liège



# Observing challenge

---

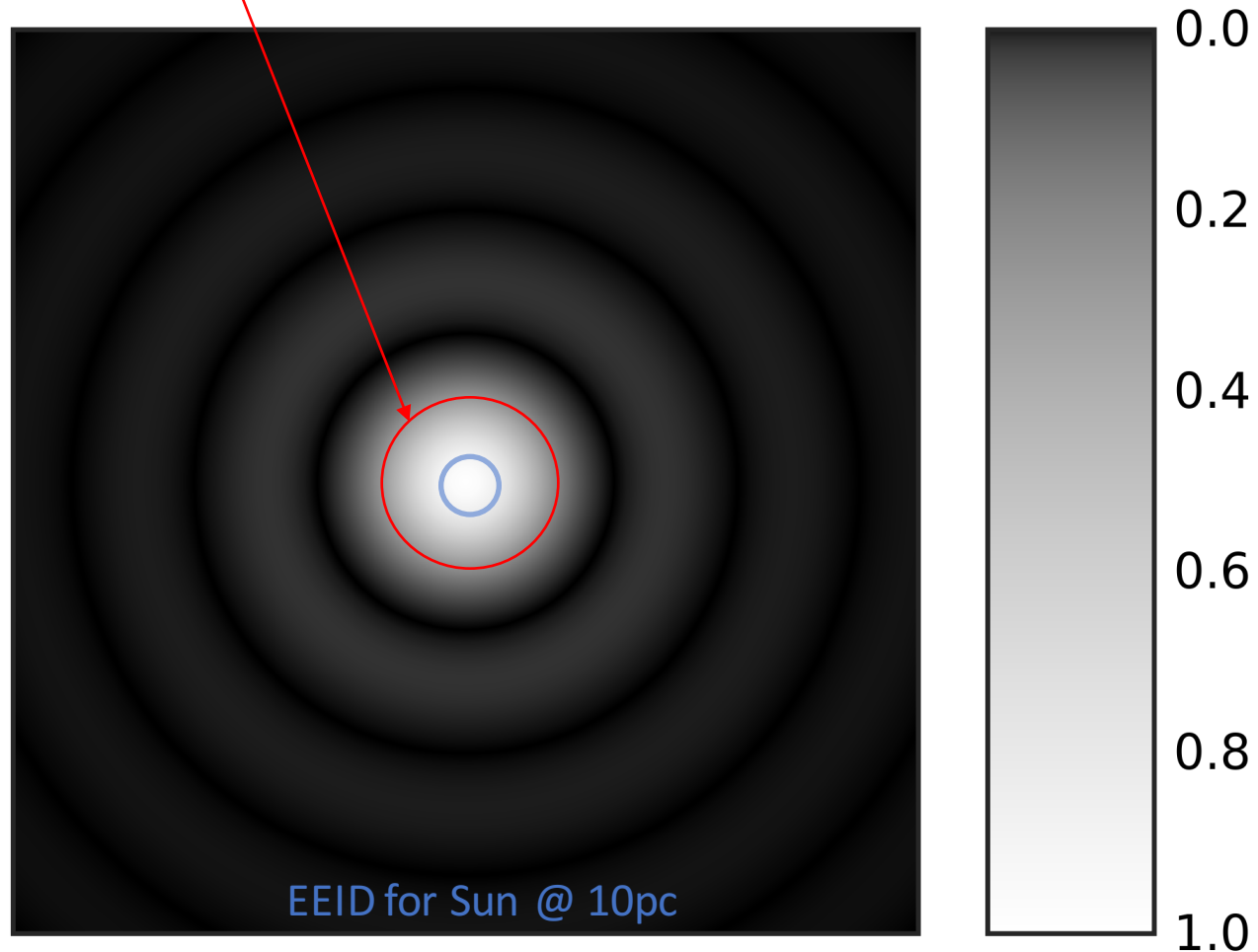
- 1 zodi around a 2-Jy star is **~1 million times dimmer** than the background and **~20000 times dimmer** than the star
- Signal mixed with the stellar PSF!





# Observing challenge

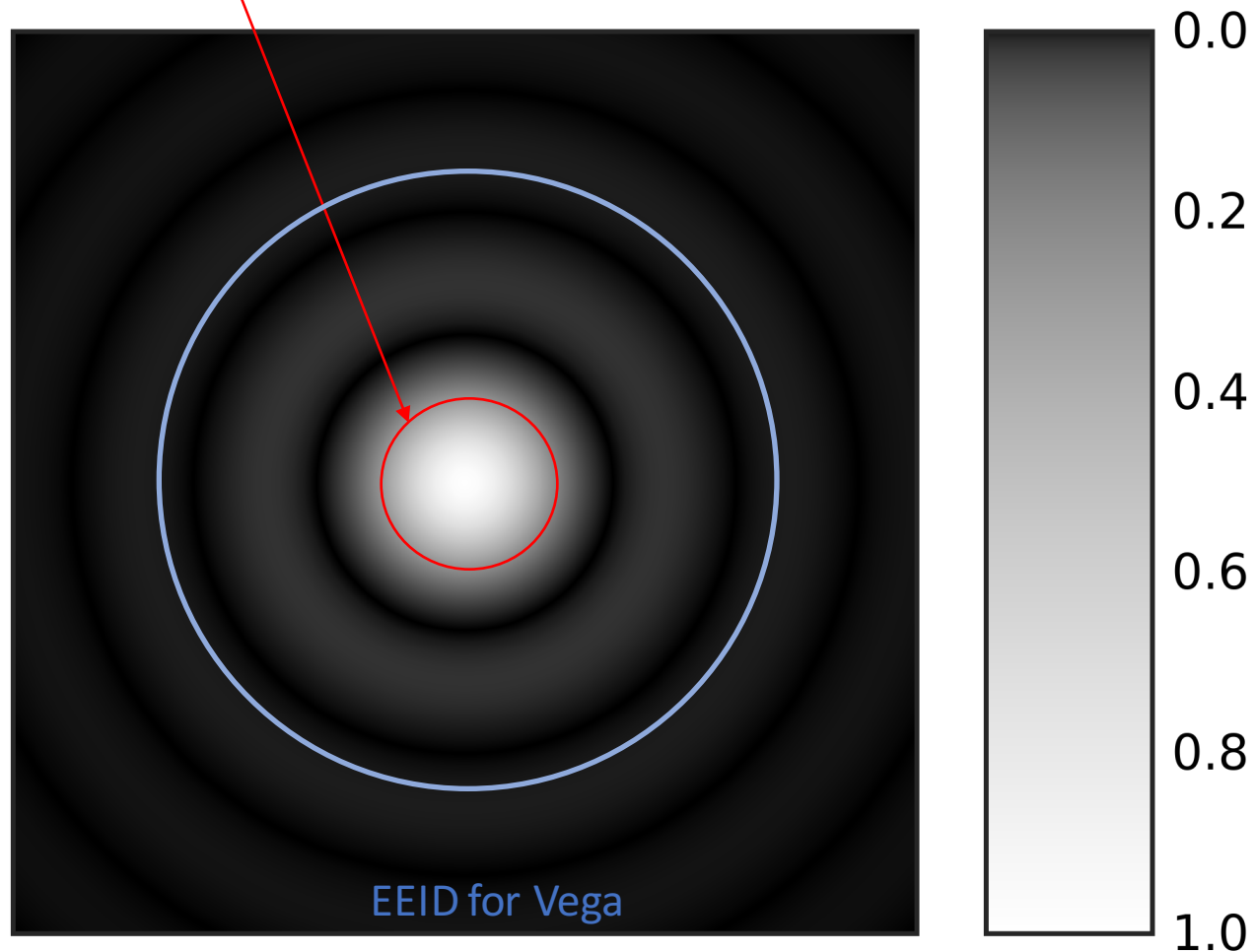
- 1 zodi around a 2-Jy star is **~1 million times** dimmer than the background and **~20000 times dimmer** than the star
- Signal mixed with the stellar PSF!





# Observing challenge

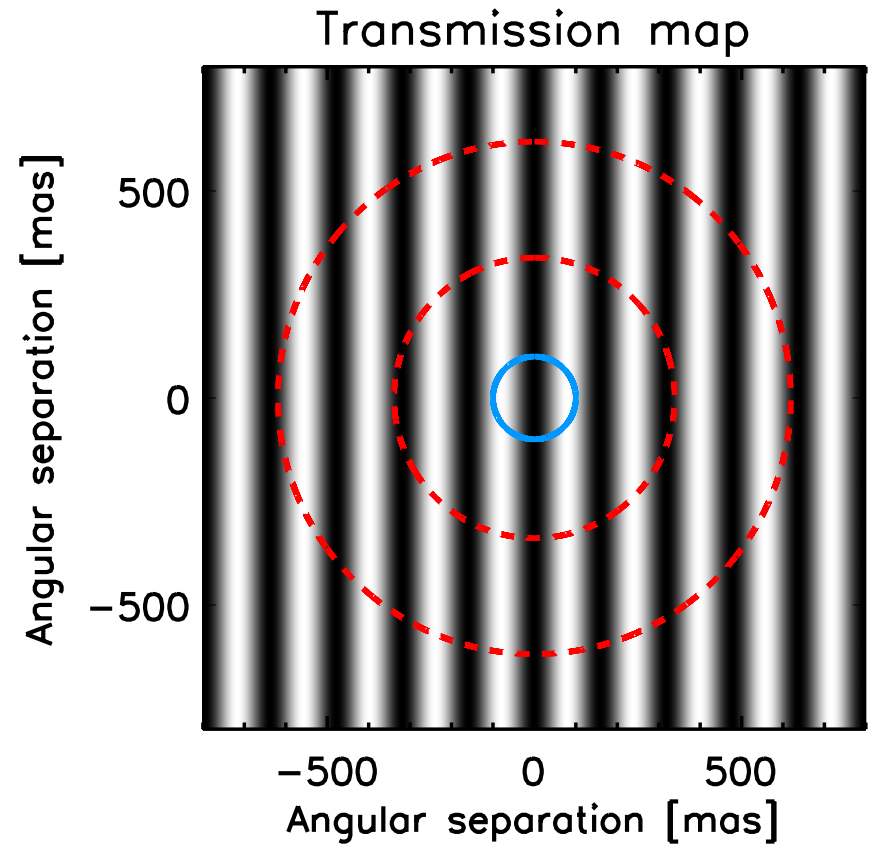
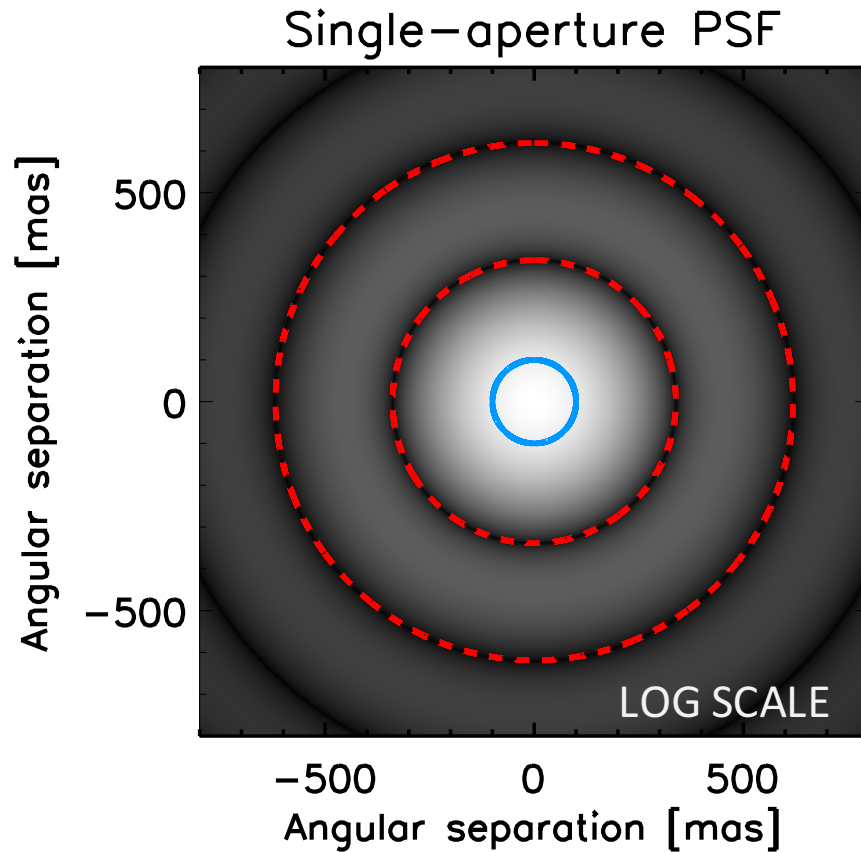
- 1 zodi around a 2-Jy star is **~1 million times** dimmer than the background and **~20000 times dimmer** than the star
- Signal mixed with the stellar PSF!





# How does it work?

- Exploit the instrumental response of the interferometer:





# How does it work?

- Exploit the instrumental response of the interferometer:

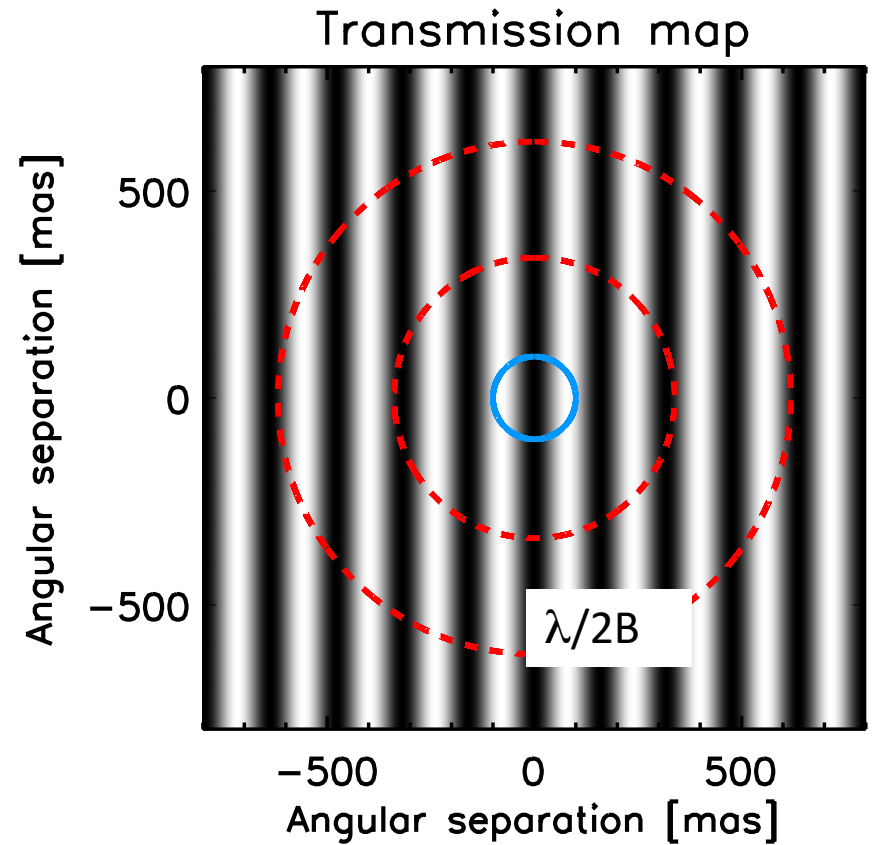
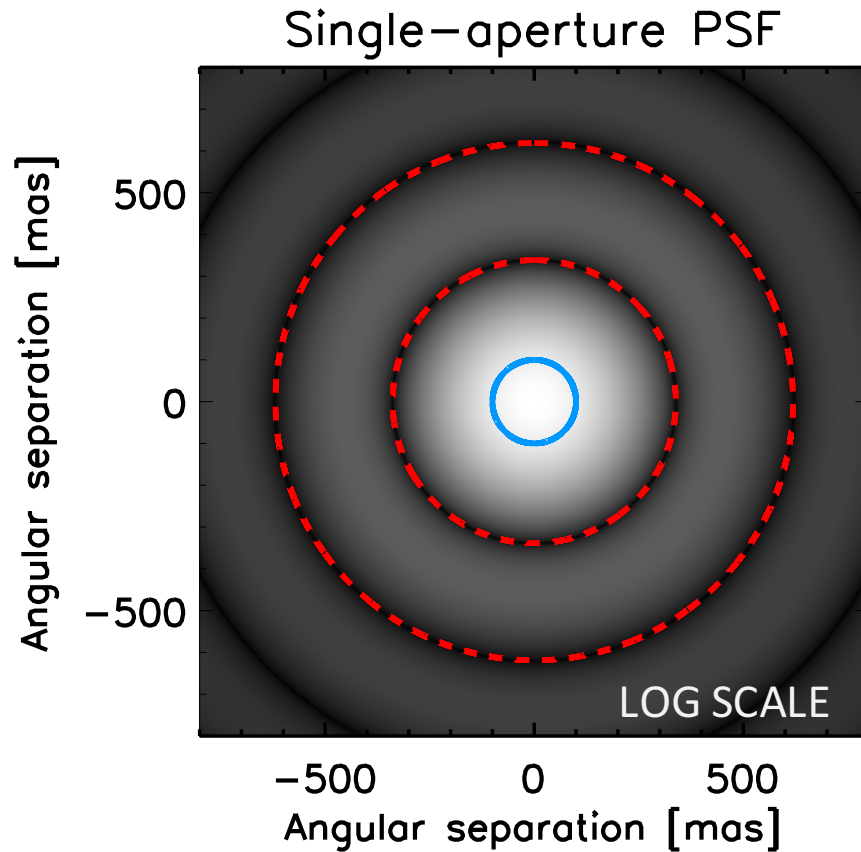




# Illustration with a binary

---

- Observations of gam per: G8III+A3IV binary system:
  - Angular separation: 250 mas
  - Estimated contrast at N band: 3.55% +/- 0.22%.
- Data obtained on December 2013 (coarse fringe tracking)

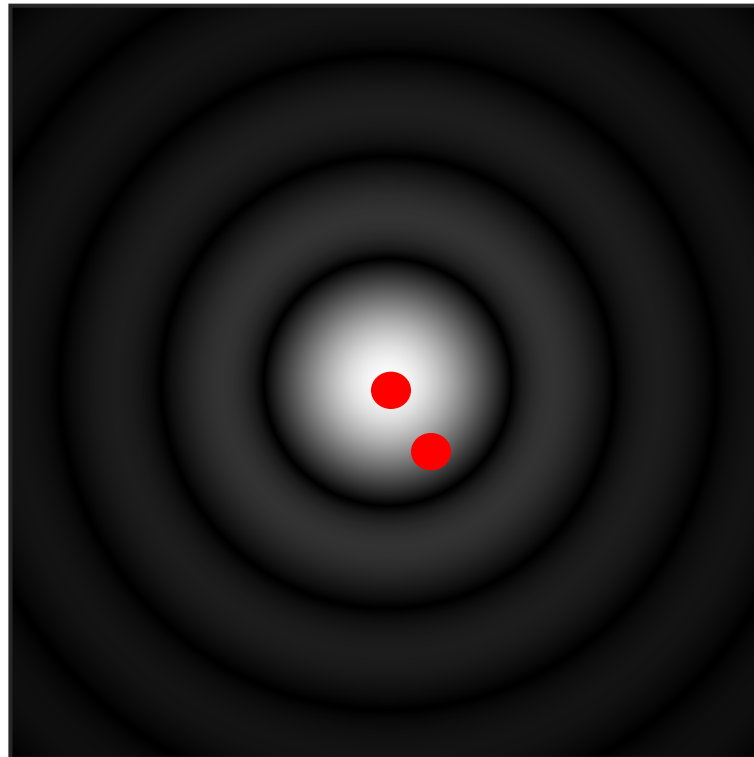




# Illustration with a binary

2013/12/31

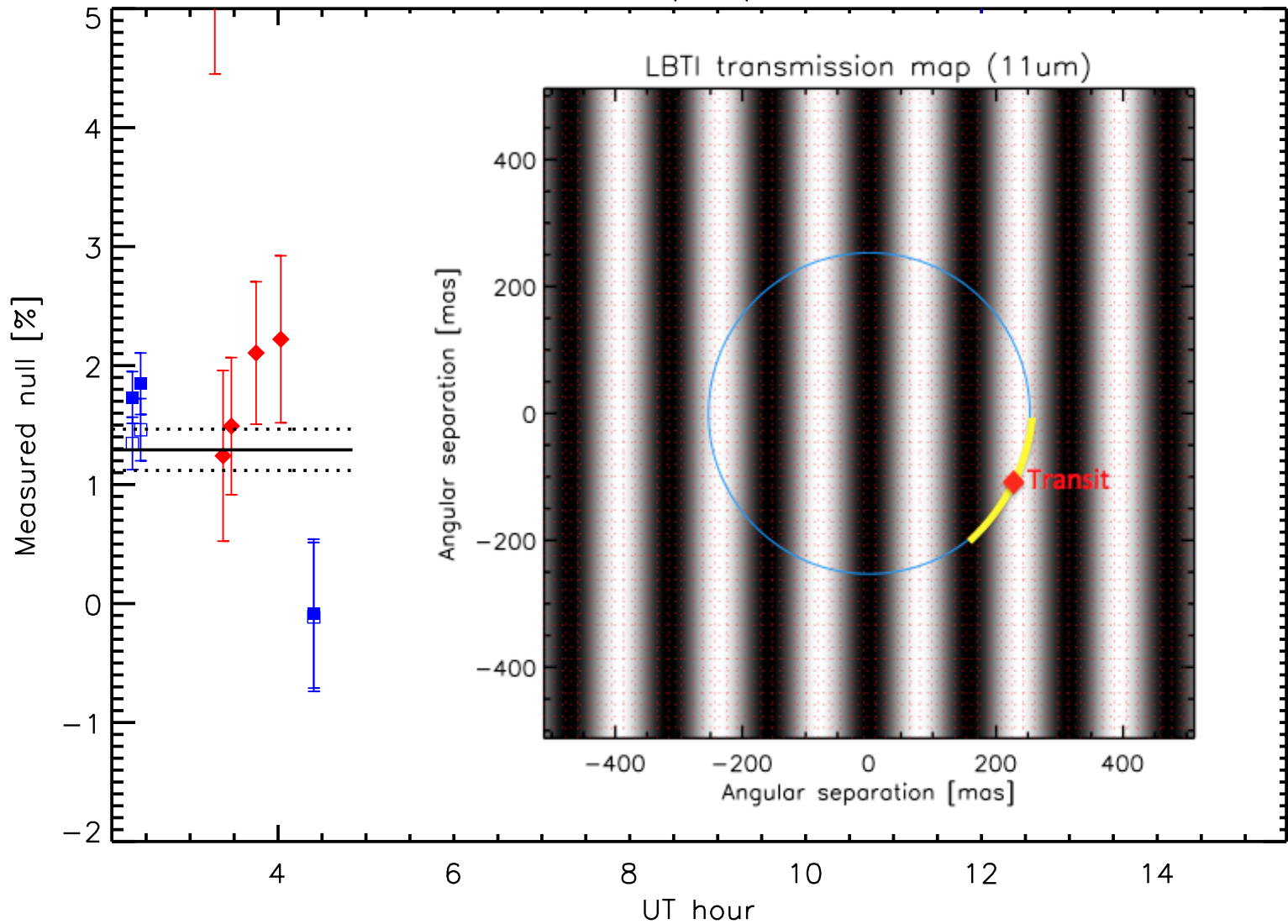




# Illustration with a binary

2013/12/31

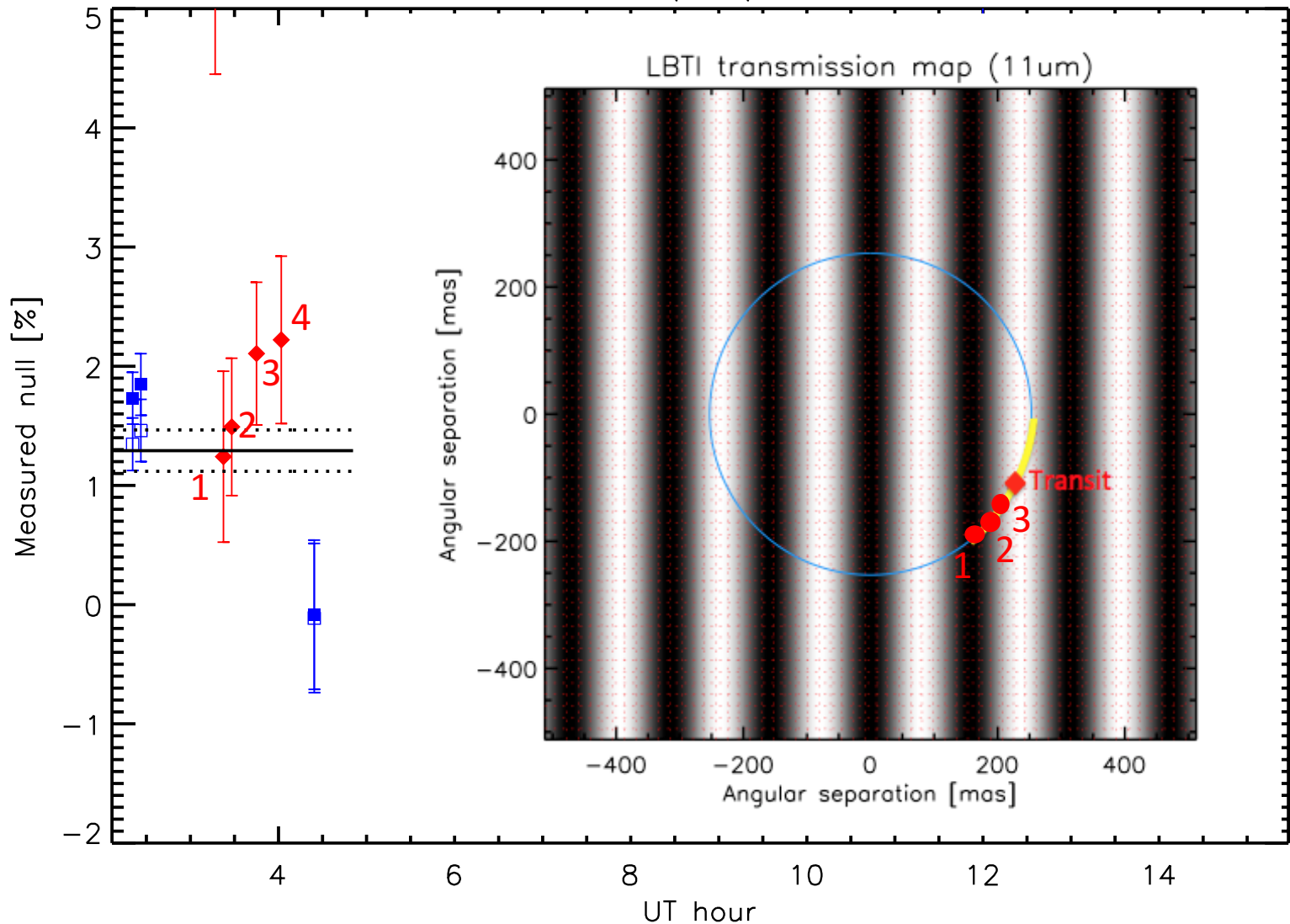




# Illustration with a binary

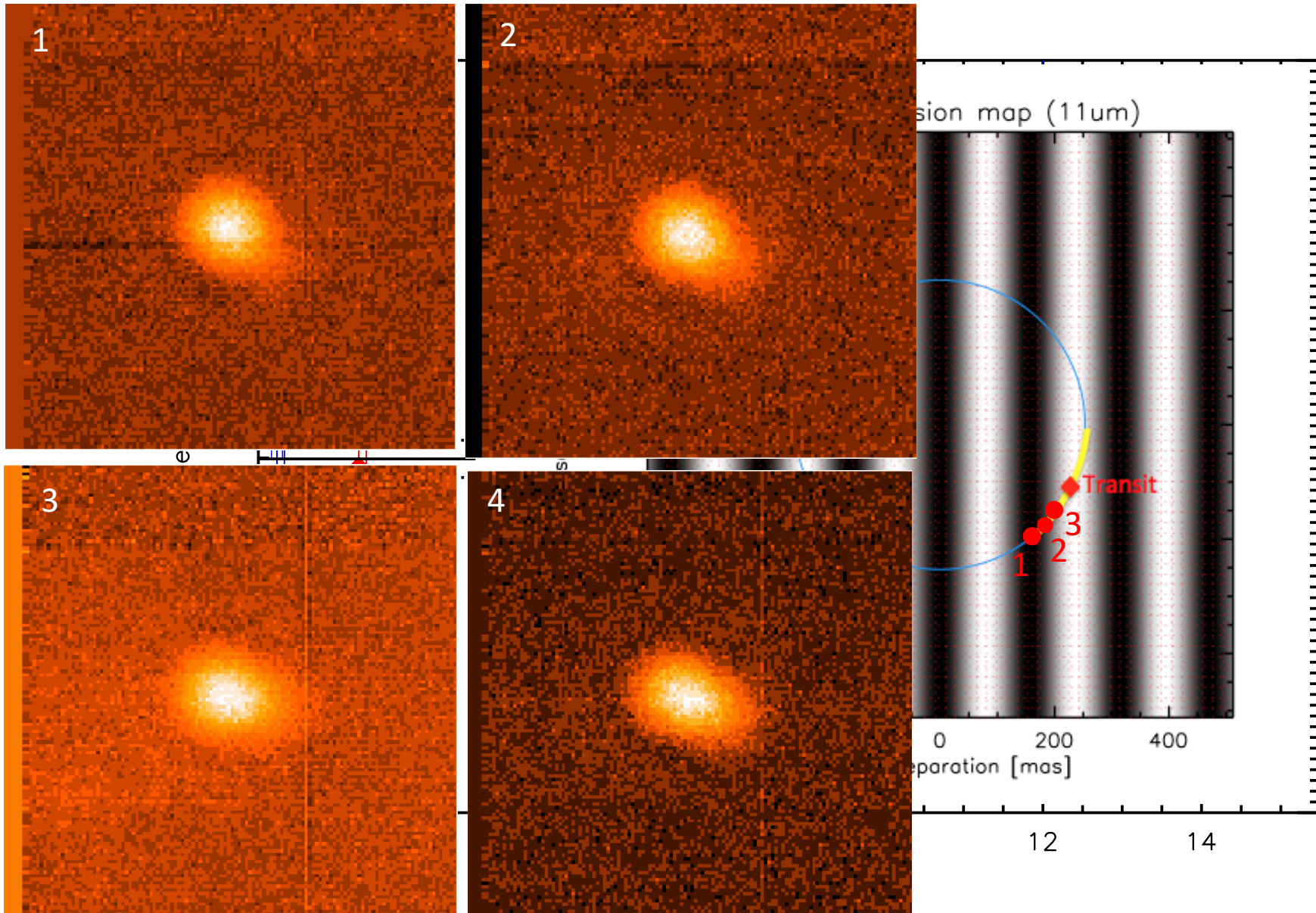
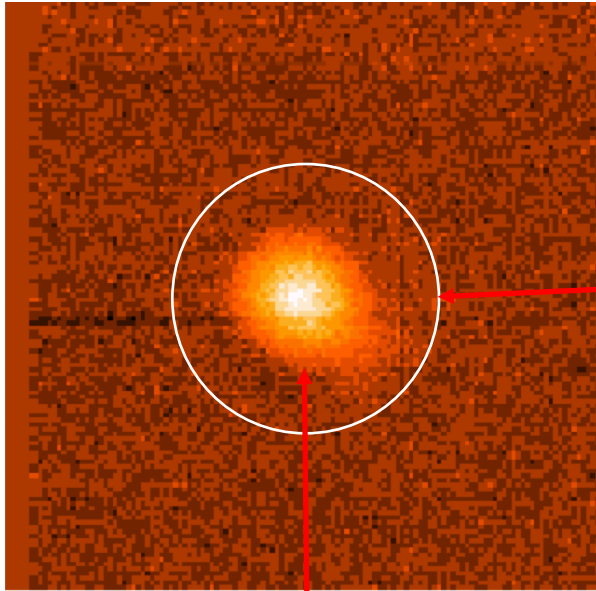




# Illustration with a binary



Flux in given aperture can be modelled (same for exozodis)

Central star not perfectly suppressed => need for calibrators

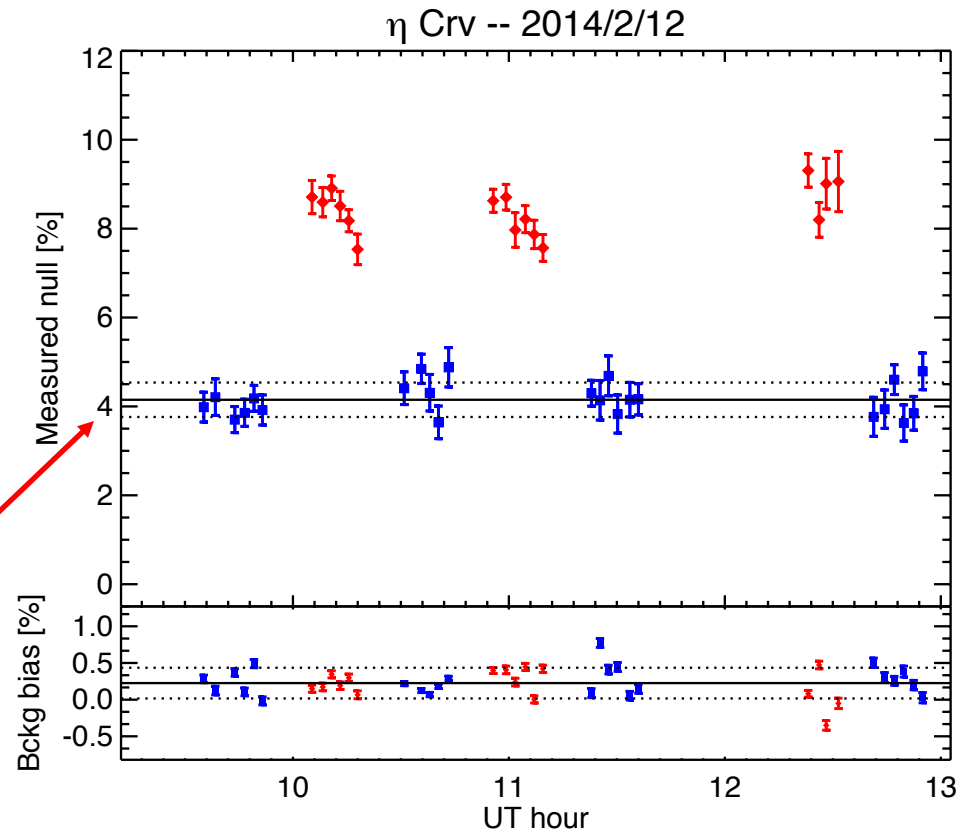
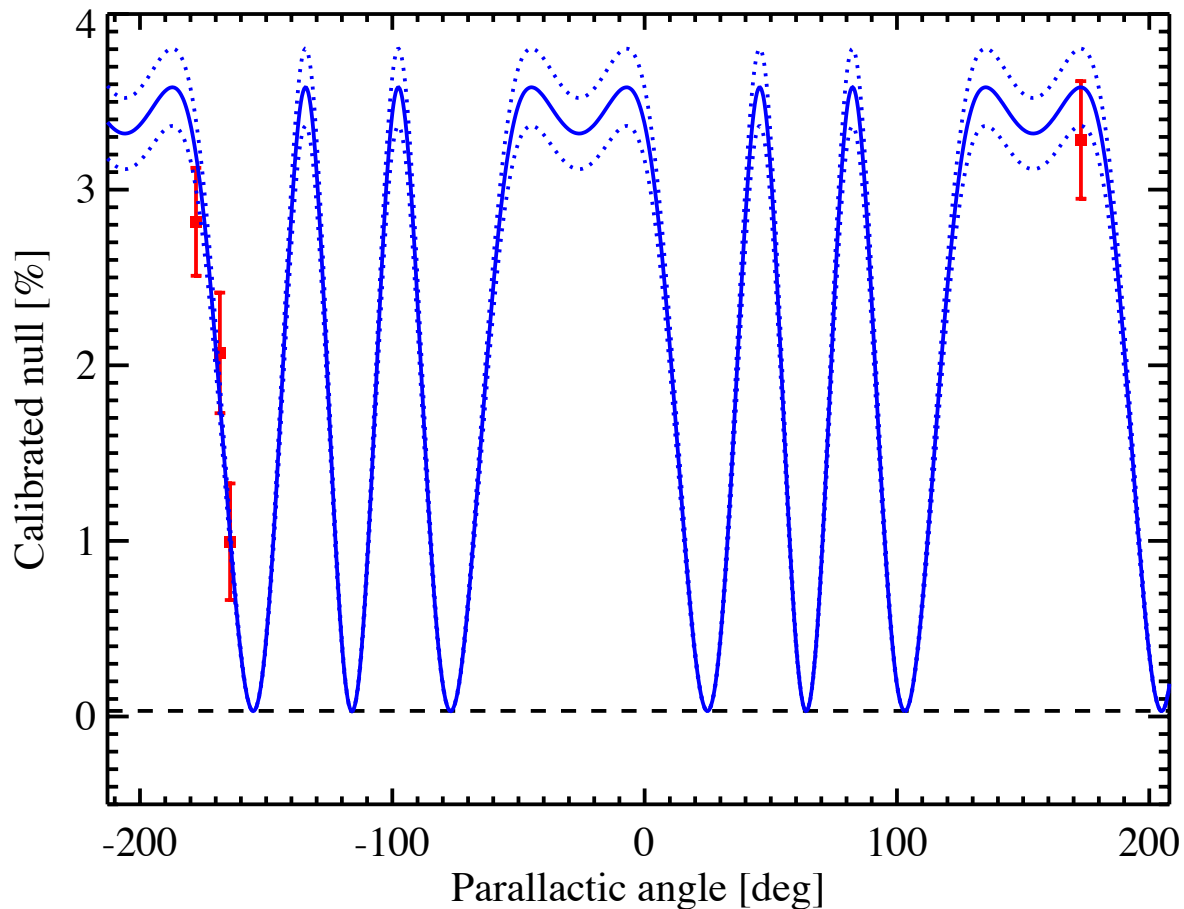




# Illustration with a binary

- Measured contrast:  $3.25\% \pm 0.40\%$ .
- Estimated contrast at N band:  $3.55\% \pm 0.22\%$ .

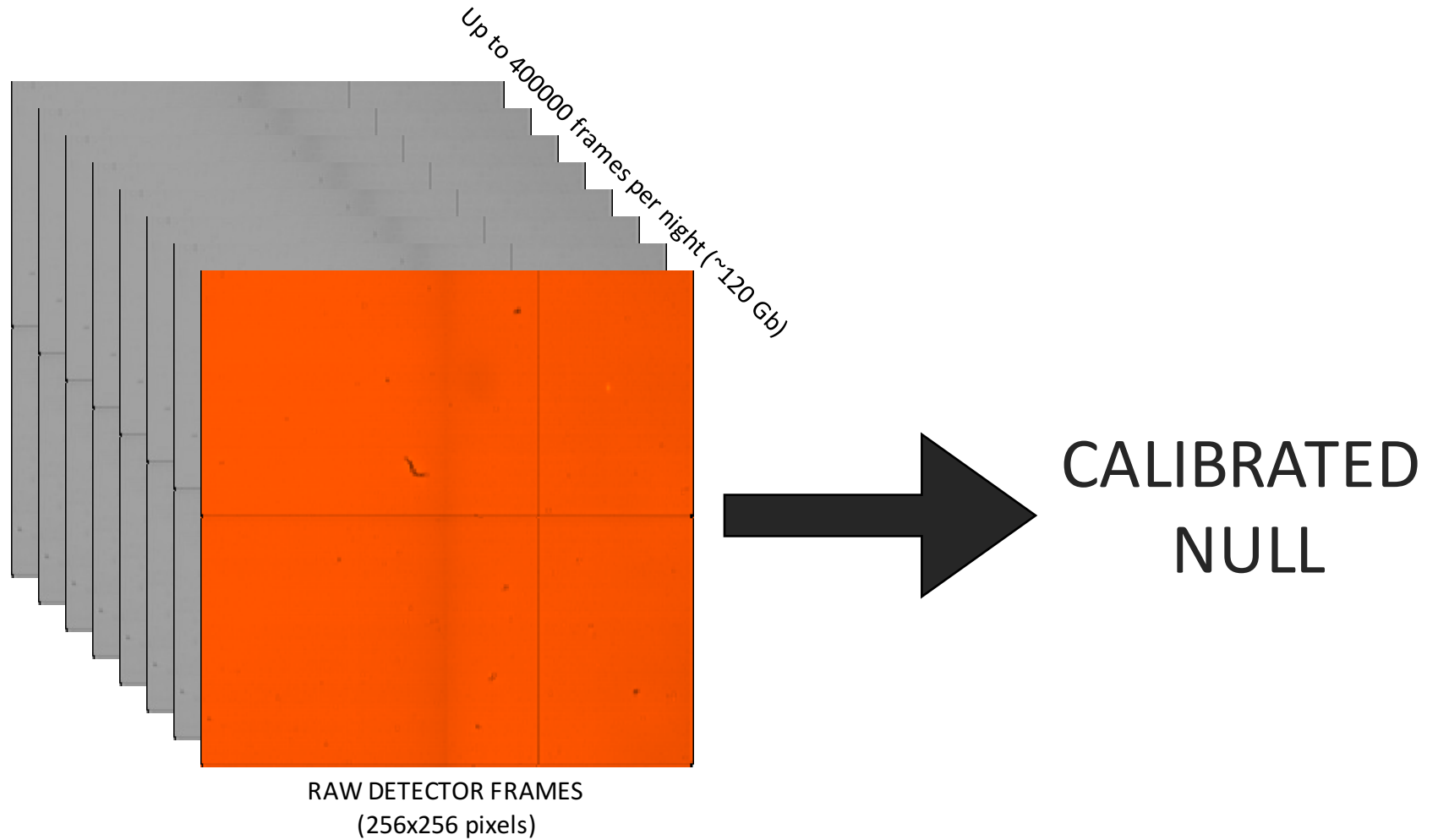


# Data analysis



# Data analysis overview

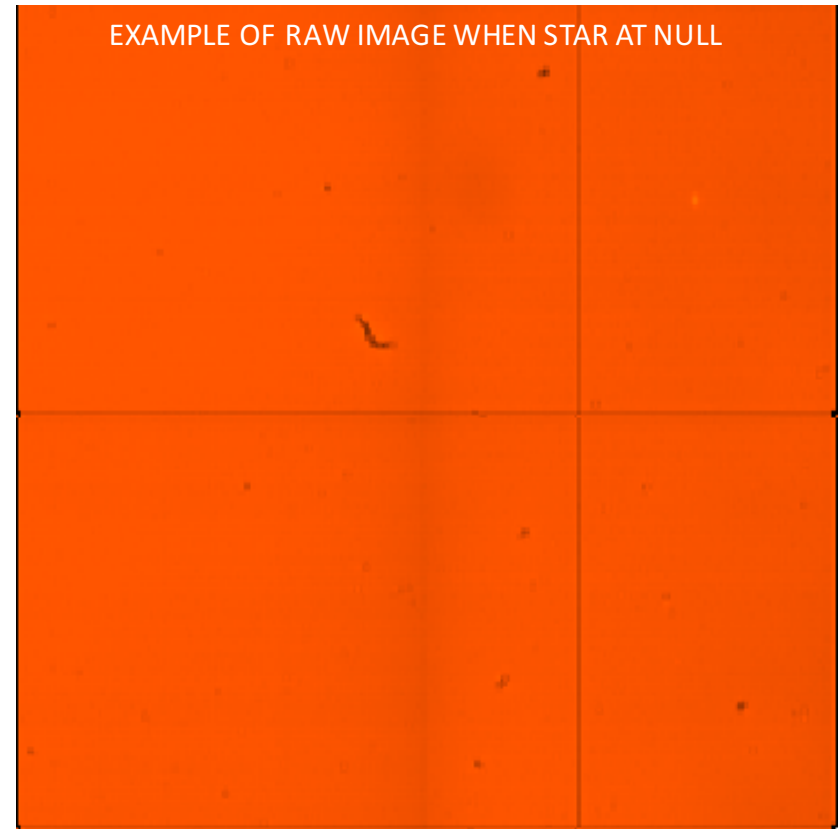
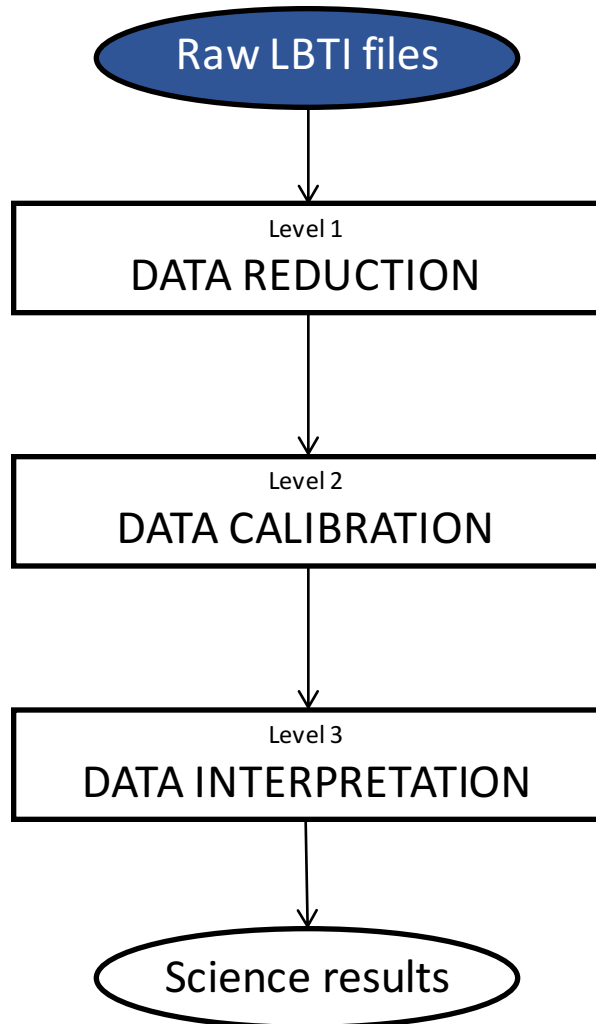
---





# Data analysis overview

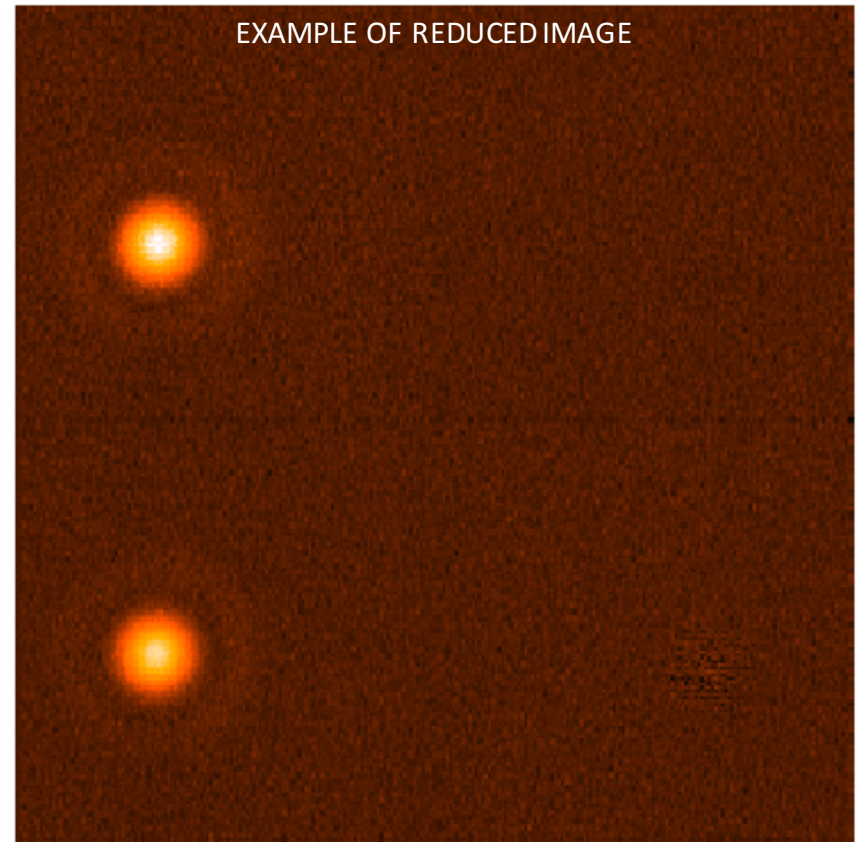
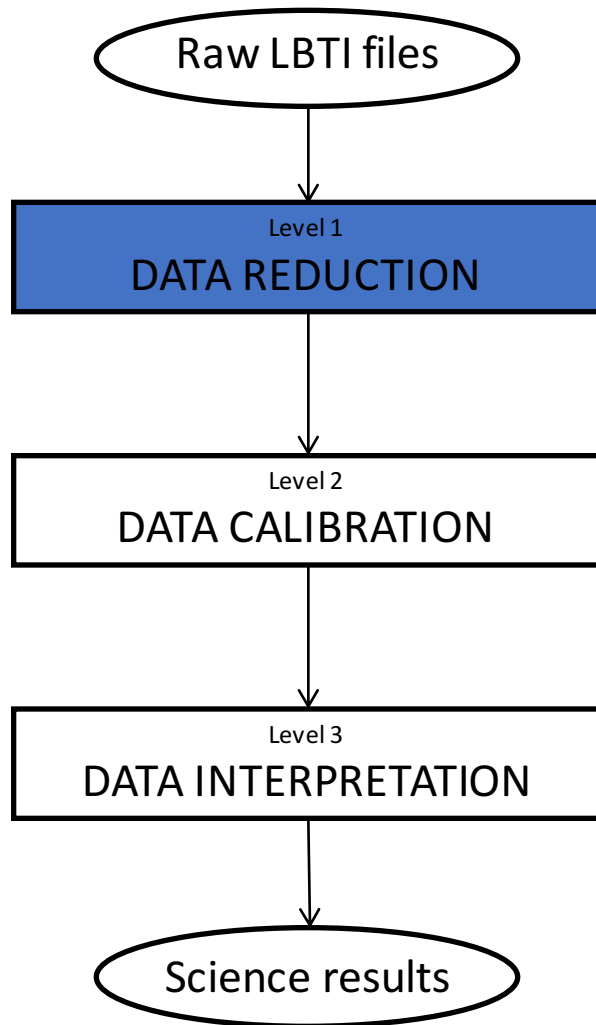
---





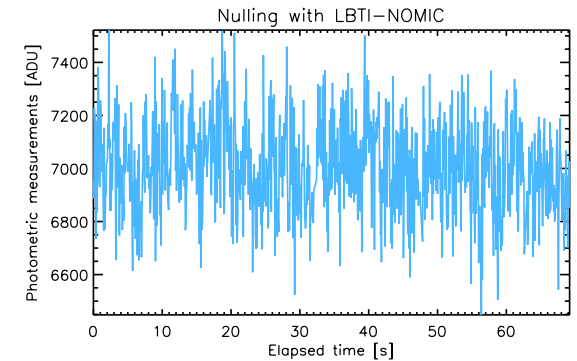
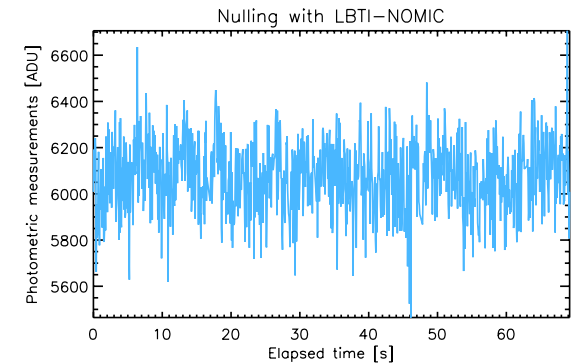
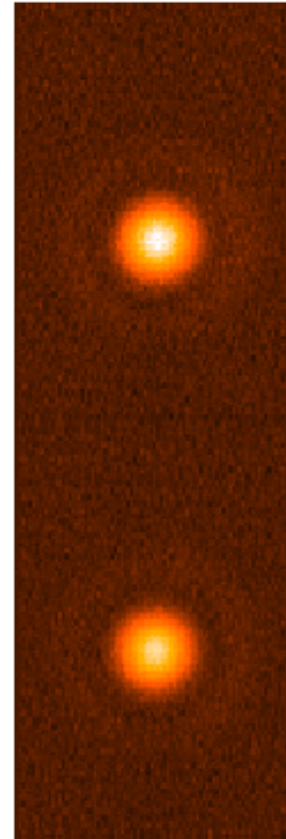
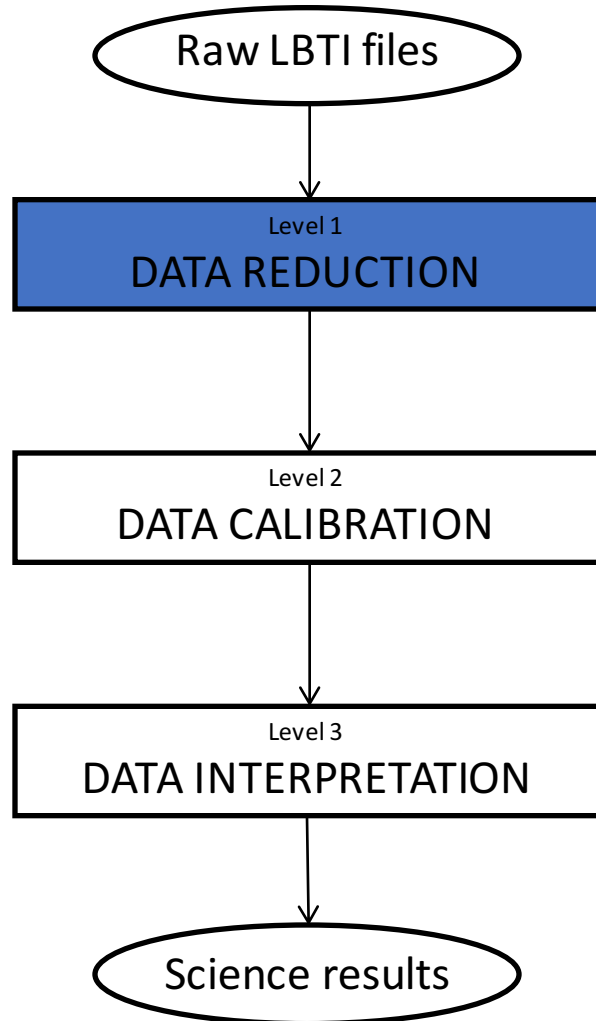
# Data analysis overview

---



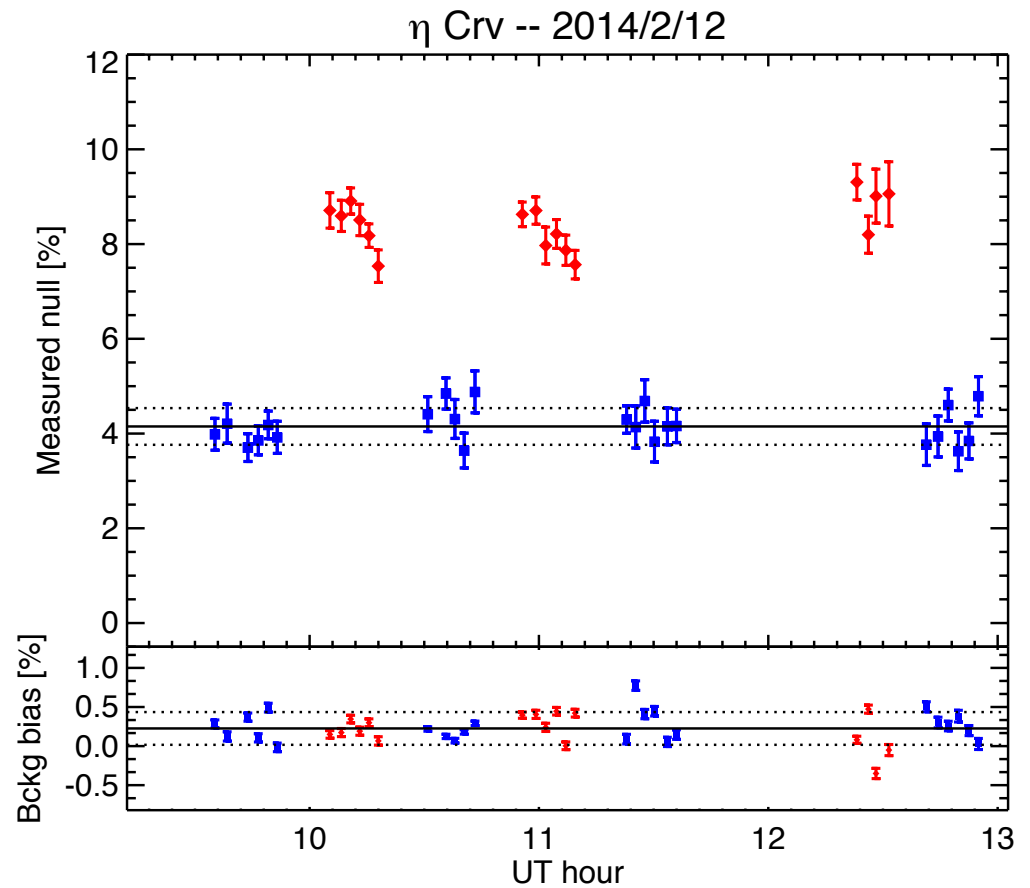
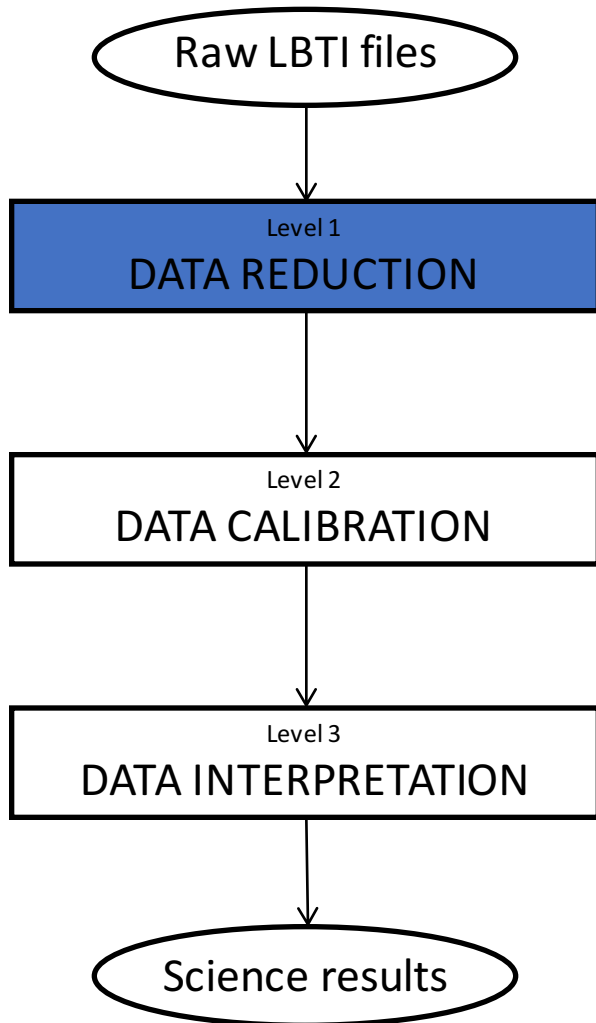


# Data analysis overview



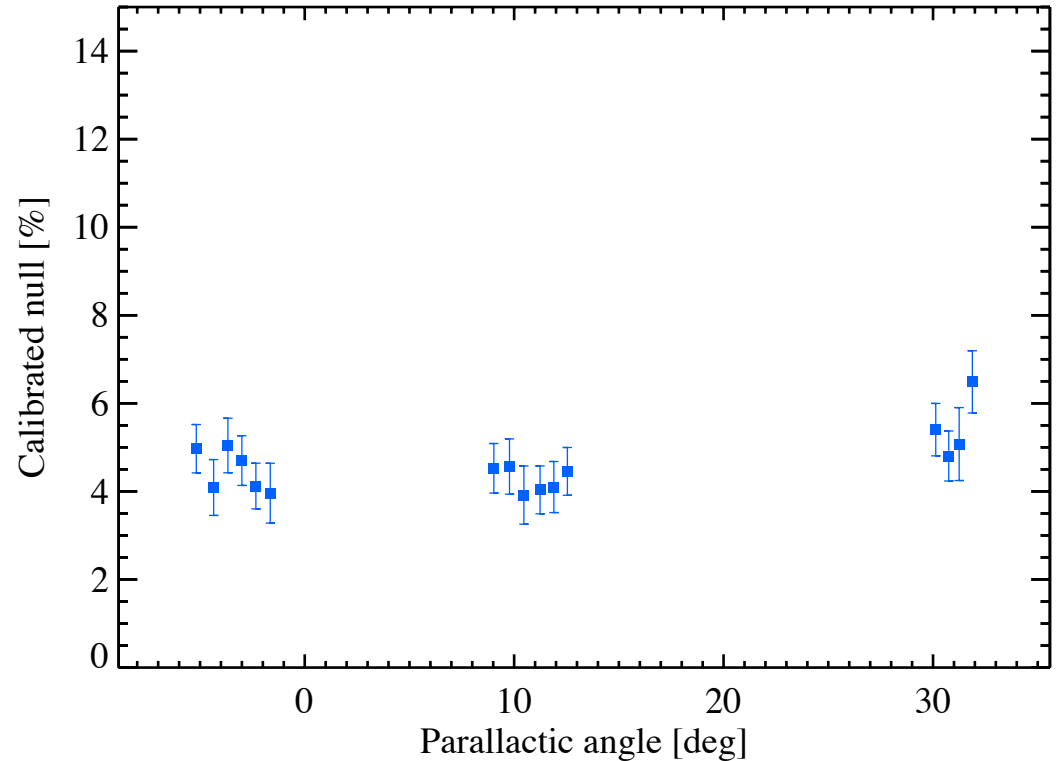
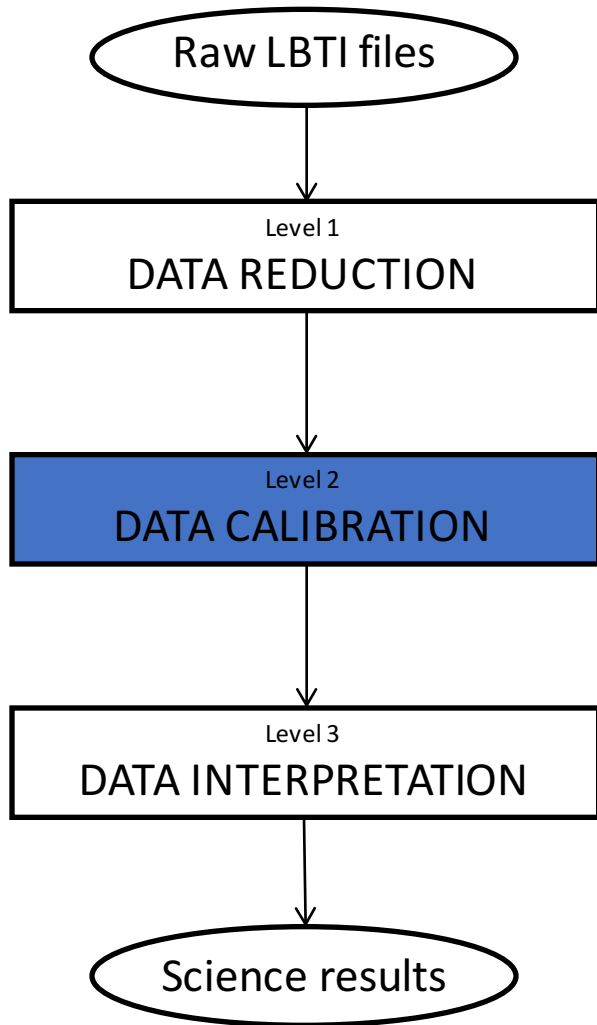


# Data analysis overview



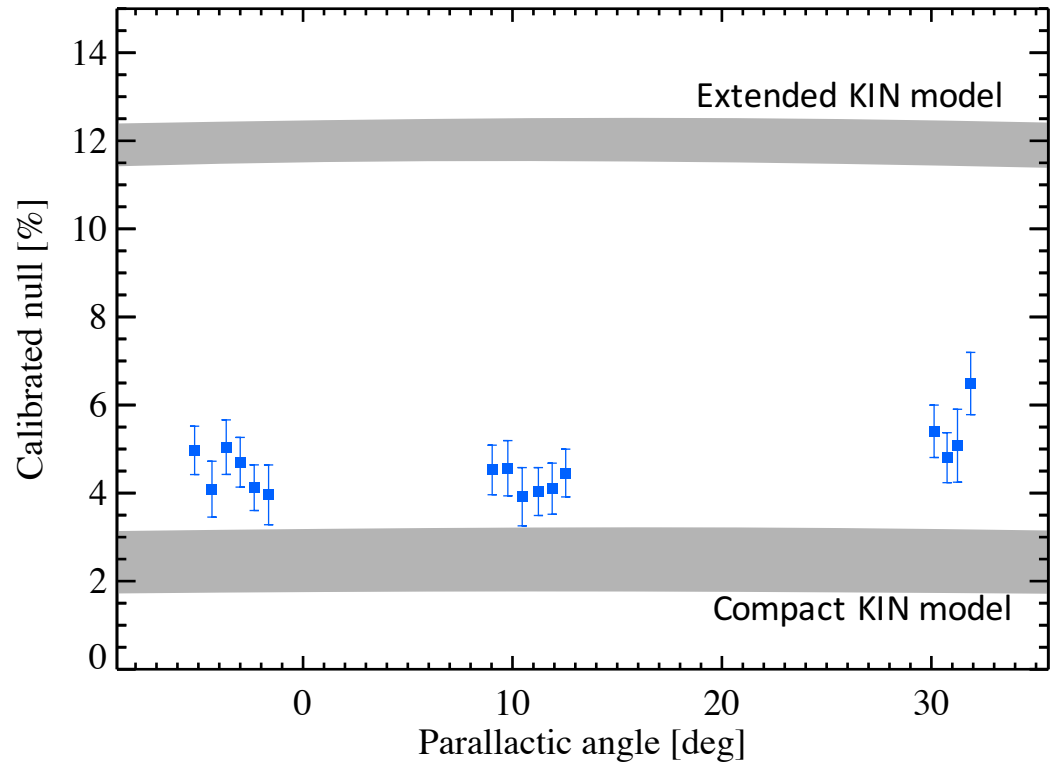
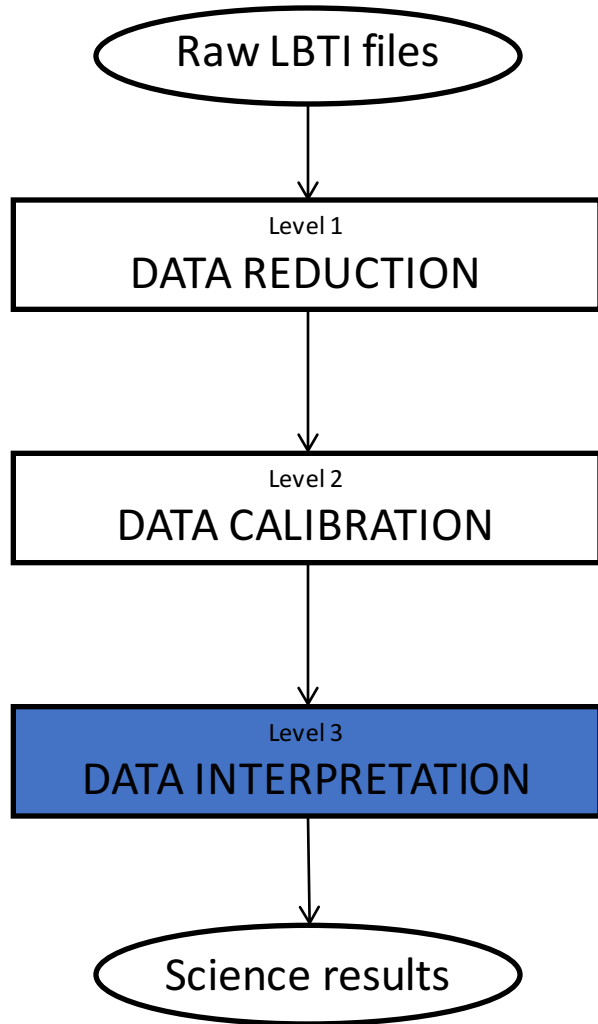


# Data analysis overview



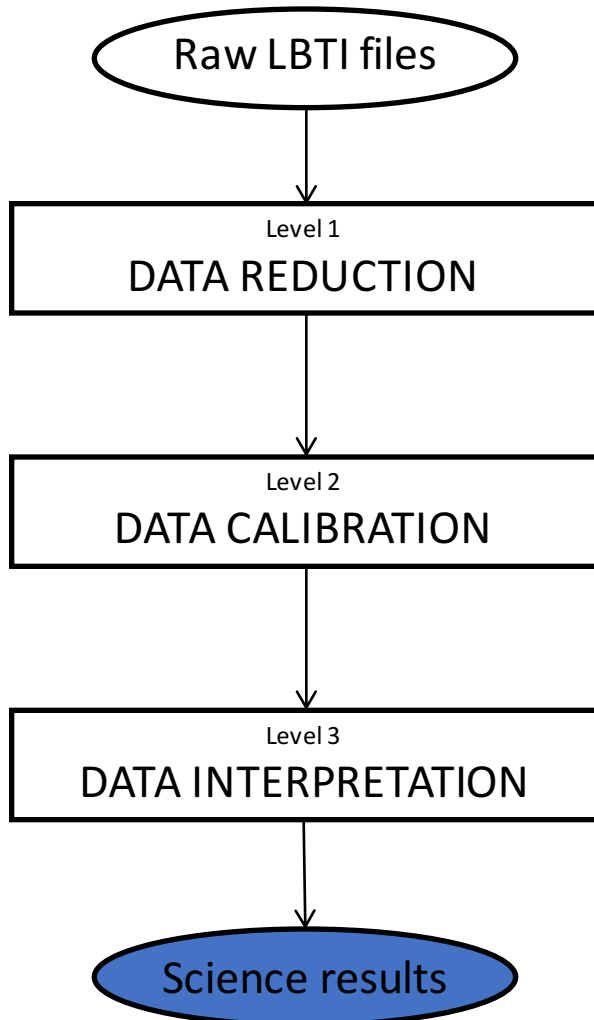


# Data analysis overview





# Data analysis overview



Jet Propulsion Laboratory  
California Institute of Technology

JPL HOME | EARTH | SOLAR SYSTEM | STARS & GALAXIES | SCIENCE & TECHNOLOGY  
BRING THE UNIVERSE TO YOU: JPL Email News | RSS | Podcast | Video

PLANET QUEST  
THE SEARCH FOR ANOTHER EARTH

3,613 CANDIDATES = 5,440 EXOPLANETS  
1,827 CONFIRMED

DISCOVER  
NEW WORLDS ATLAS  
a visual guide to exoplanets

NEWS | SCIENCE & TECHNOLOGY | IMAGES & VIDEO | INTERACTIVES | EDUCATION | FOR PROFESSIONALS | SEARCH | GO

NEWS  
LATEST | 2015 | 2014 | 2013 | 2012 | 2011 | 2010 | 2008 | 2007 | 2006 | 2005 | 2004 | 2003 | 2002

### LBTI hits the dusty trail of Earth-like planets

Artist's concept

THE ASTROPHYSICAL JOURNAL, 799:42 (9pp), 2015 January 20  
© 2015. The American Astronomical Society. All rights reserved.

doi:10.1088/0004-637X/799/1/42

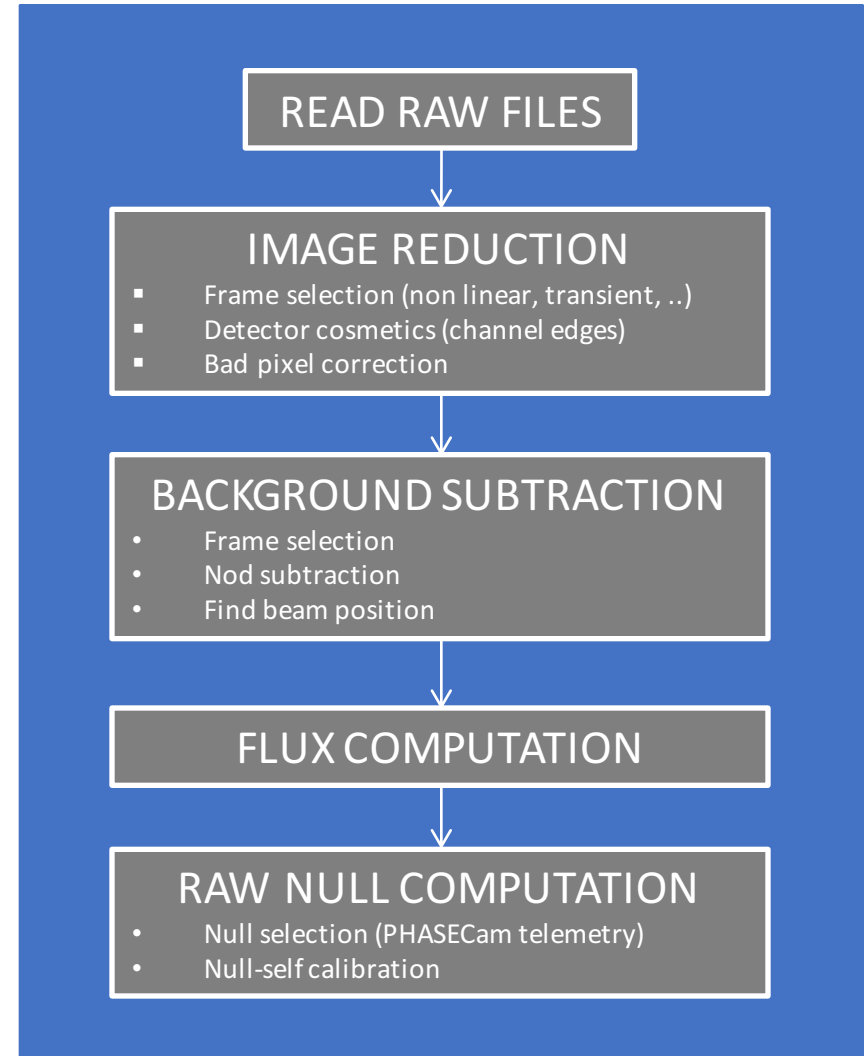
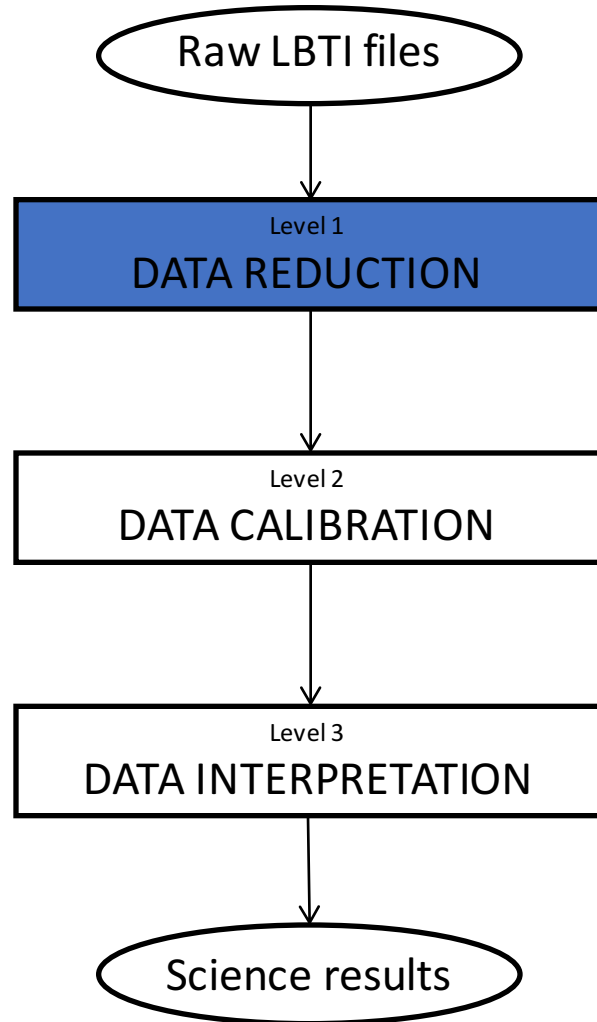
## FIRST-LIGHT LBT NULLING INTERFEROMETRIC OBSERVATIONS: WARM EXOZODIACAL DUST RESOLVED WITHIN A FEW AU OF $\eta$ Crv

D. DEFRÈRE<sup>1</sup>, P. M. HINZ<sup>1</sup>, A. J. SKEMER<sup>1</sup>, G. M. KENNEDY<sup>2</sup>, V. P. BAILEY<sup>1</sup>, W. F. HOFFMANN<sup>1</sup>, B. MENNESSON<sup>3</sup>, R. MILLAN-GABET<sup>4</sup>, W. C. DANCHI<sup>5</sup>, O. ABSIL<sup>6,11</sup>, P. ARBO<sup>1</sup>, C. BEICHMAN<sup>4</sup>, G. BRUSA<sup>1</sup>, G. BRYDEN<sup>3</sup>, E. C. DOWNY<sup>1</sup>, O. DURNAY<sup>1</sup>, S. ESPOSITO<sup>7</sup>, A. GASPAR<sup>1</sup>, P. GRENZ<sup>1</sup>, C. HANIFF<sup>8</sup>, J. M. HILL<sup>9</sup>, J. LEBRETON<sup>4</sup>, J. M. LEISENRING<sup>1</sup>, J. R. MALES<sup>1,12</sup>, L. MARION<sup>6</sup>, T. J. MCMAHON<sup>1</sup>, M. MONTOYA<sup>1</sup>, K. M. MORZINSKI<sup>1,12</sup>, E. PINNA<sup>7</sup>, A. PUGLISI<sup>7</sup>, G. RIEKE<sup>1</sup>, A. ROBERGE<sup>5</sup>, E. SERABYN<sup>3</sup>, R. SOSA<sup>1</sup>, K. STAPELDFELDT<sup>5</sup>, K. SU<sup>1</sup>, V. VAITHEESWARAN<sup>1</sup>, A. VAZ<sup>1</sup>, A. J. WEINBERGER<sup>10</sup>, AND M. C. WYATT<sup>2</sup>

<sup>1</sup> Steward Observatory, Department of Astronomy, University of Arizona, 933 North Cherry Avenue, Tucson, AZ 85721, USA; [ddefre@email.arizona.edu](mailto:ddefre@email.arizona.edu)

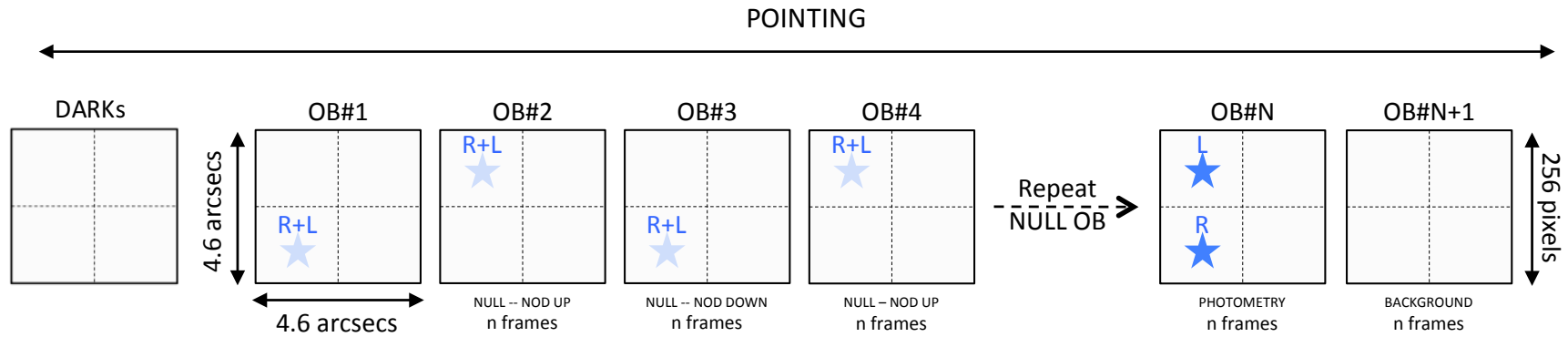


# Data analysis overview



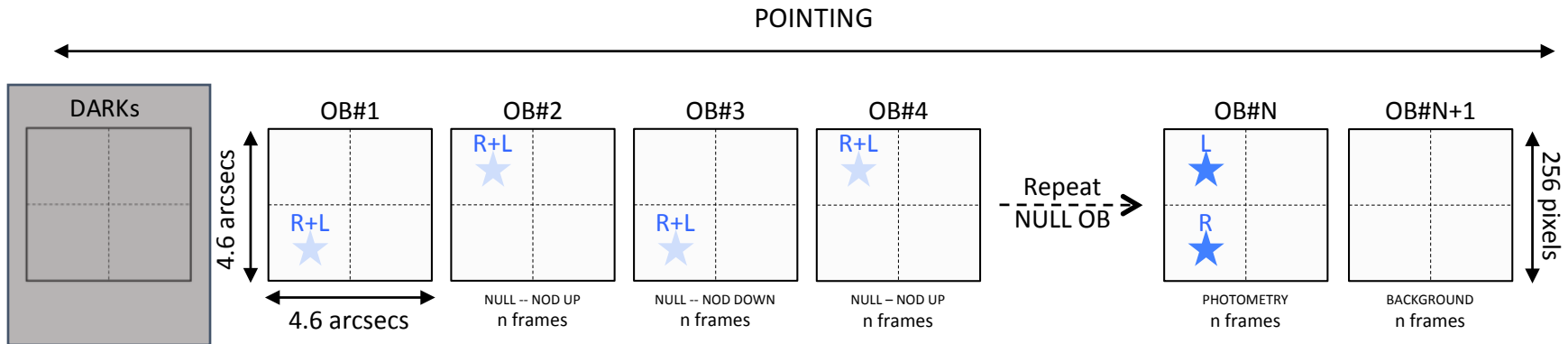


# Observing strategy





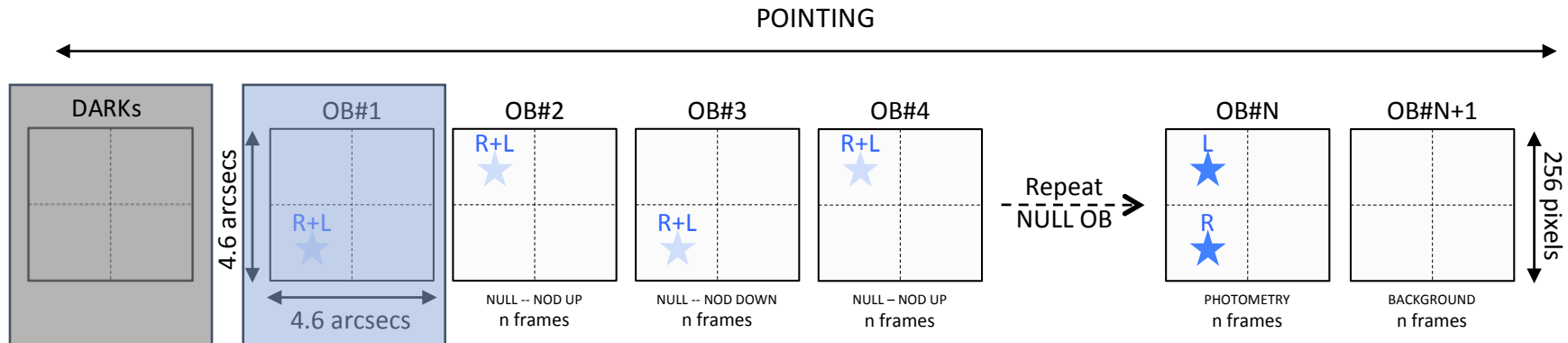
# Observing strategy



- DARKS: used for hot bad pixel identification



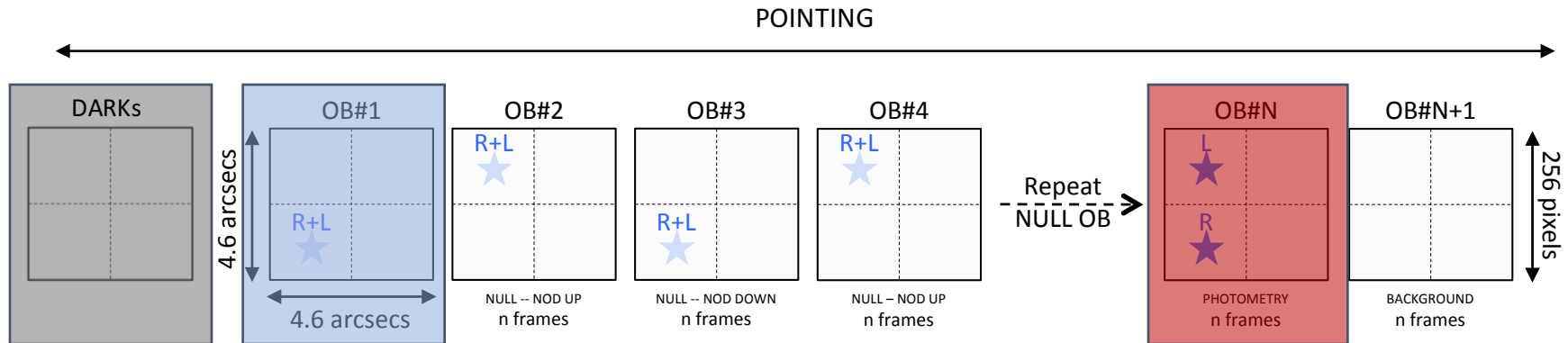
# Observing strategy



- DARKS: used for cold bad pixel identification
- NULL observing block (OB): overlapped beams in phase opposition.



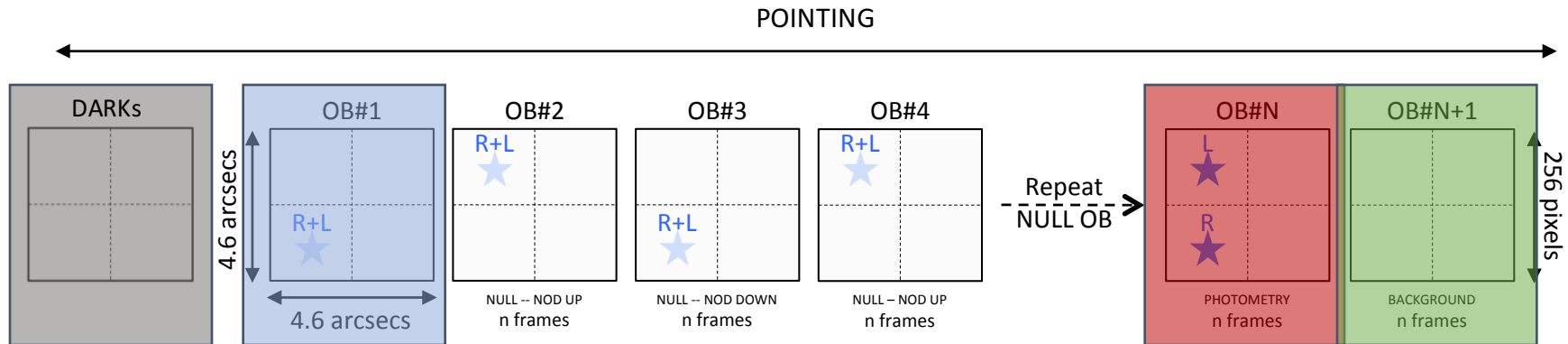
# Observing strategy



- DARKS: used for hot bad pixel identification
- NULL observing block (OB): overlapped beams in phase opposition.
- PHOTOMETRY OB: separated beams, used for normalization



# Observing strategy



- DARKS: used for hot bad pixel identification
- NULL observing block (OB): overlapped beams in phase opposition.
- PHOTOMETRY OB: separated beams, used for normalization
- BACKGROUND OB: used for flat fielding and cold bad pixel identification



# Observing strategy

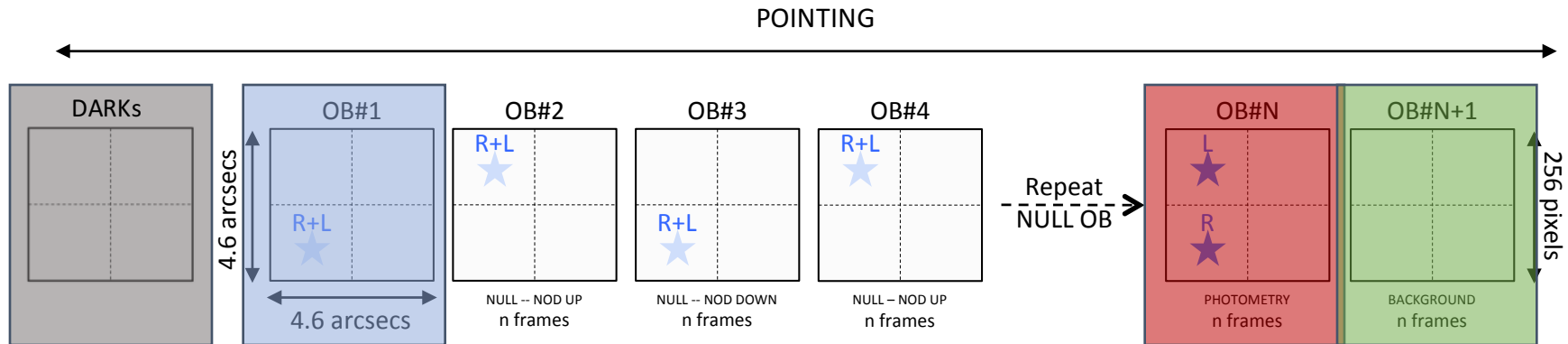


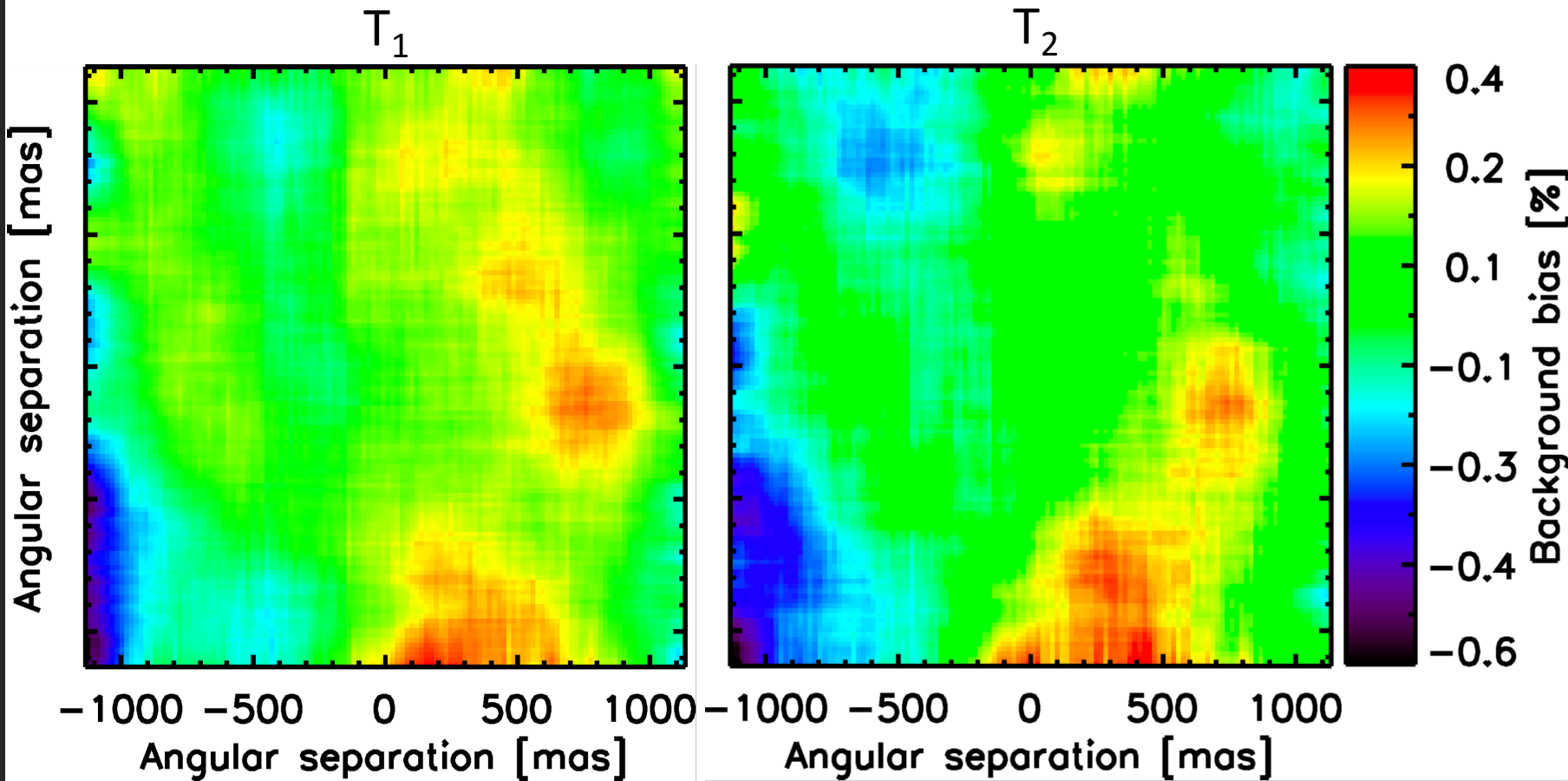
## IMAGE HEADER

- Target info (e.g., name, RA, DEC, ...)
- Telescope telemetry (e.g., elevation, ...)
- Detector and filter configuration (e.g., DIT, mode, filter position, ...)
- AO telemetry (e.g., loop status, loop frequency, loop gains, ...)
- PHASECam telemetry (e.g., loop status, SNR, speed, OPD RMS, tip/tilt RMS, ...)
- Weather information (e.g., seeing, PWV, wind, ...)



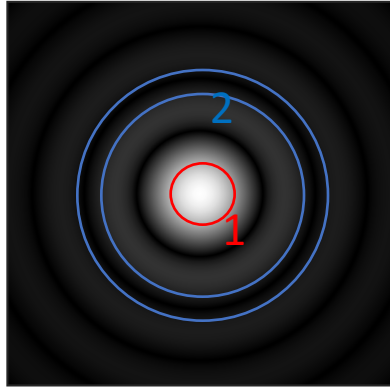
# Background subtraction

- Complex spatiotemporal fluctuations
- Flux-dependent detector behavior
- Temporal and spatial noise correlation
- Must be corrected for accurate null measurements



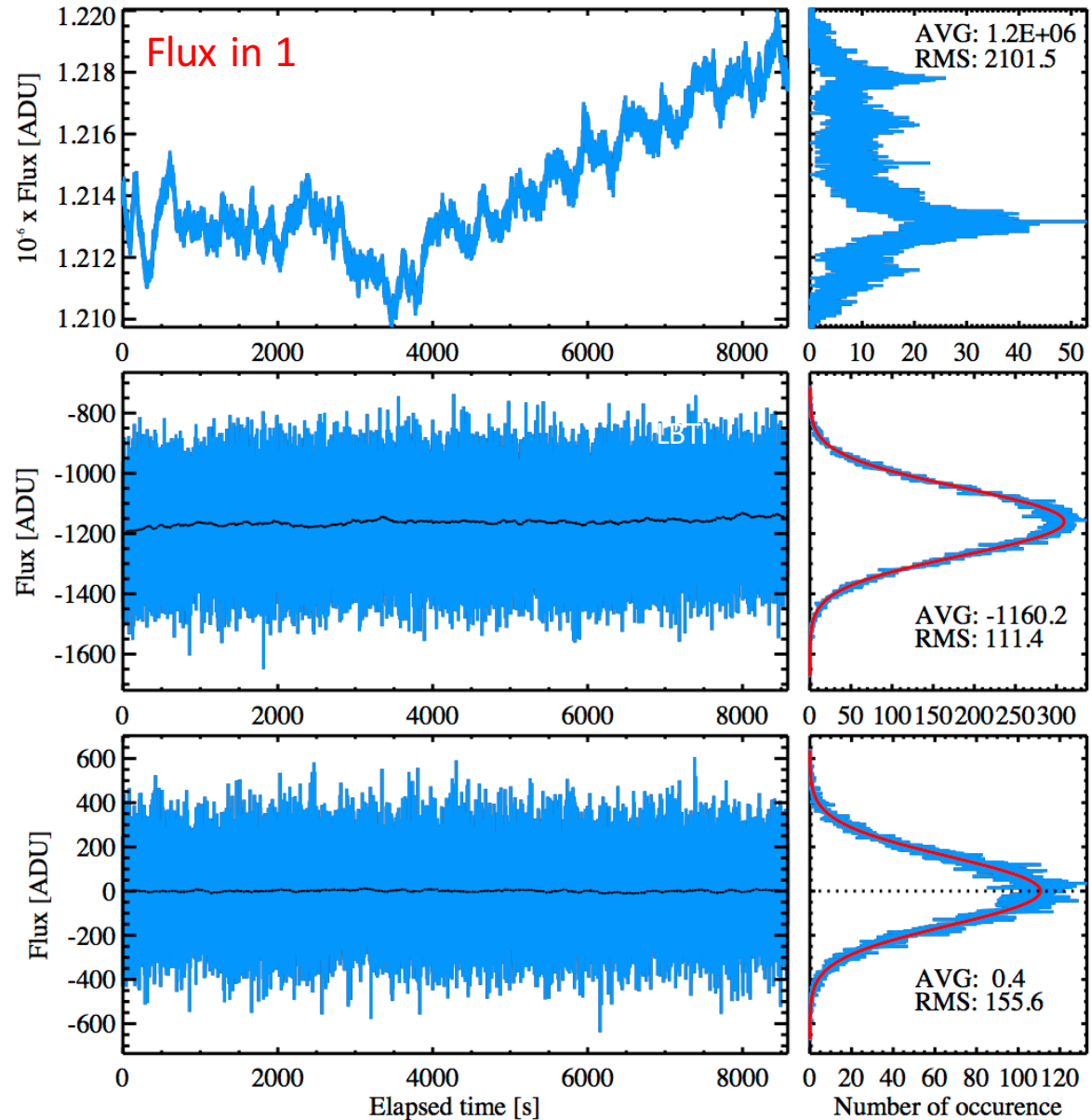


# Background subtraction



Flux in region 1 – region 2  
Large variation corrected  
Large offset  
Slow drift

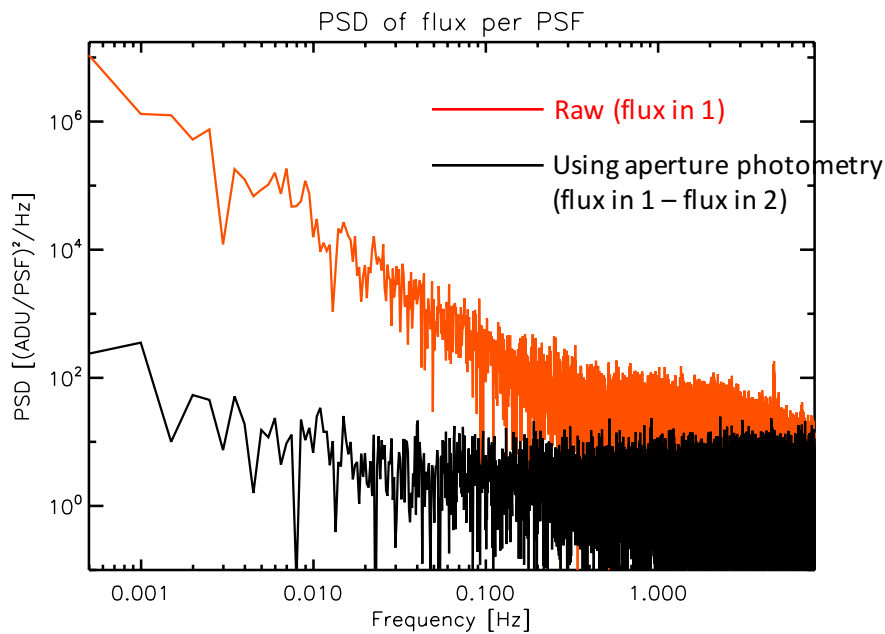
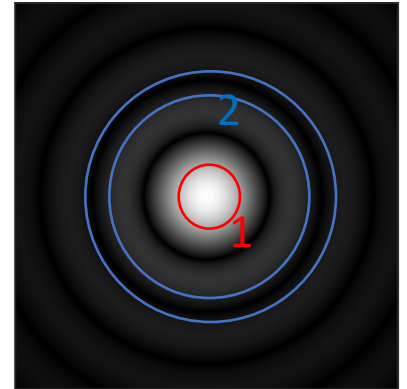
Flux in region 1 – region 2 -  
(estimate in next nod)  
Offset corrected  
Slow drift removed



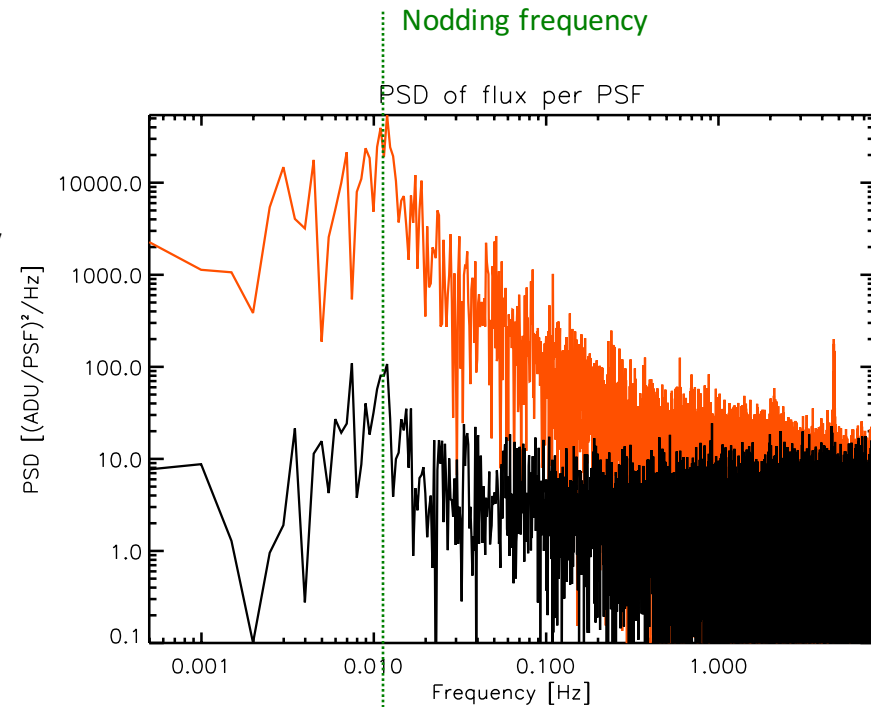


# Background subtraction

- High nodding frequency!



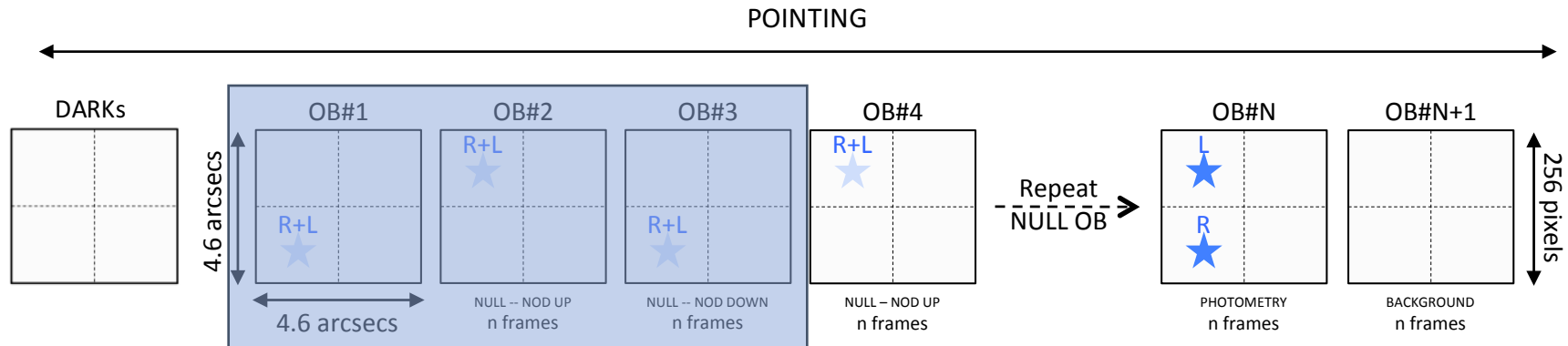
**WITHOUT NODDING SUBTRACTION**



**WITH NODDING SUBTRACTION**



# Observing strategy

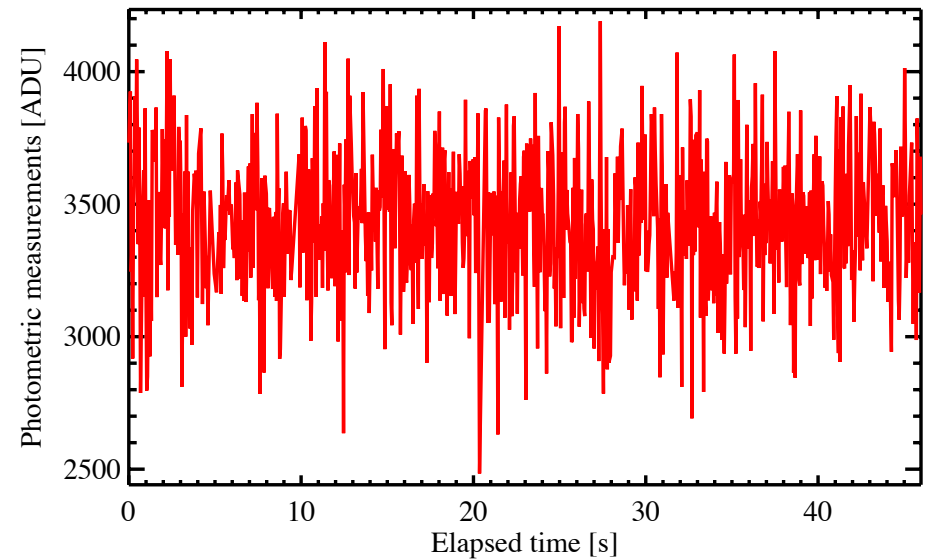
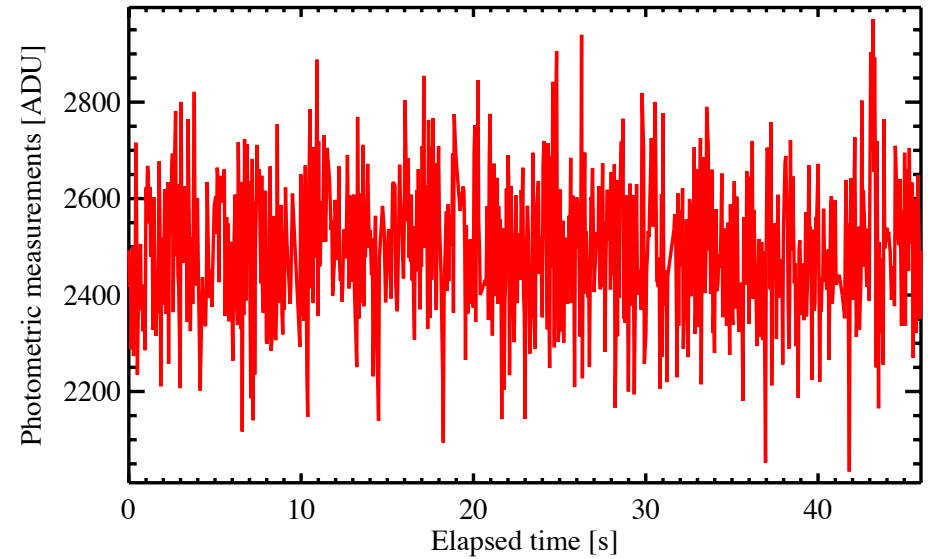
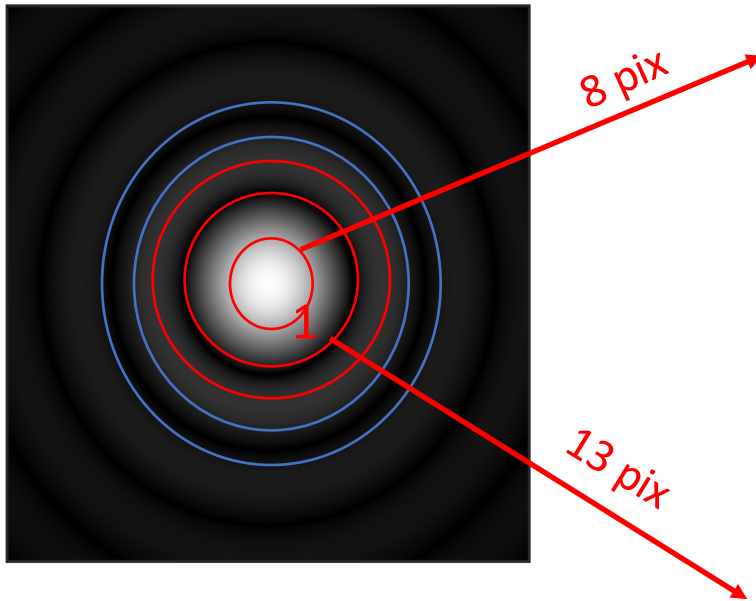


- Two-step approach:
  1. SPATIAL ESTIMATOR (simultaneous, different position): aperture photometry
  2. TIME ESTIMATOR (different time, same position): median of frames in neighboring nods
- Frame selection is critical:
  - Several possibilities: proximity in time, flux, elevation, ...
  - Weighted-combination (e.g. Bottom et al. 2017)?



# Flux computation

- Performed by aperture photometry over different aperture radii

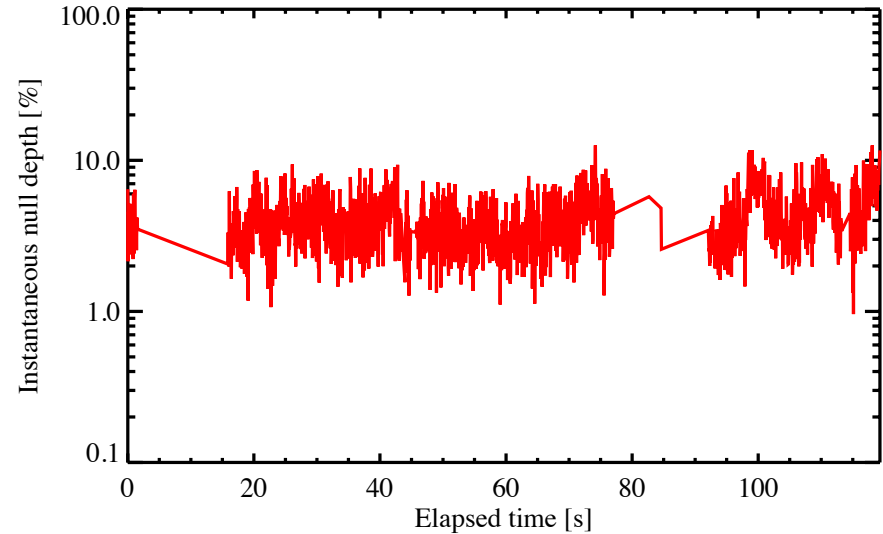
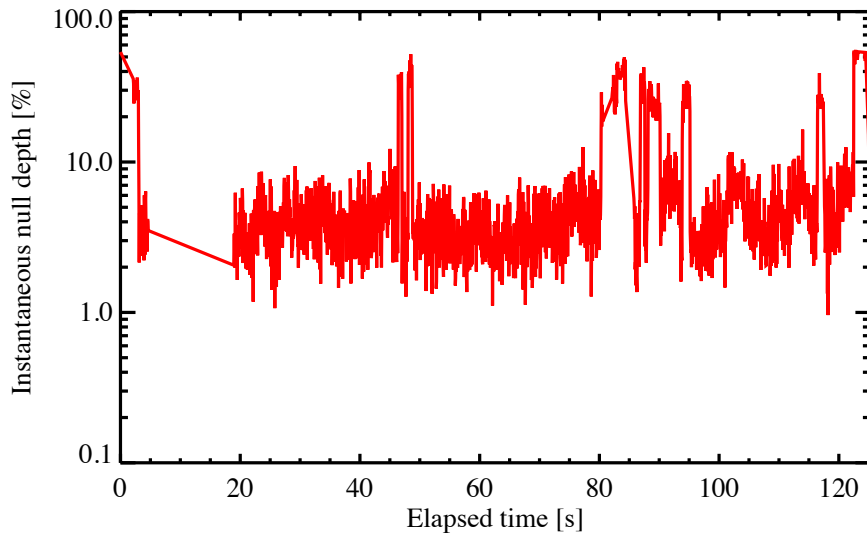




# Null computation

## Step 1: frame selection

- Reject open-loop frames (AO and phase)
- Reject fringe jumps
- Reject frames associated to low-quality 2- $\mu\text{m}$  fringes
- Reject frames associated to high phase noise (measured by PHASECam)
- Keep only nulls in the  $[-0.02, 0.95]$  range



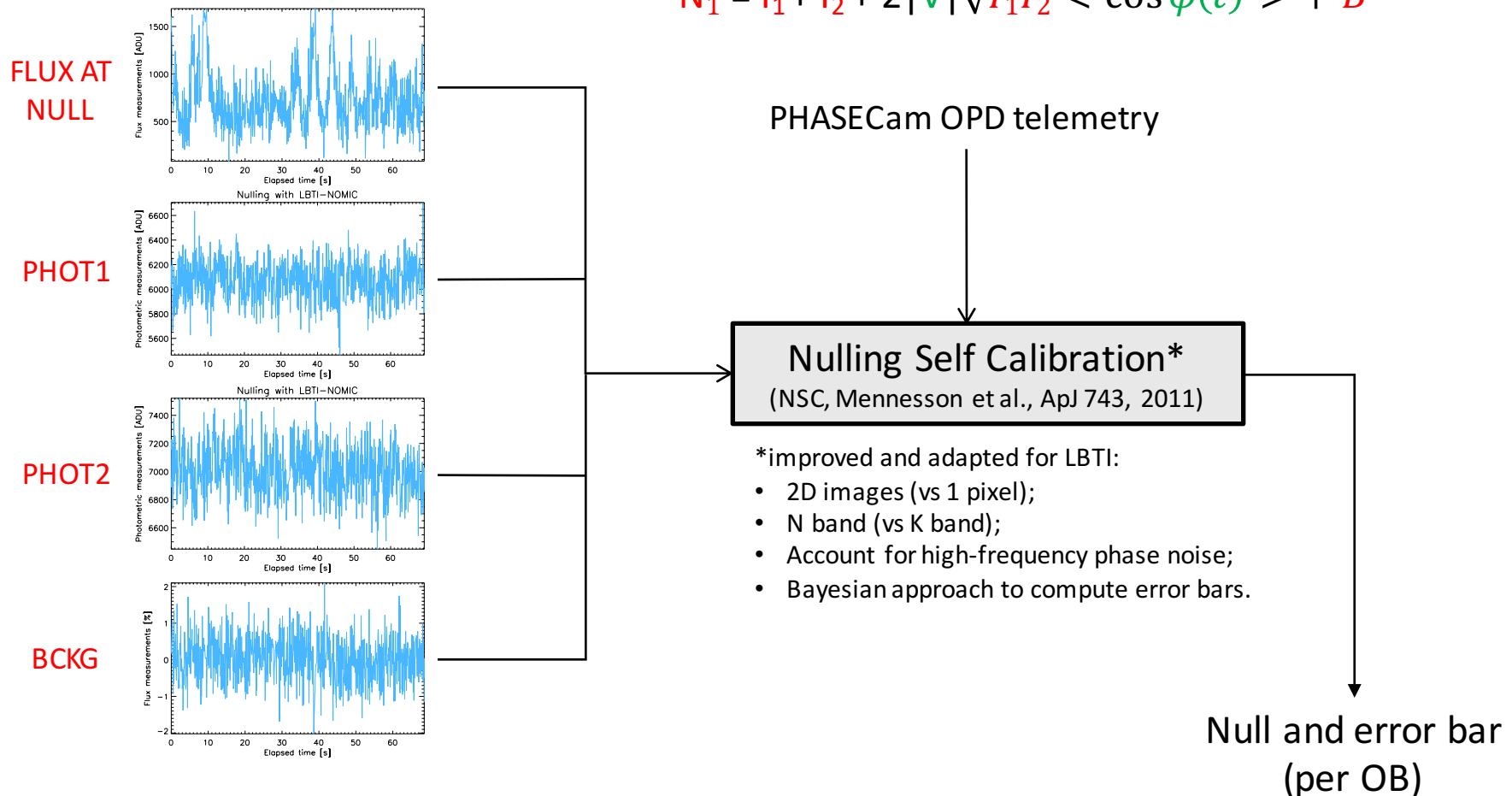


# Null computation

## Step 2: convert flux measurements at null of each OB to a single null value

- Assume Gaussian phase  $\phi$  ( $\mu ; \sigma$ ), adjust ( $\mu, \sigma, V$ ) to build fake data set and match observed distribution:

$$N_1 = I_1 + I_2 + 2|V|\sqrt{I_1 I_2} \langle \cos \phi(t) \rangle + B$$





# Null Self Calibration

---

- The average measured null (or visibility) is NOT the best observable !! The analysis of the distribution provides a much better and more robust estimator
- Deconvolution of instrumental effects (piston and intensity mismatch) making use of *whole* dataset
- Can work with average nulls as bad as 10% and fluctuating by the same amount, and still measure underlying astro nulls  $< 0.001$  with a few  $10^{-4}$  accuracy
- Works as well on resolved objects, measuring accurate visibilities (tested on archival KI FT data)
- Single-mode monochromatic assumption for the interferometric signal:

$$= I_1(t) + I_2(t) + 2|V| \cdot \sqrt{I_1(t)I_2(t)} \cdot \cos(\phi(t) + \phi_V) + D(t)$$

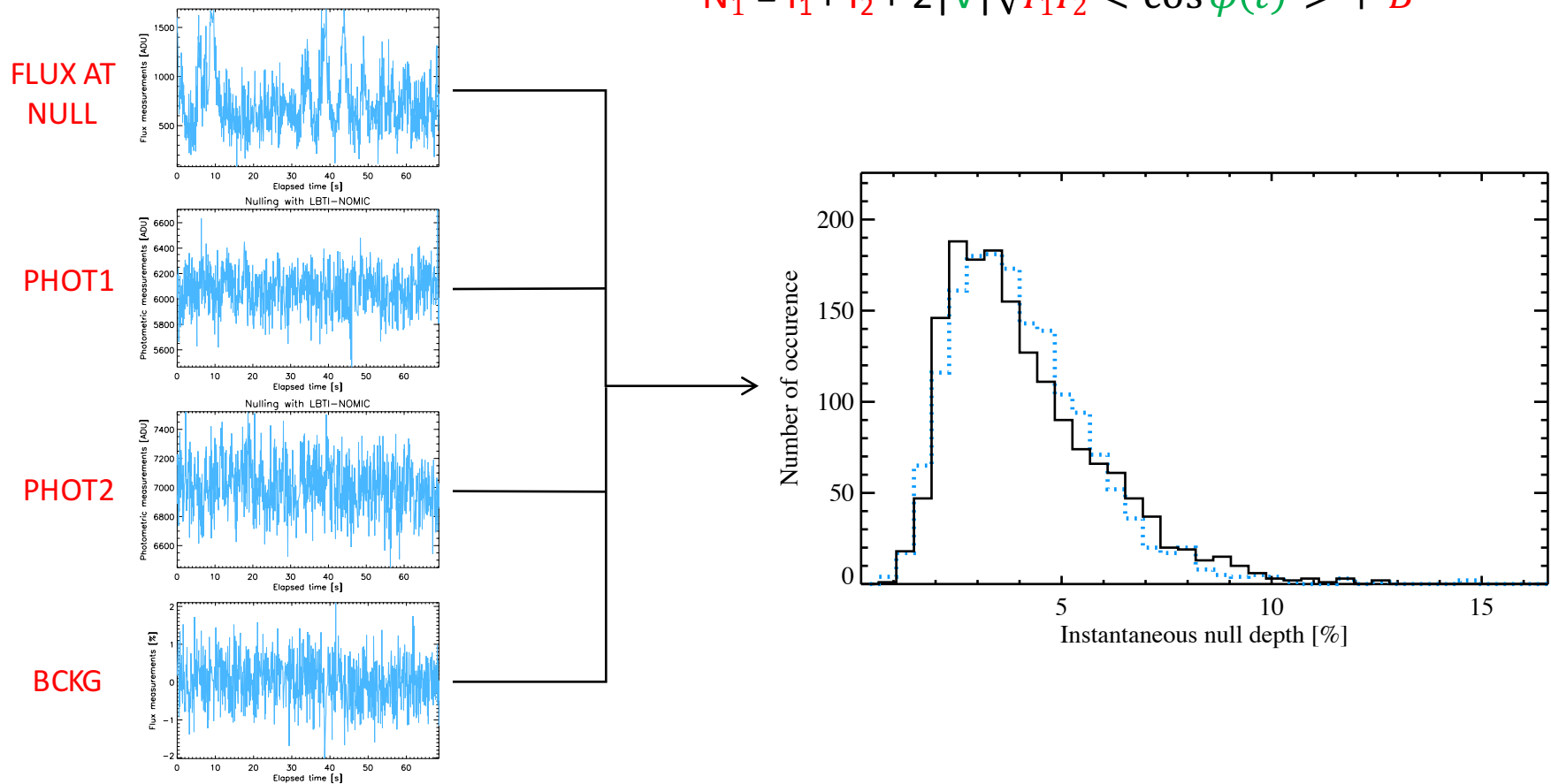


# Null computation

Step 2: convert flux measurements at null of each OB to a single null value

- Assume Gaussian phase  $\phi$  ( $\mu ; \sigma$ ), adjust ( $\mu, \sigma, V$ ) to build fake data set and match observed distribution:

$$N_1 = I_1 + I_2 + 2|V|\sqrt{I_1 I_2} \langle \cos \phi(t) \rangle + B$$

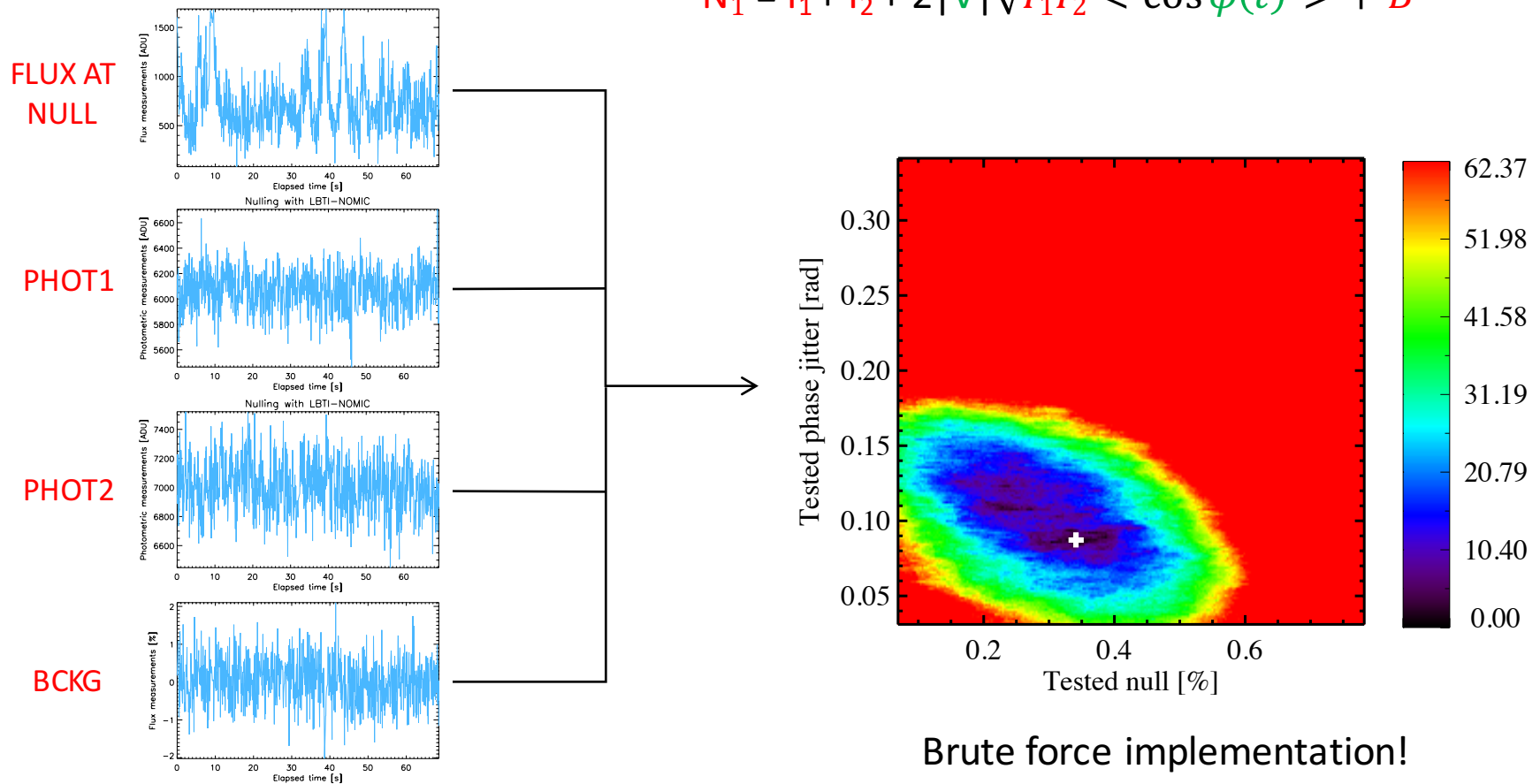


# Null computation

Step 2: convert flux measurements at null of each OB to a single null value

- Assume Gaussian phase  $\phi$  ( $\mu ; \sigma$ ), adjust ( $\mu, \sigma, V$ ) to build fake data set and match observed distribution:

$$N_1 = I_1 + I_2 + 2|V|\sqrt{I_1 I_2} \langle \cos \phi(t) \rangle + B$$

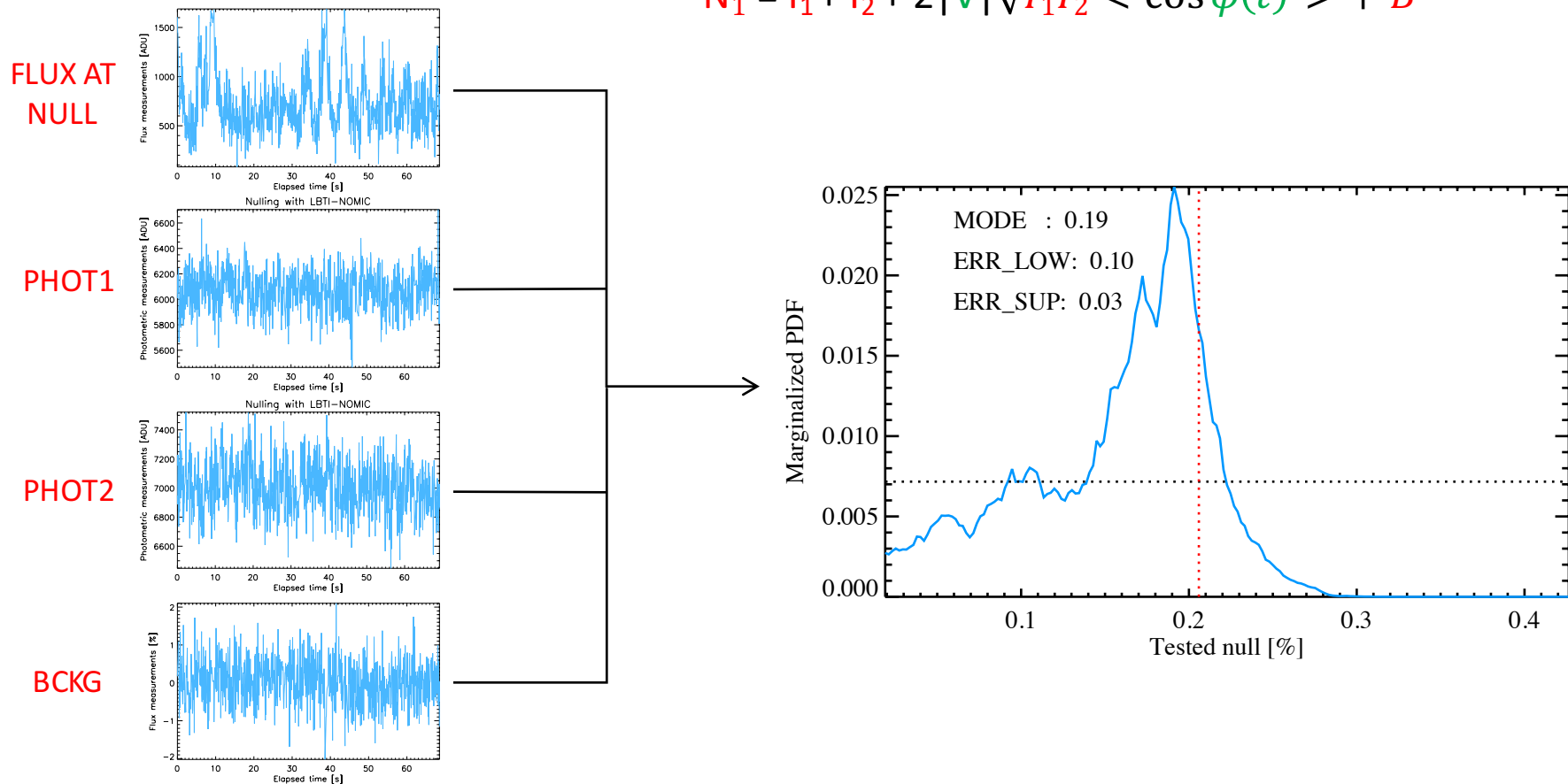


# Null computation

## Step 2: convert flux measurements at null of each OB to a single null value

- Assume Gaussian phase  $\phi$  ( $\mu ; \sigma$ ), adjust ( $\mu, \sigma, V$ ) to build fake data set and match observed distribution:

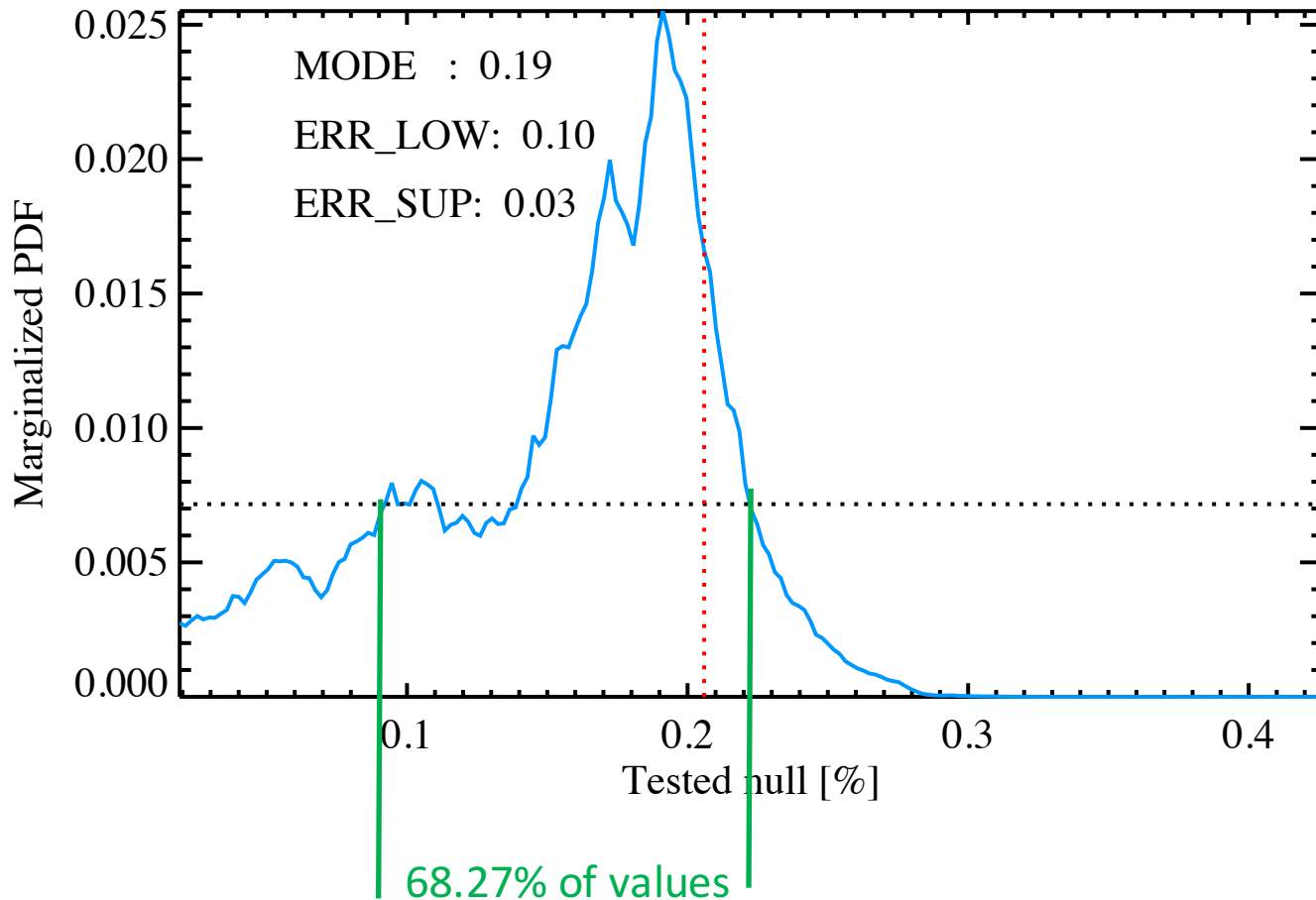
$$N_1 = I_1 + I_2 + 2|V|\sqrt{I_1 I_2} \langle \cos \phi(t) \rangle + B$$





# Null computation

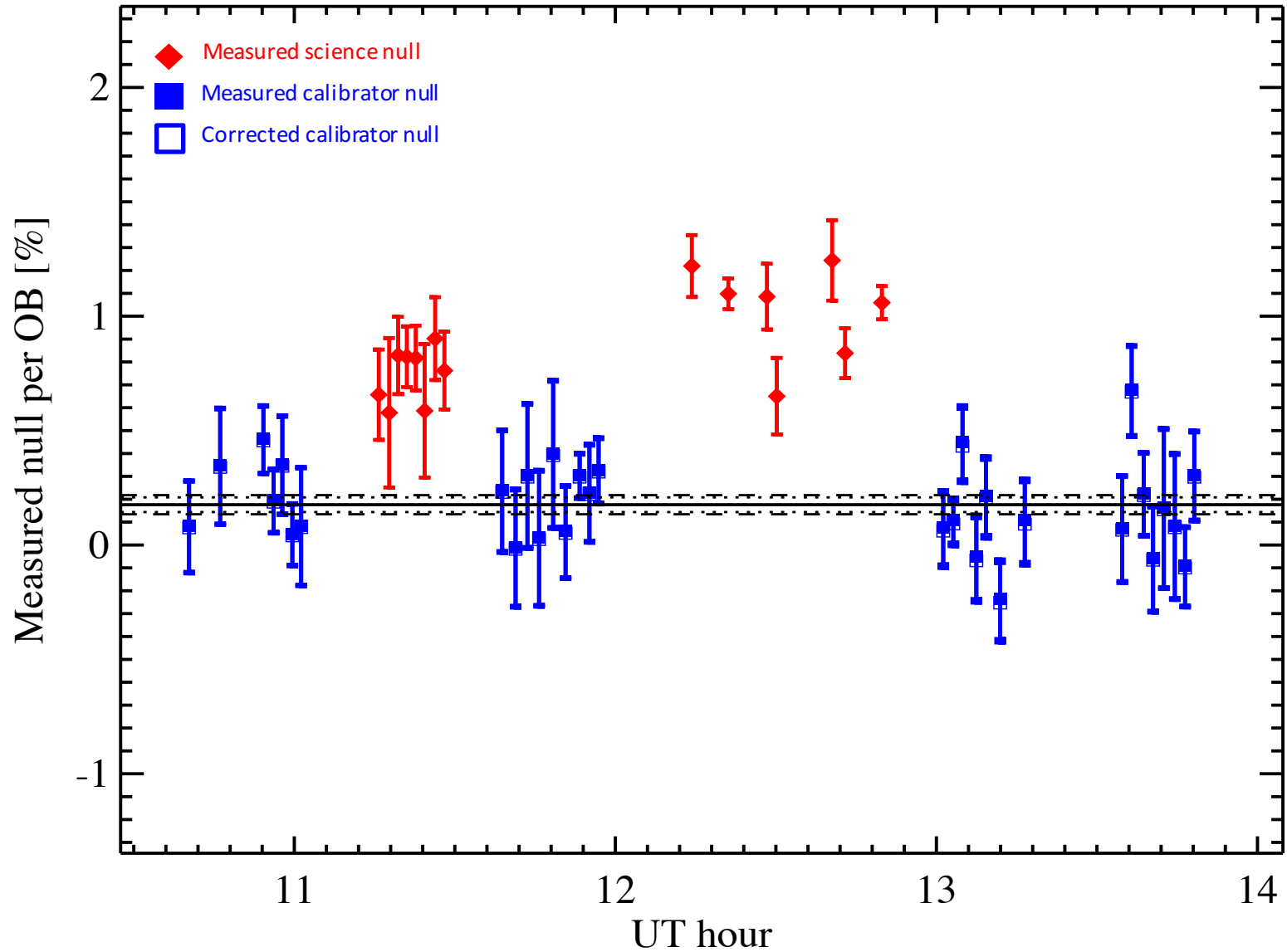
- Error bar computed using high-density regions described by Hyndman, R. J. 1996, The American Statistician, 50, 120:





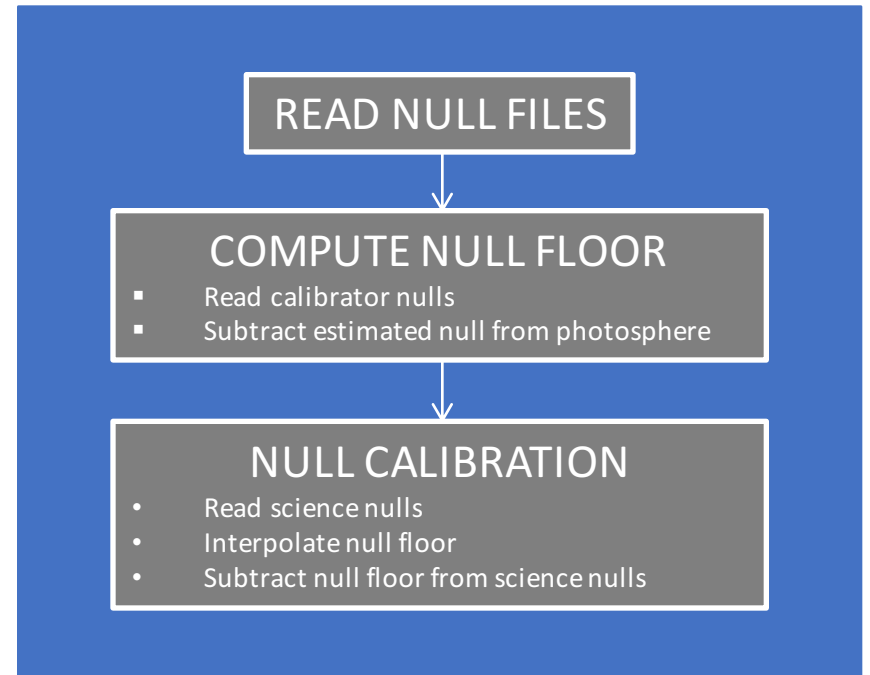
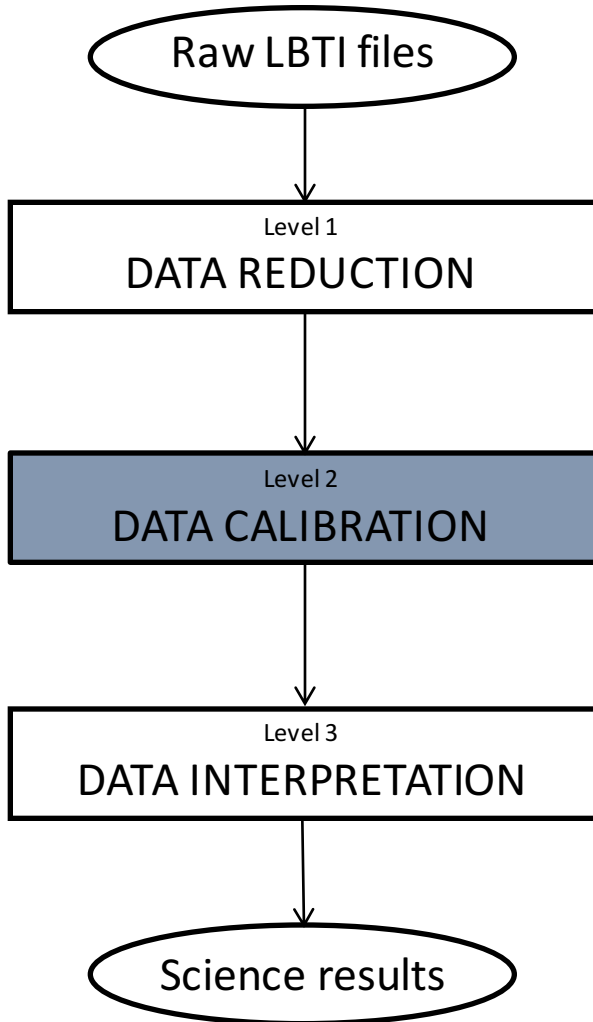
# Null computation

2015/2/8



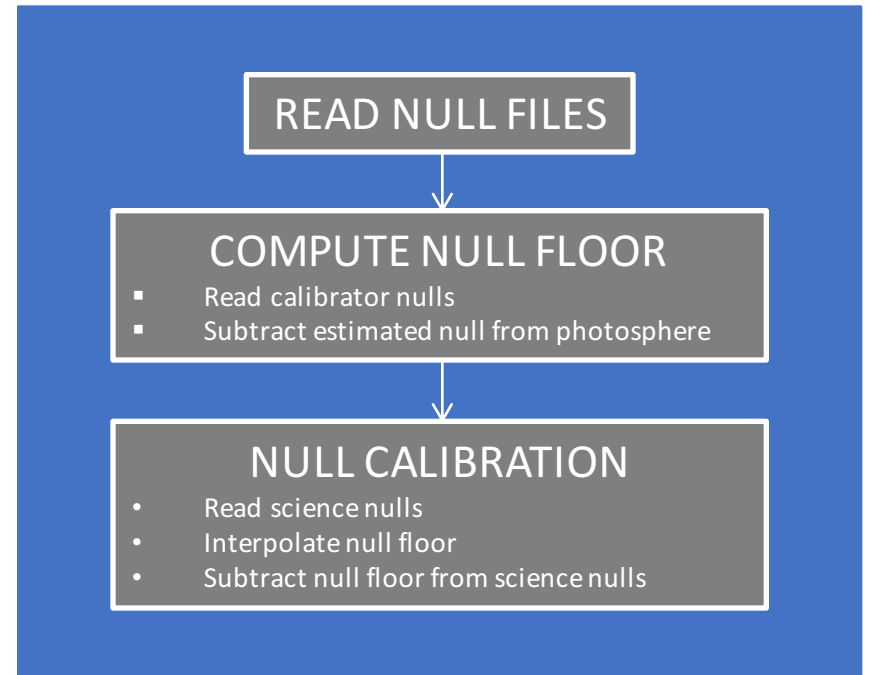
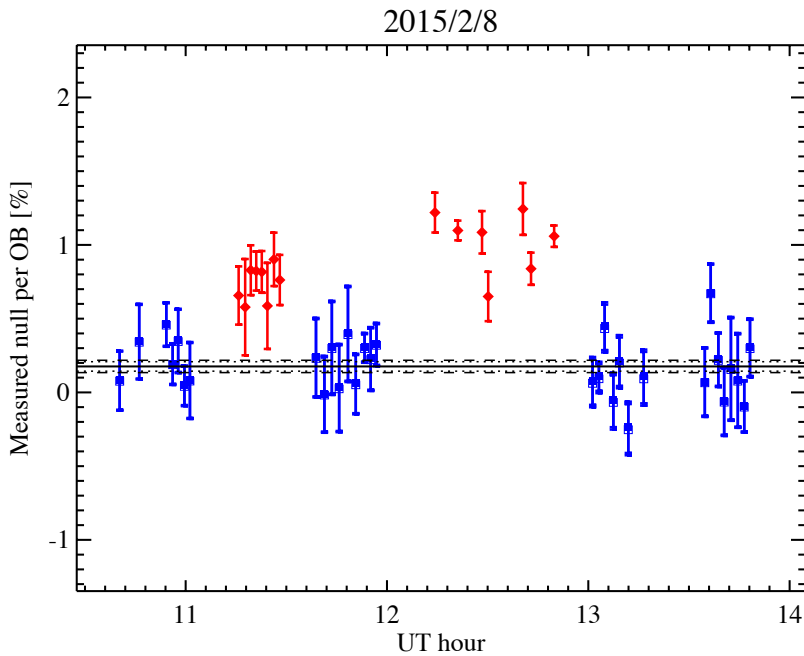


# Null calibration





# Null calibration





# Analysis and pipeline limitations

---

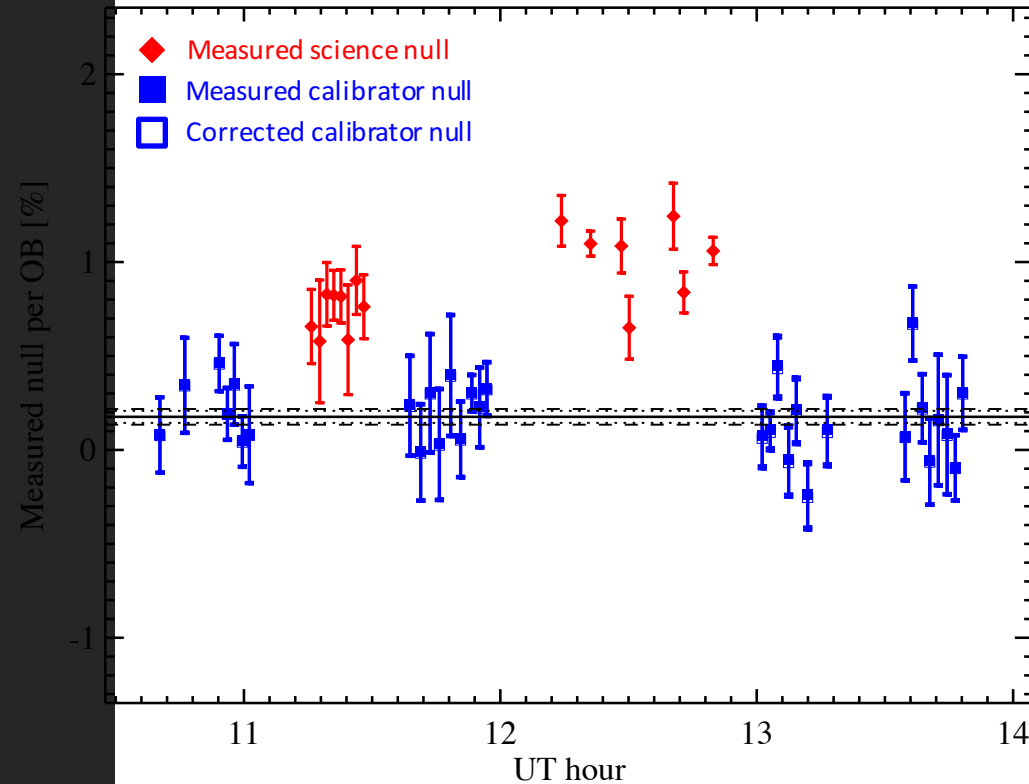
- Need to test more advanced nod-subtraction techniques (e.g. parameter weighted approach, gain of  $\sim 20\%$ , see Bottom et al. 2017)
- Replace brute-force computer-intensive NSC approach by MCMC
- Asymmetric error bars not propagated (only the maximum of the 2)
- Implement and test null calibration using images rather than fluxes



# Data calibration

## NOTATIONS AND ERROR BARS

2015/2/8



— Weighted mean transfer function (TF, cal. only):

$$TF = \frac{\sum_i n_i / \sigma_i^2}{\sum_i 1 / \sigma_i^2}$$

..... 1- $\sigma$  propagated statistical error on mean TF (cal. only):

$$\sigma_{stat} = \frac{1}{\sqrt{\sum_i 1 / \sigma_i^2}}$$

----- 1- $\sigma$  unbiased weighted error on the weighted mean:

$$\sigma_{sys} = \sqrt{\frac{\sum_i 1 / \sigma_i^2 \sum_i (n_i - TF)^2 / \sigma_i^2}{(\sum_i 1 / \sigma_i^2)^2 \frac{(N-1)}{N} \sum_i 1 / \sigma_i^2}}$$

+ error due to diameter uncertainty (generally negligible)

# LBTI's nulling performance limitations and prospects

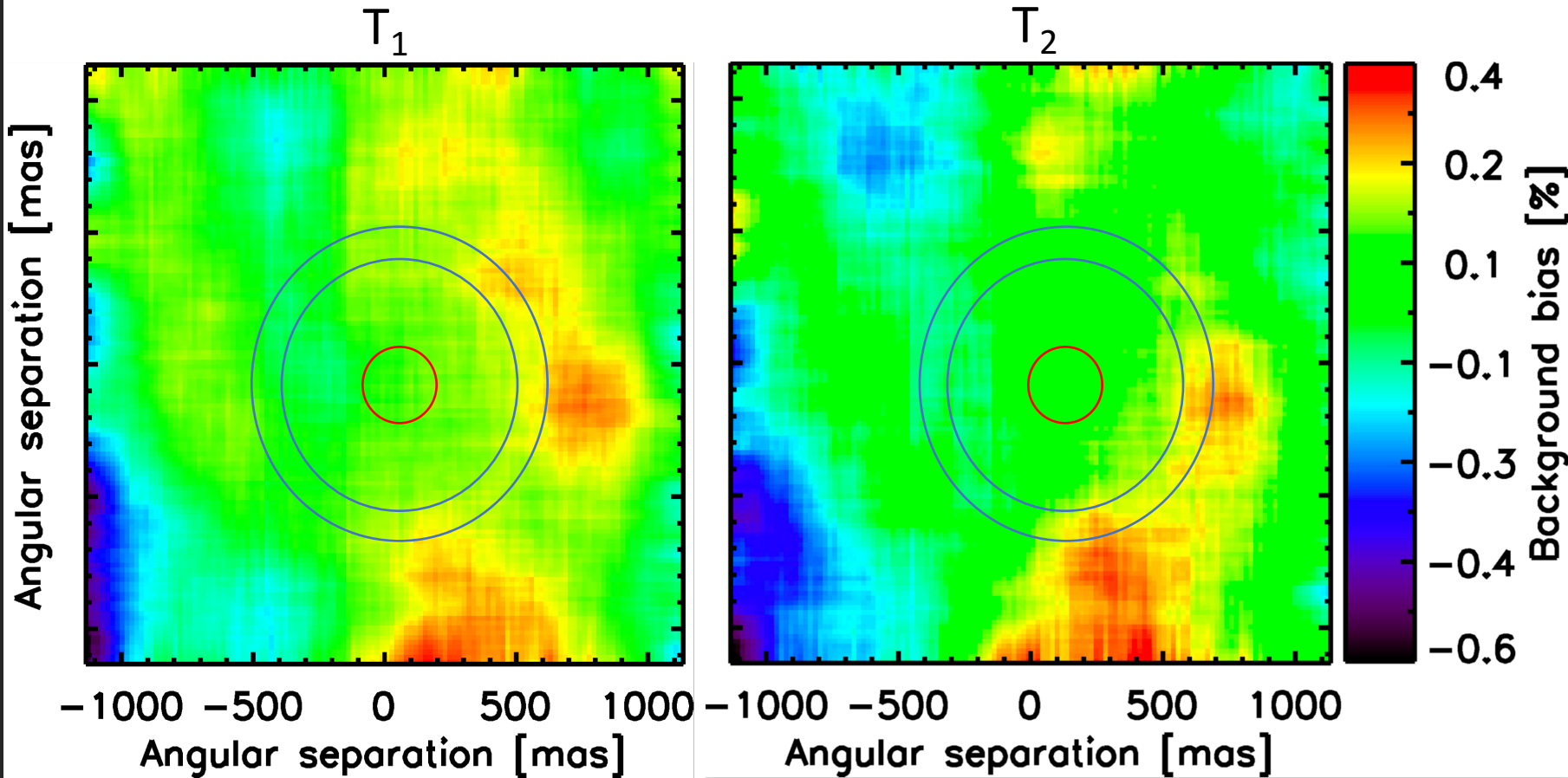
D. Defrère

University of Liège



# Background bias

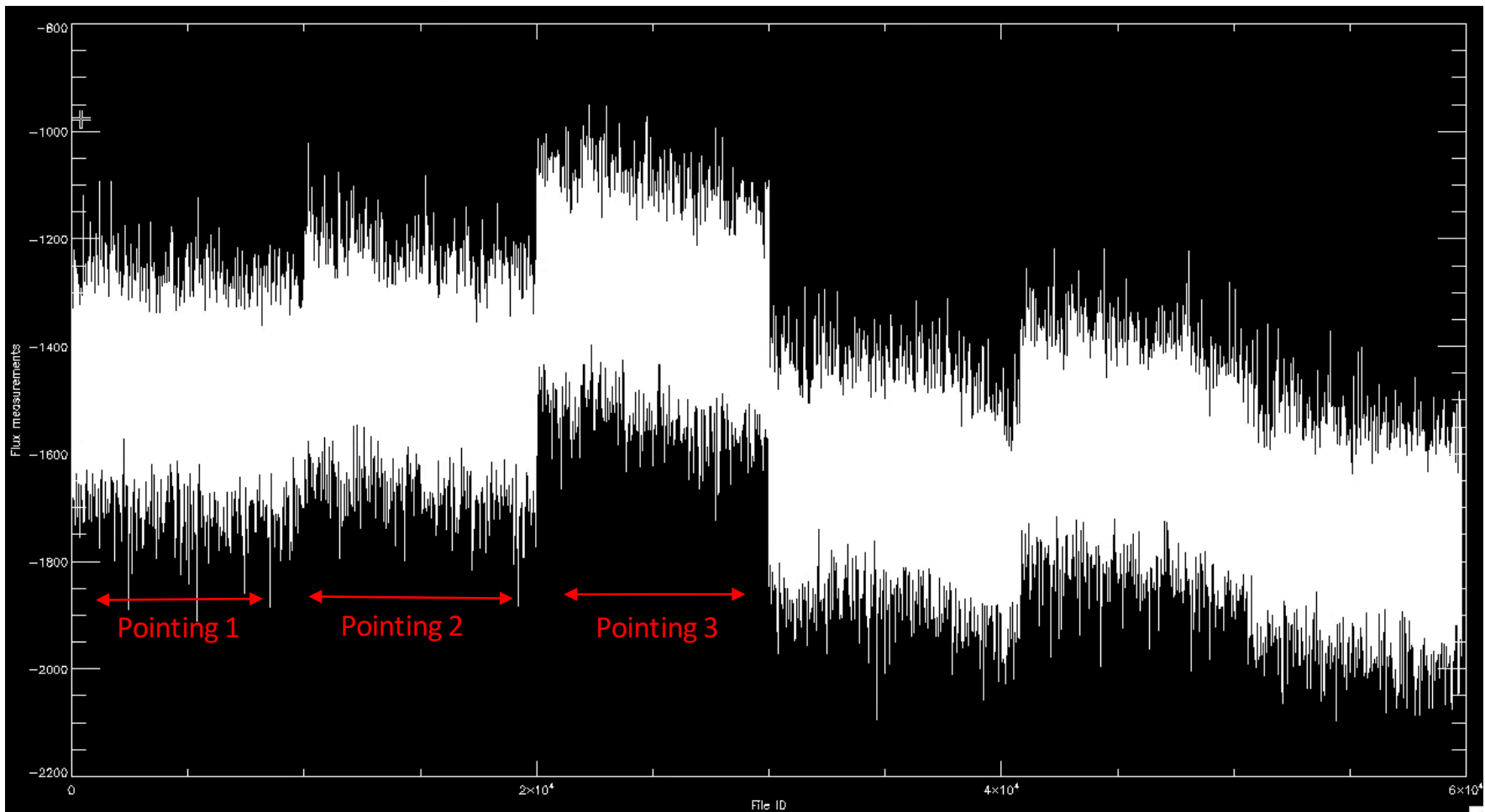
- Empty region of the detector at two different times:





# Example of nulling sequence

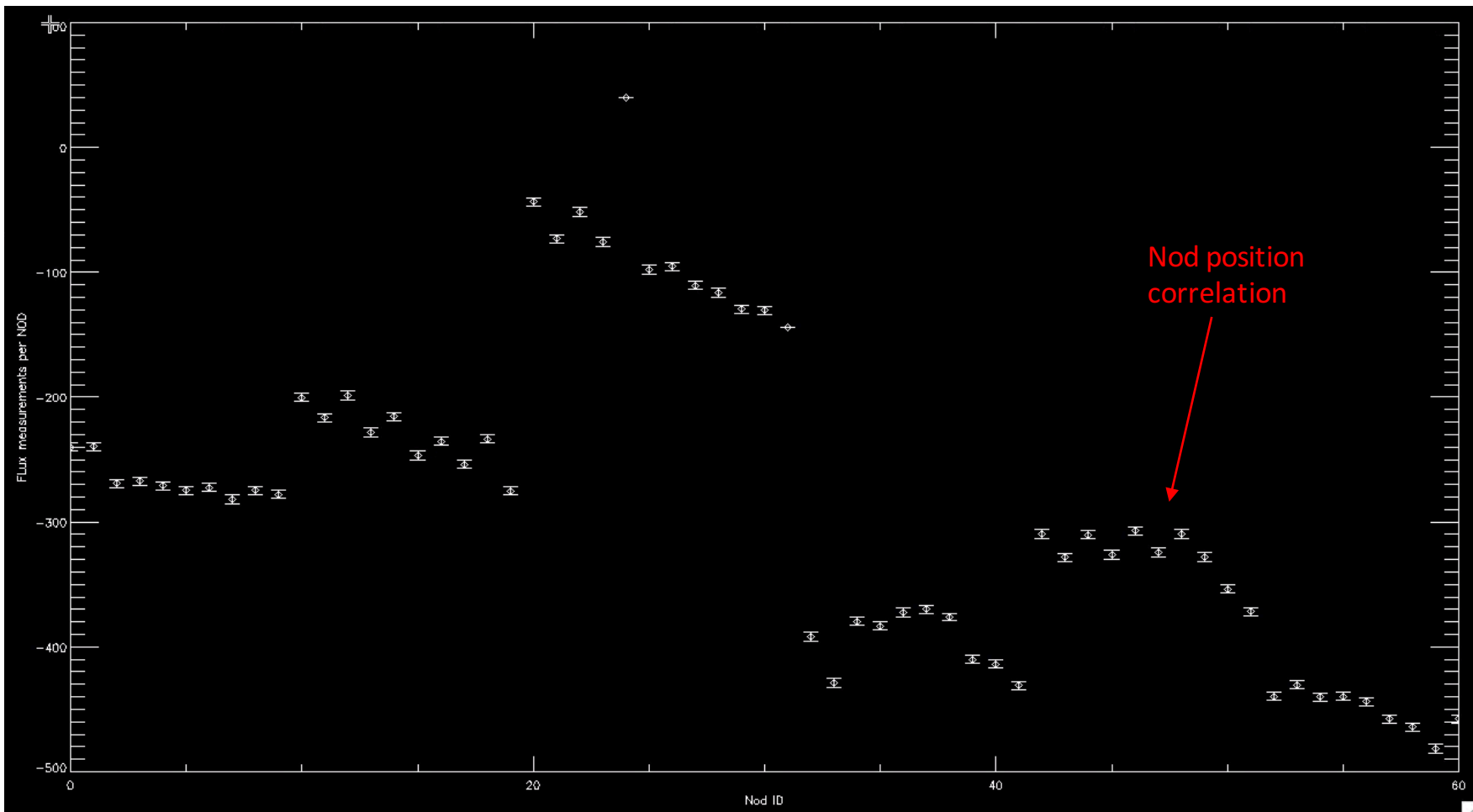
- The plot below shows the background bias looking at **an empty region of the sky** (60000 frames).
- Each pointing can be clearly identifies by a jump in background bias.





# Example of nulling sequence

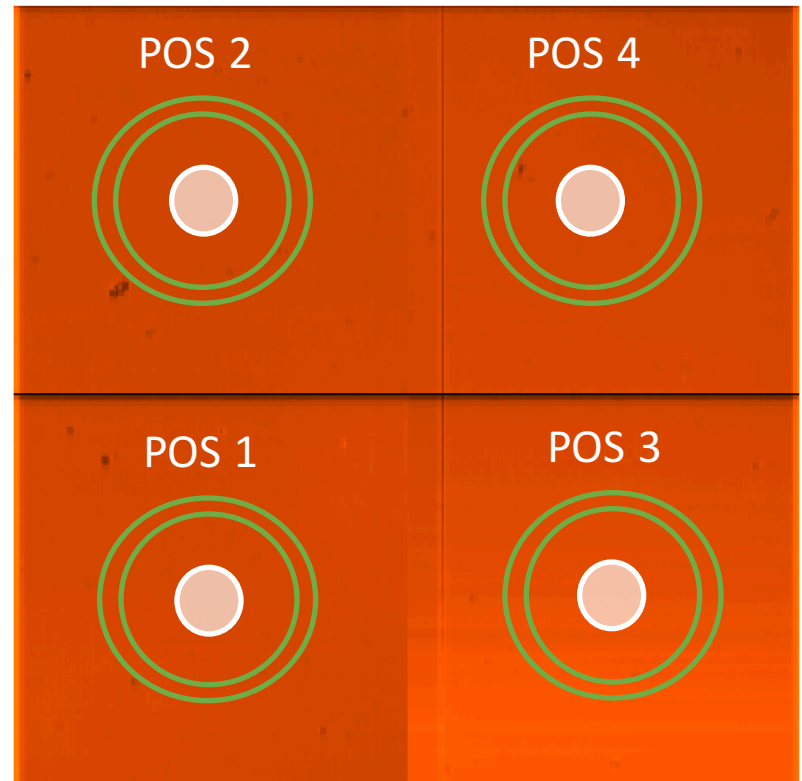
- Within each pointing, the flux measurements are not stable and are often correlated by NOD position (but not always!).
- The difference in flux per NOD for successive NODS within a given pointing can be as large as 20 ADU or **0.2% of beta Leo** flux over the same aperture! (~10000 ADU)





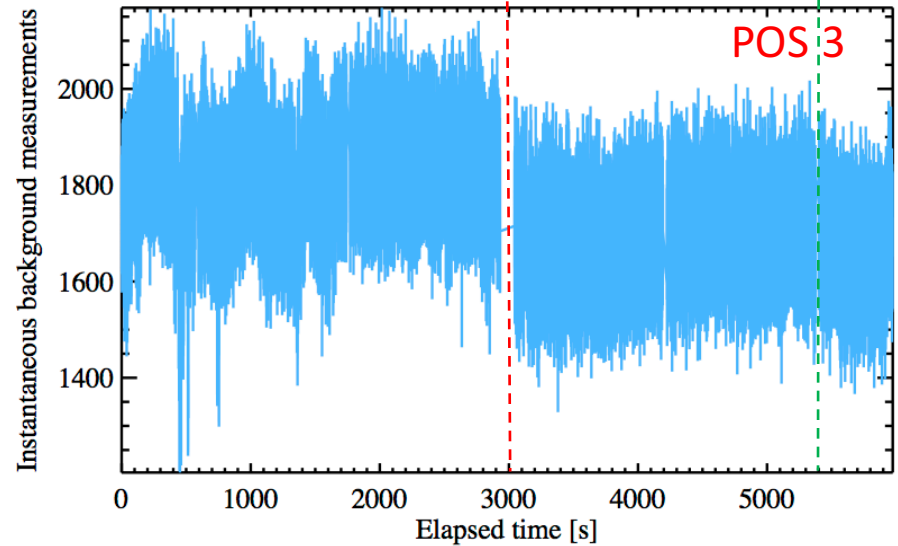
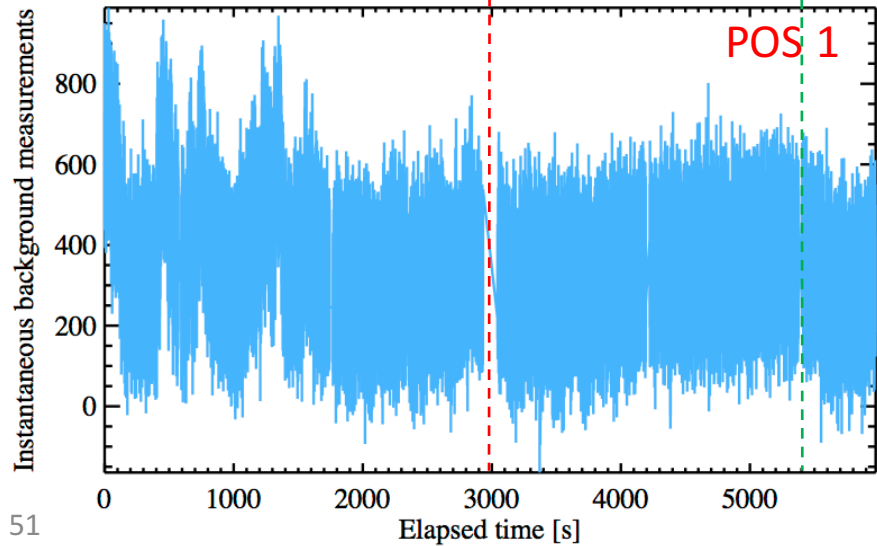
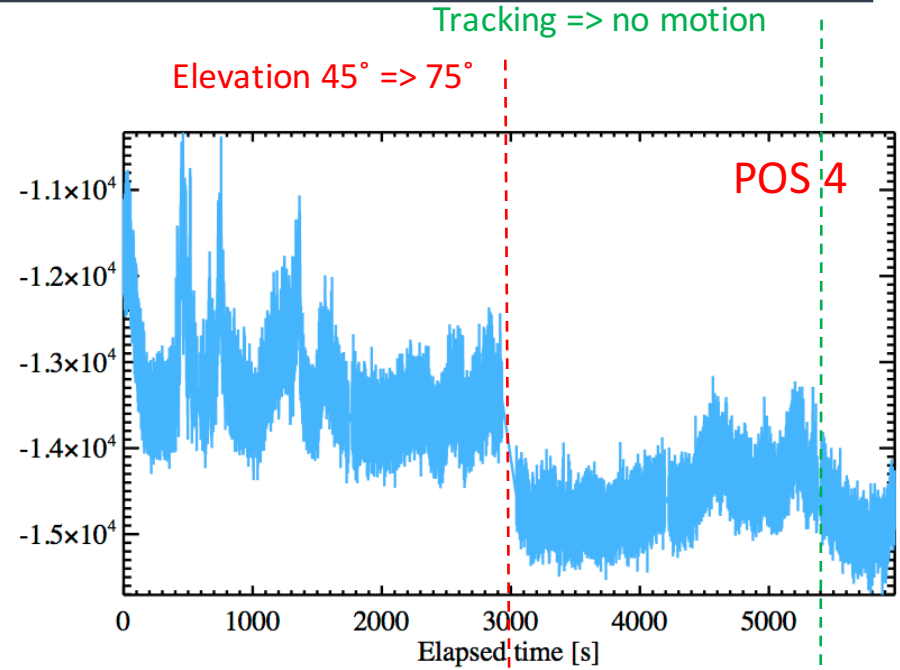
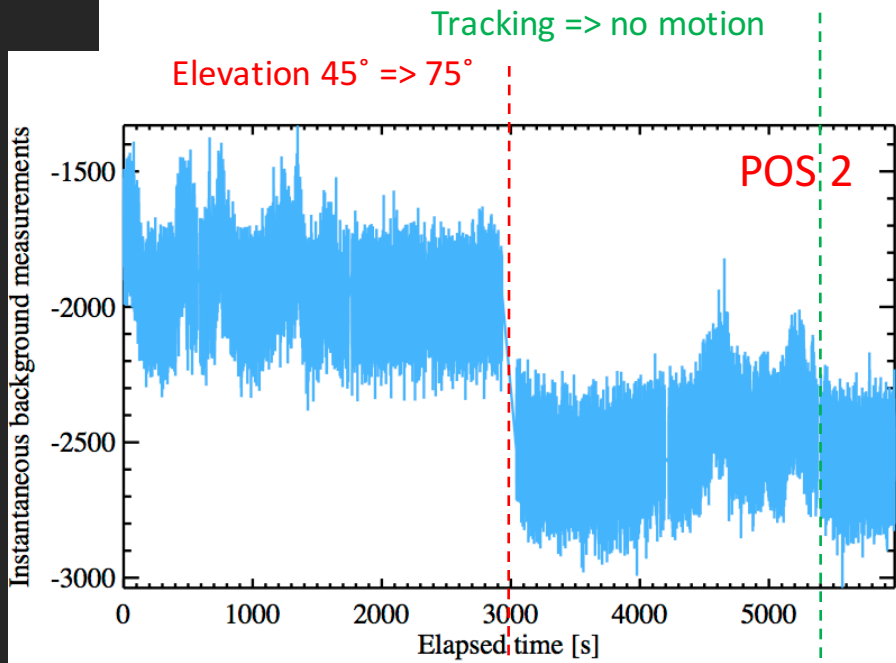
# Origin of the background bias?

- Based on data from March 9<sup>th</sup> 2016 and March 26<sup>th</sup> data;
- Approach follows default procedure of nulling pipeline, i.e. a photometric aperture of 8 pixels in radius and a background annulus which has an inner radius of 31 pixels and the same number of pixels as the photometric aperture;
- Following slides show the results for 4 different positions on the array (corresponding to the middle of each channel of the default 256x256 sub-array). **POS1 and POS2 are default for nulling;**
- The background bias is defined as the offset between the flux measured in the photometric aperture and that estimated from the background annulus;



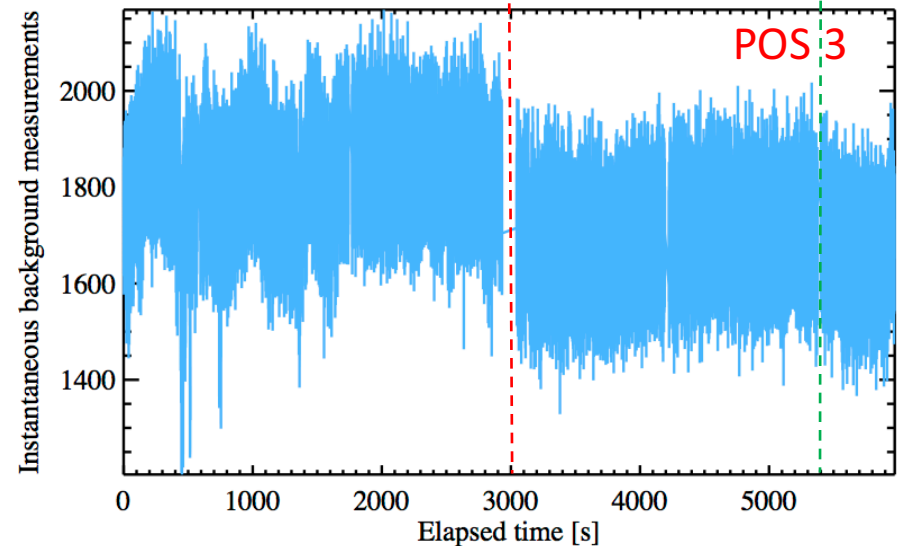
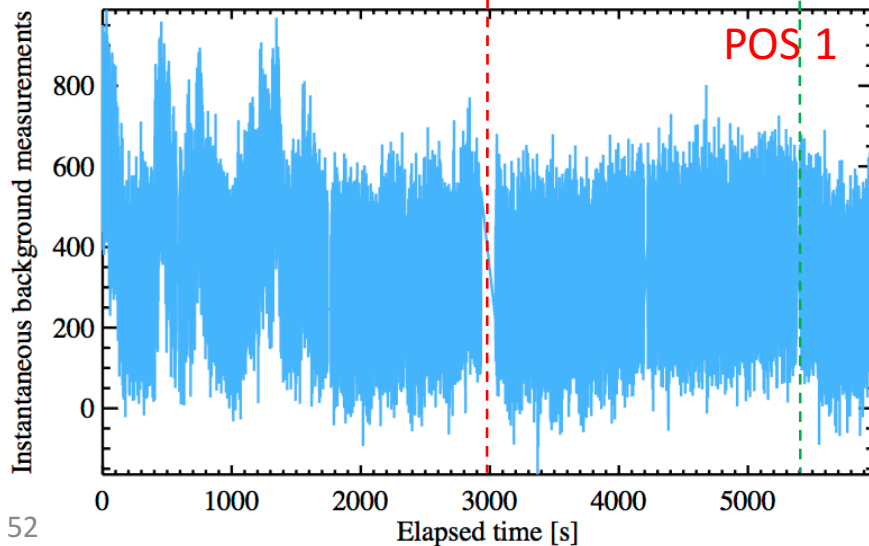
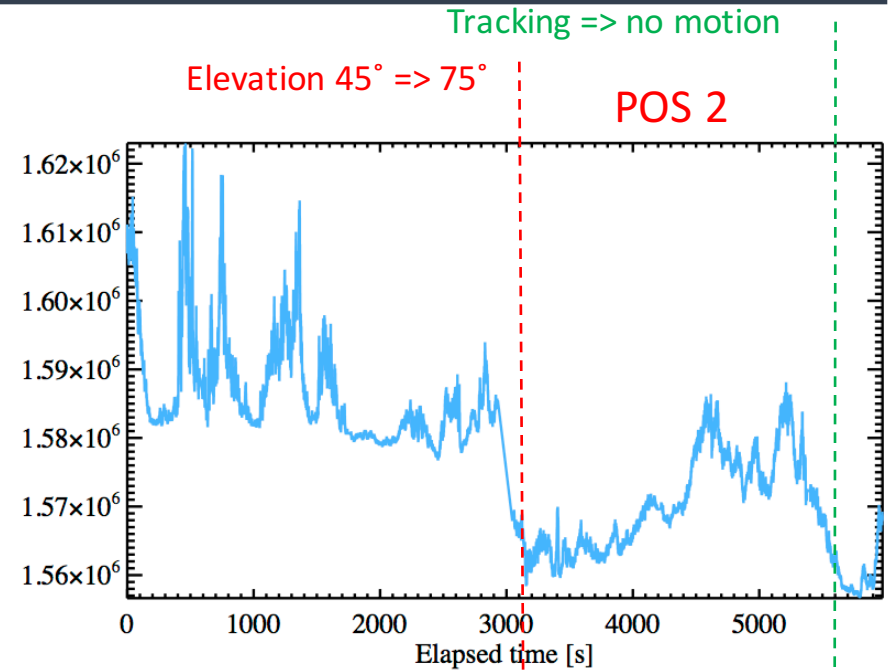
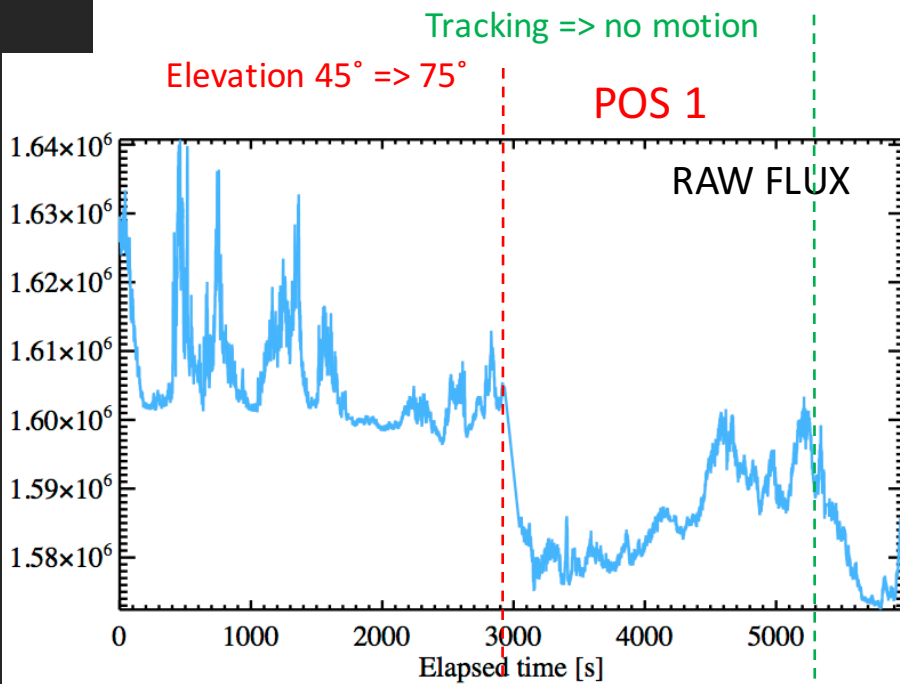


# Origin of the background bias?



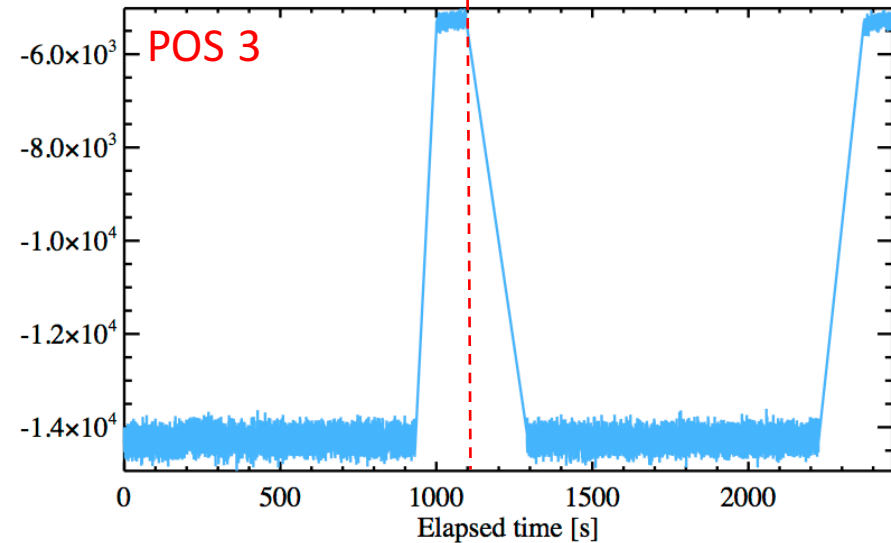
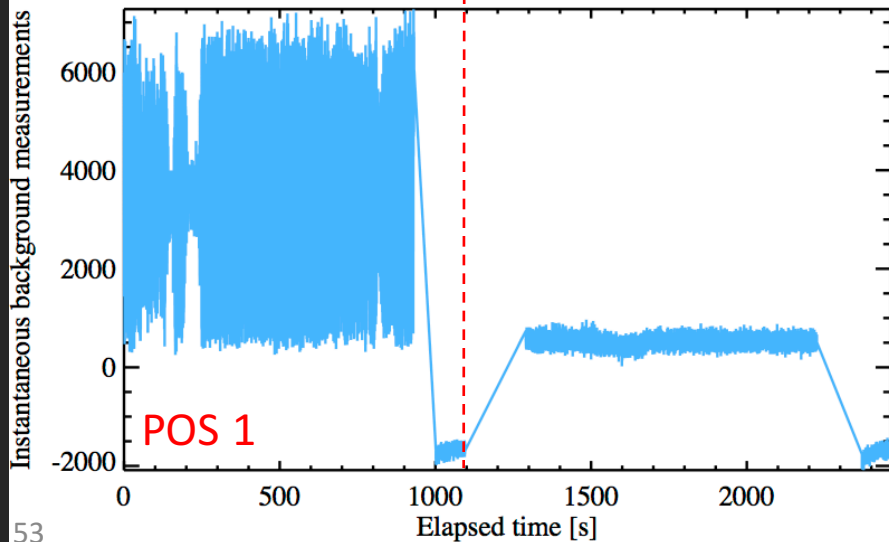
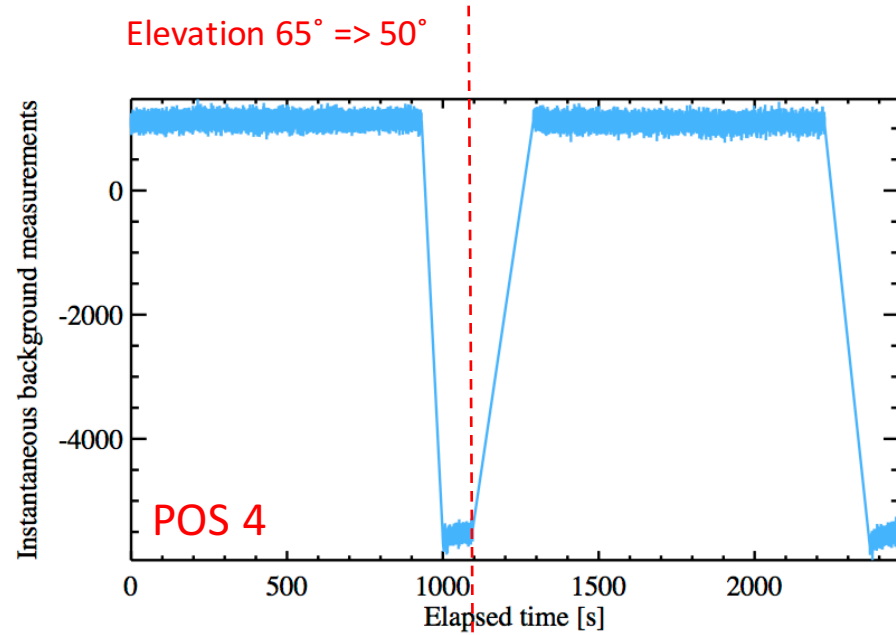
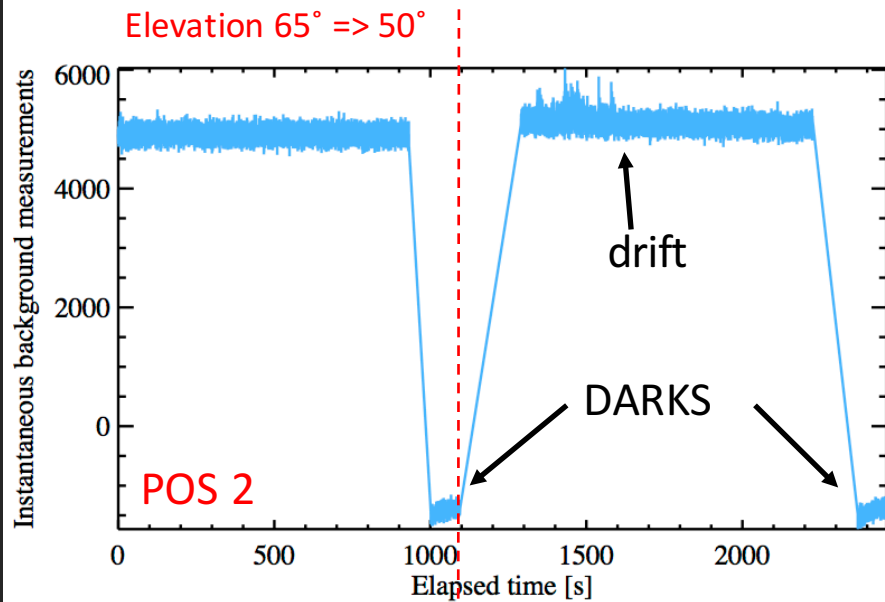


# Origin of the background bias?





# Origin of the background bias?

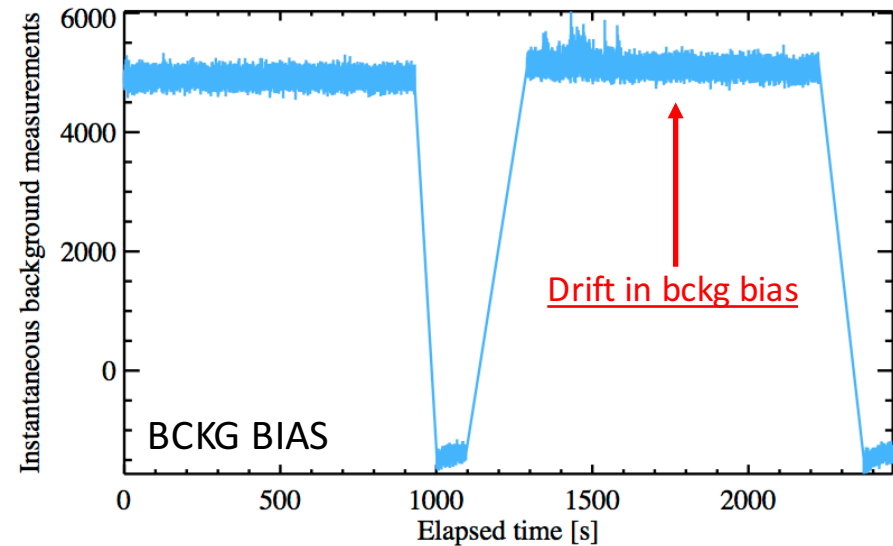
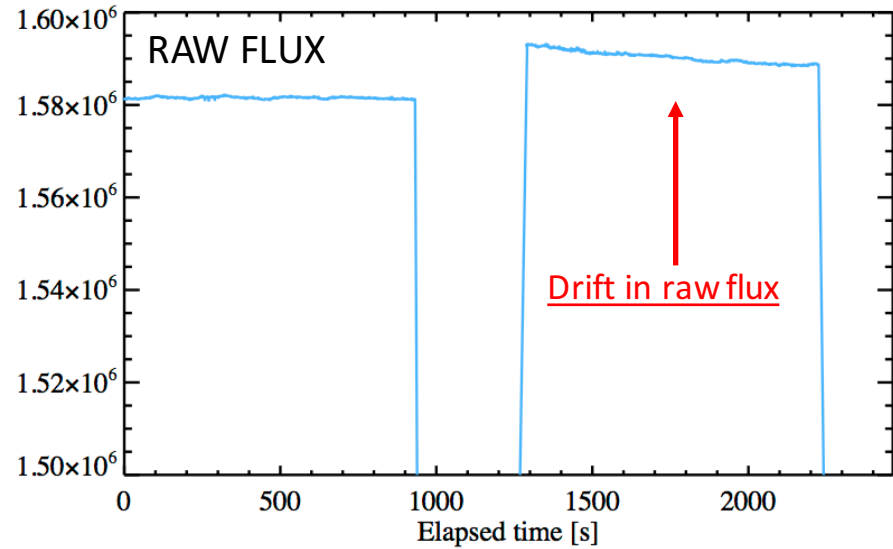
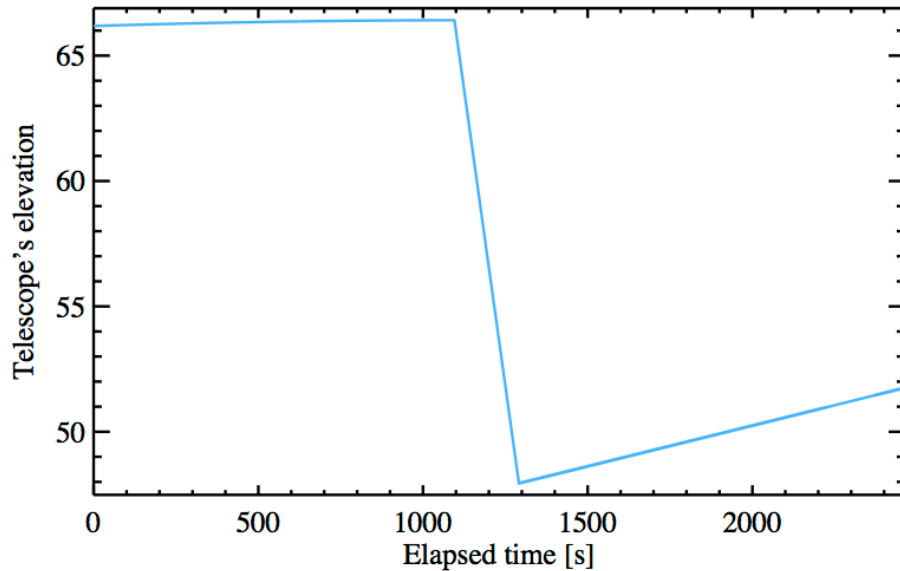




# Origin of the background bias?

POS 2

Drift in raw flux related to elevation changes

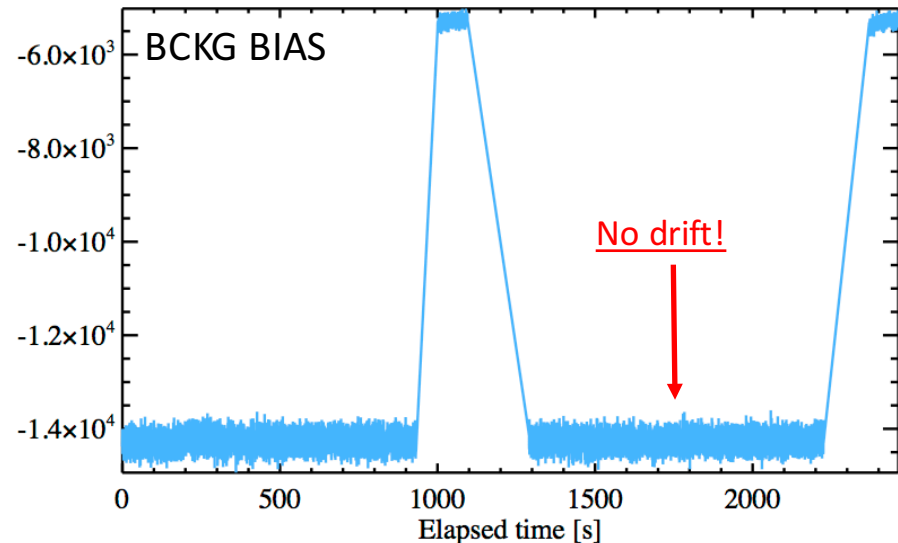
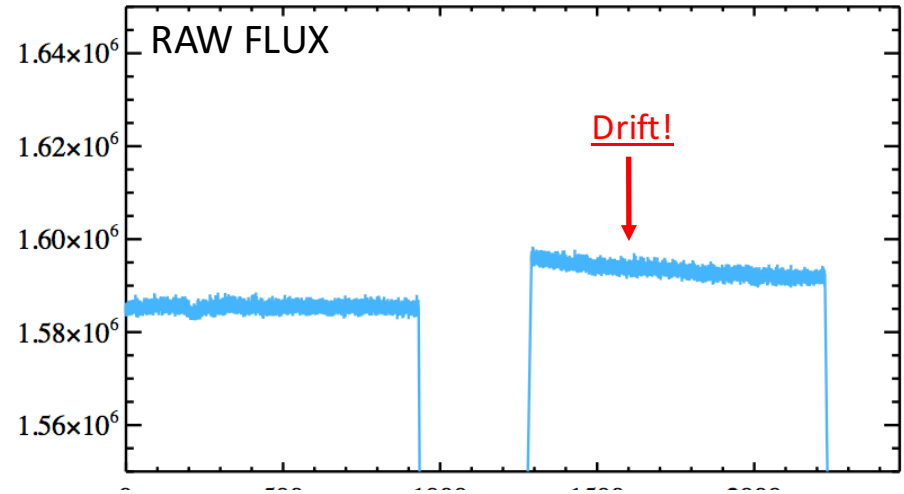
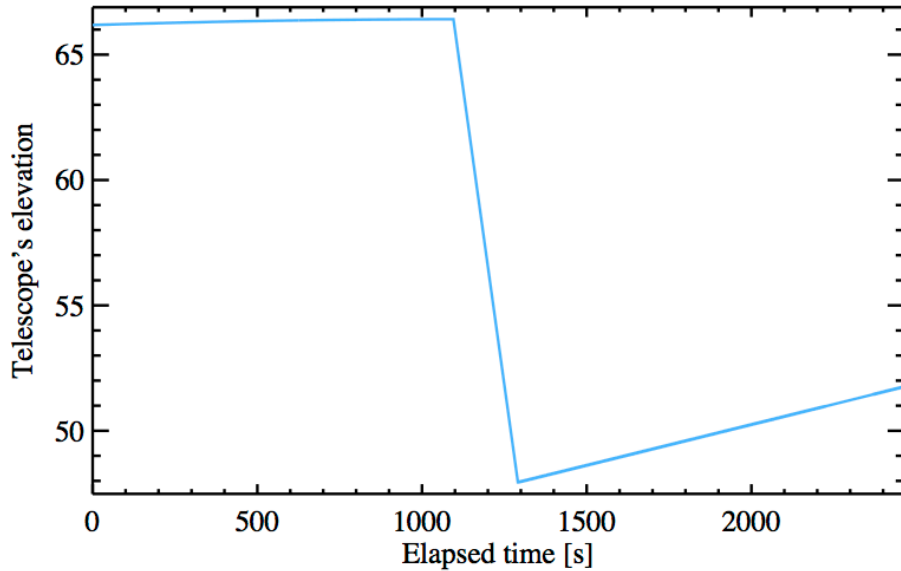




# Origin of the background bias?

POS 3

But this doesn't always produce a drift of the background bias, e.g. POS 3





# Conclusion on background bias

---

- The background bias depends on raw flux, but not always! (e.g., POS1 at ~3000s for March 9<sup>th</sup> data)
- The raw flux depends on elevation and, therefore, the background bias depends on the elevation, but not always!! (e.g., POS3 for March 26<sup>th</sup> data)
- Some channels show excessive noise at a given elevation (e.g., POS1 on March 26<sup>th</sup>). This problem goes away at a different elevation with similar raw flux levels. This points to temperature problems but needs to be checked.
- **These points suggest that NOMIC has a significant pixel-to-pixel differential flux response but also an elevation/temperature-dependent flux response per pixel!**

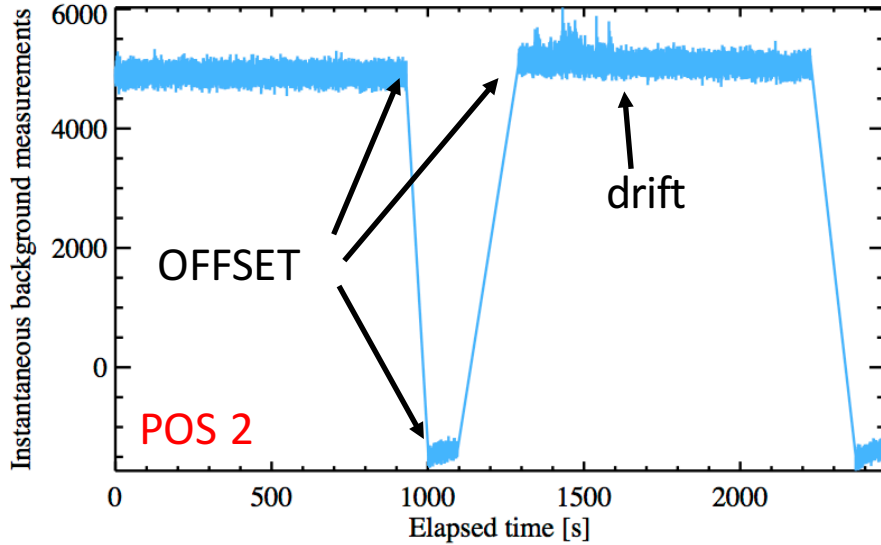


# Removing the background bias

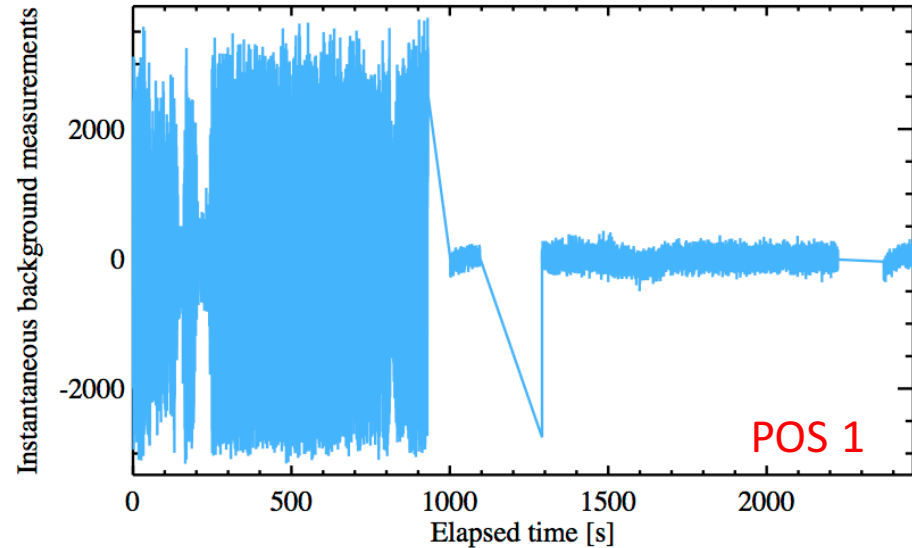
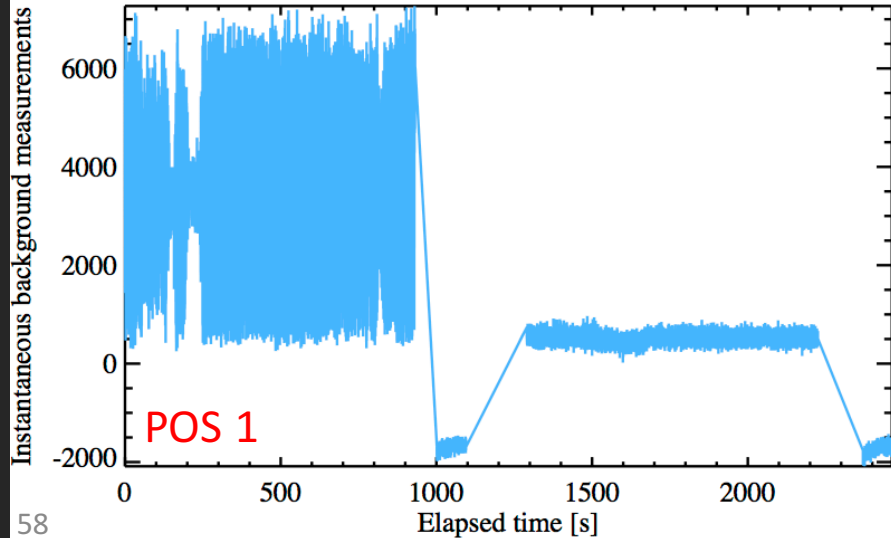
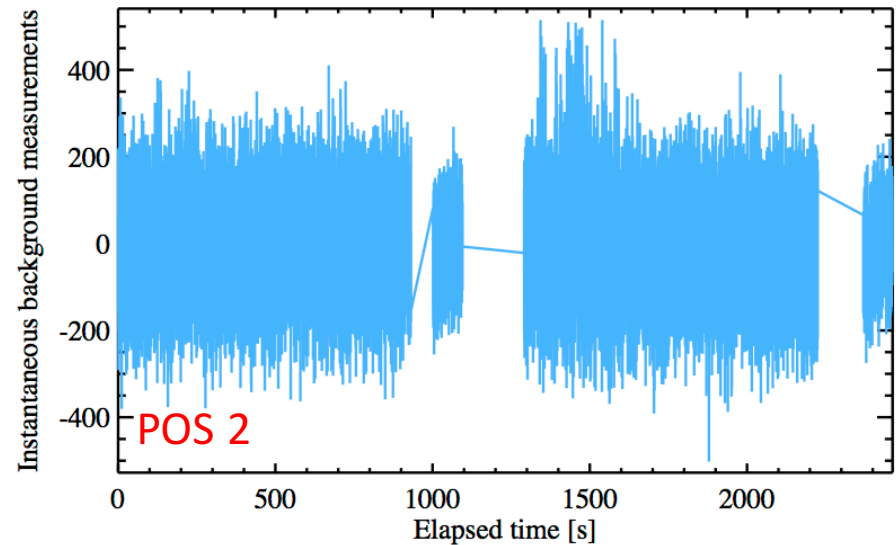


# Approach 1: flat fielding

NO FLAT FIELD



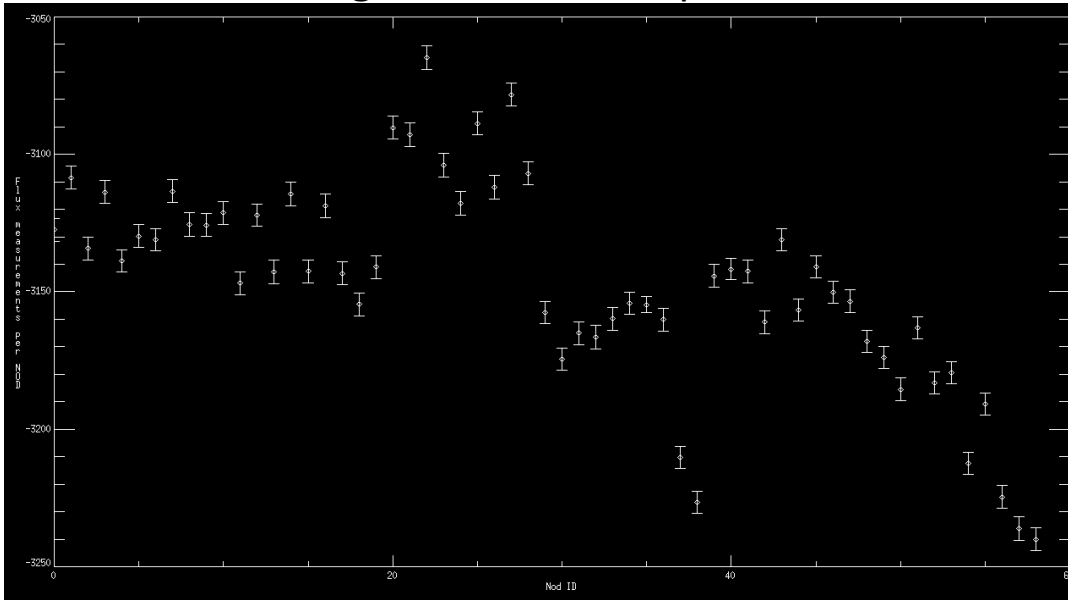
FLAT FIELD





# Approach 1: flat fielding

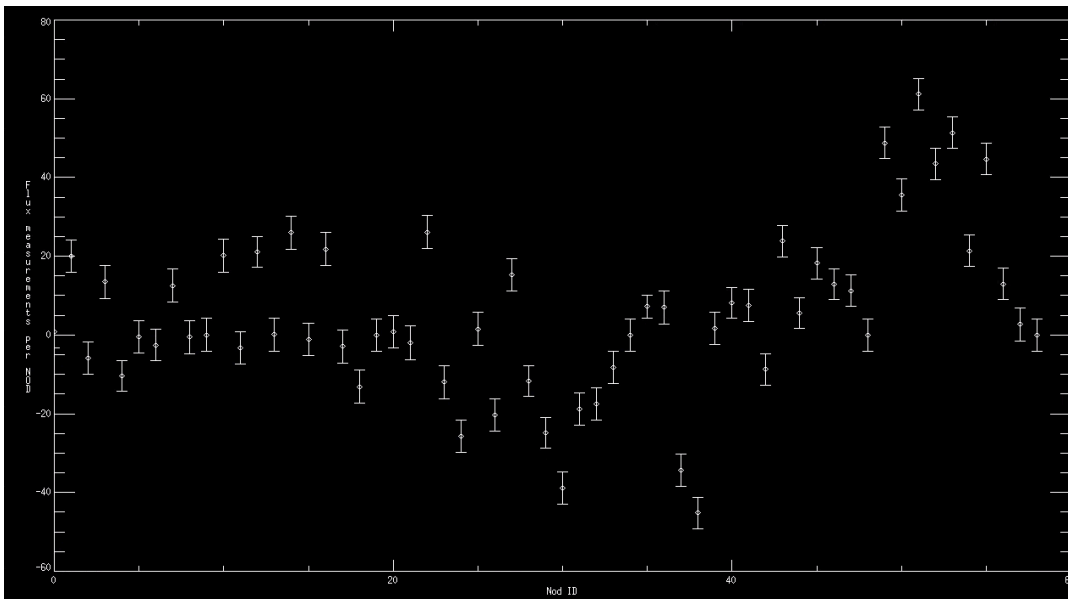
## Background estimate per nod



No flat fielding

RMS of background estimates: 38 ADU

Expected RMS: 4 ADU



Flat fielding

No offset

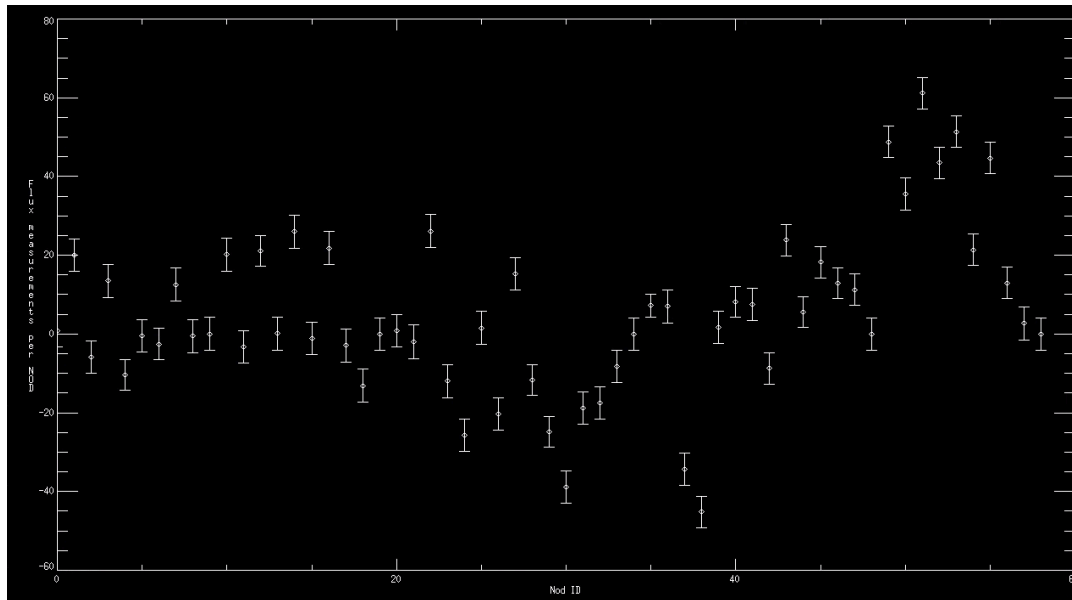
RMS of background estimates: 21 ADU

Expected RMS: 4 ADU



# Approach 2: nod subtraction

## Background estimate per nod

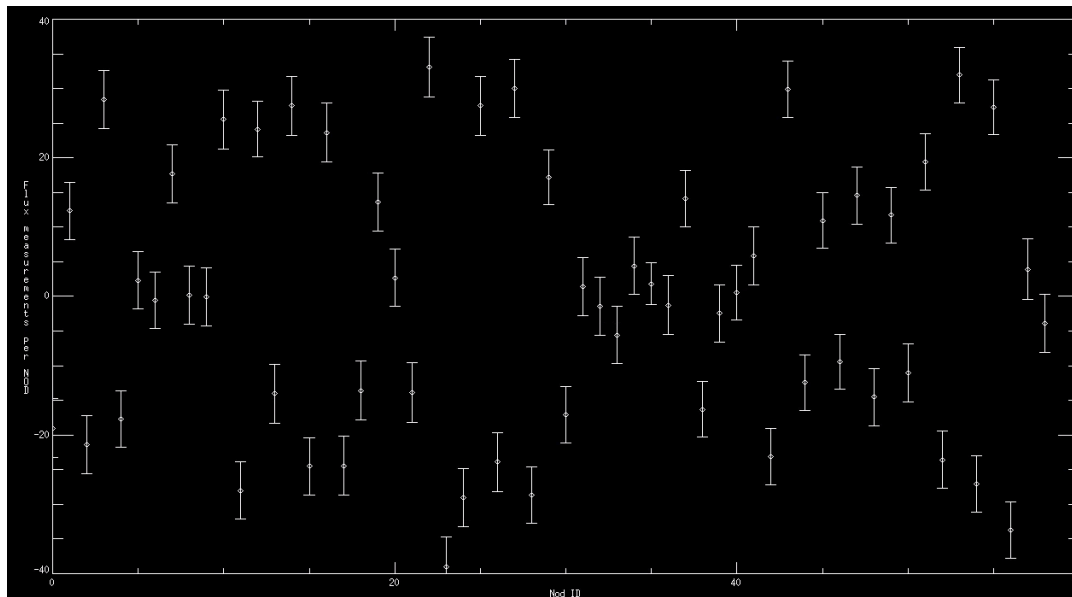


### Flat fielding

No offset

RMS of background estimates: 21 ADU

Expected RMS: 4 ADU



### Nod subtraction

No offset

RMS of background estimates: 19 ADU

Expected RMS: 4 ADU



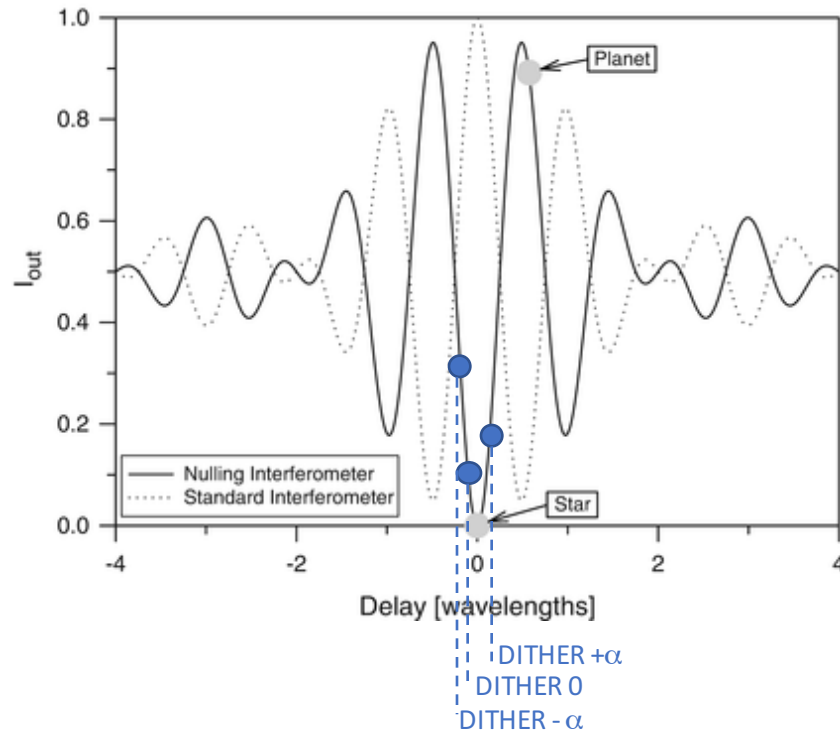
# Conclusions

---

- Flat fielding helps but nod subtraction gives slightly better results
- With current approach, error on background estimate **~5x larger** than based on pure photon noise
- New idea: fast dithering



# Fast dithering principle



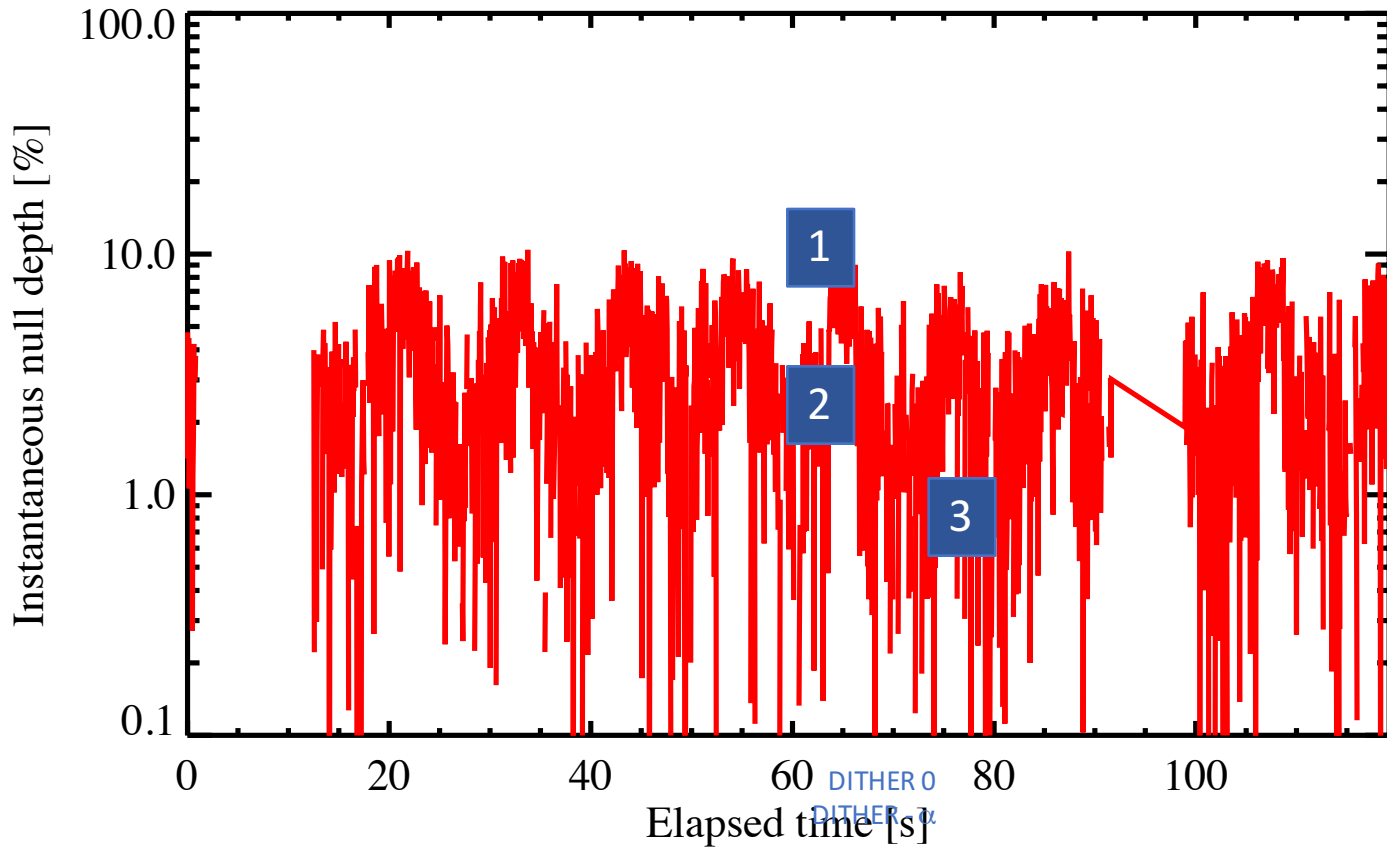
$$N_1 = \langle I_1(t) \rangle = I_1 + I_2 + 2|V|\sqrt{I_1 I_2} \langle \cos \phi_1(t) \rangle + B_1$$

$$N_2 = \langle I_2(t) \rangle = I_1 + I_2 + 2|V|\sqrt{I_1 I_2} \langle \cos(\phi_2(t) + \alpha) \rangle + B_2$$

$$N_3 = \langle I_3(t) \rangle = I_1 + I_2 + 2|V|\sqrt{I_1 I_2} \langle \cos(\phi_3(t) - \alpha) \rangle + B_3$$



# Fast dithering principle



$$N_1 = \langle I_1(t) \rangle = I_1 + I_2 + 2|V|\sqrt{I_1 I_2} \langle \cos \phi_1(t) \rangle + B_1$$

$$N_2 = \langle I_2(t) \rangle = I_1 + I_2 + 2|V|\sqrt{I_1 I_2} \langle \cos(\phi_2(t) + \alpha) \rangle + B_2$$

$$N_3 = \langle I_3(t) \rangle = I_1 + I_2 + 2|V|\sqrt{I_1 I_2} \langle \cos(\phi_3(t) - \alpha) \rangle + B_3$$



# Fast dithering principle

---

$$N_1 = \langle I_1(t) \rangle = I_1 + I_2 + 2|V|\sqrt{I_1 I_2} \langle \cos \phi_1(t) \rangle + B_1$$

$$N_2 = \langle I_2(t) \rangle = I_1 + I_2 + 2|V|\sqrt{I_1 I_2} \langle \cos(\phi_2(t) + \alpha) \rangle + B_2$$

$$N_3 = \langle I_3(t) \rangle = I_1 + I_2 + 2|V|\sqrt{I_1 I_2} \langle \cos(\phi_3(t) - \alpha) \rangle + B_3$$

$$\phi_1 = s_1 + \varepsilon_1$$

- Fit the null equation to null measurements at 3 dither positions:  
⇒ 1 null estimate per dither cycle  
⇒ Average nulls per dither cycle to get 1 null per OB
- Assumptions:
  1. Background bias constant between 3 dither positions ( $B_1=B_2=B_3$ );
  2. Phase setpoint constant between 3 dither positions ( $s_1=s_2=s_3$ );
  3. Stable high-frequency phase jitter between the 3 dither positions ( $\varepsilon_1=\varepsilon_2=\varepsilon_3$ );

- Analytical solution:

$$B = \frac{N_1 + N_2 - 2 \cos \alpha N_1}{2(1 - \cos \alpha)} - (I_1 + I_2)$$

$$\tan \phi = \frac{N_2 - N_3}{2(N_1 - I_1 - I_2 - B) \sin \alpha}$$

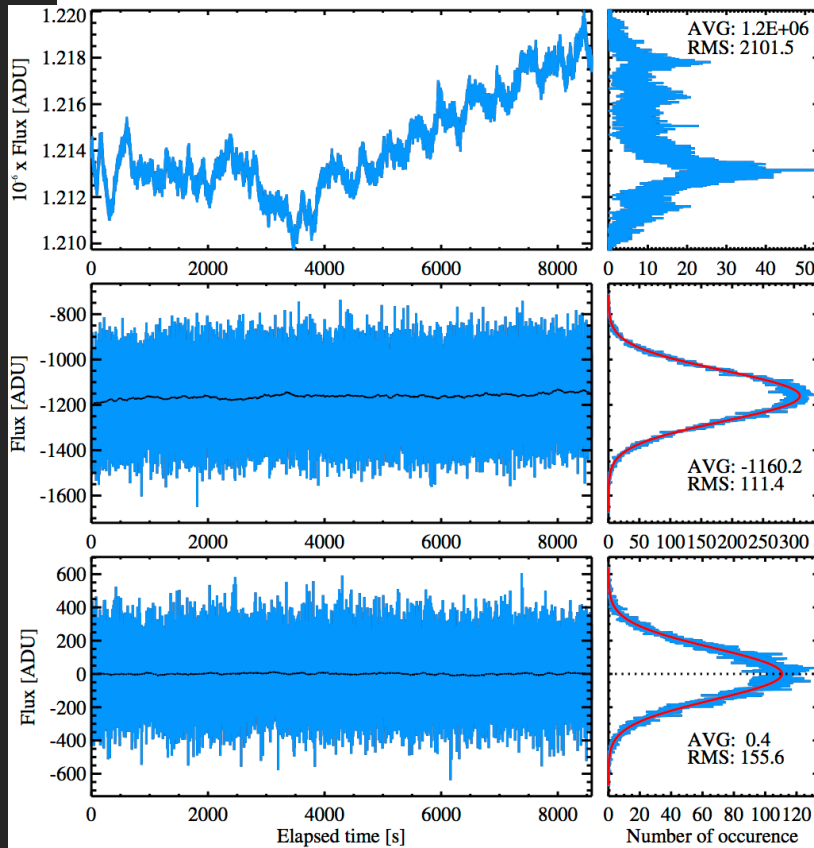
$$|V| = \frac{N_1 - (I_1 + I_2) - B}{2 \cos \alpha \sqrt{I_1 I_2}}$$



# Fast dithering principle

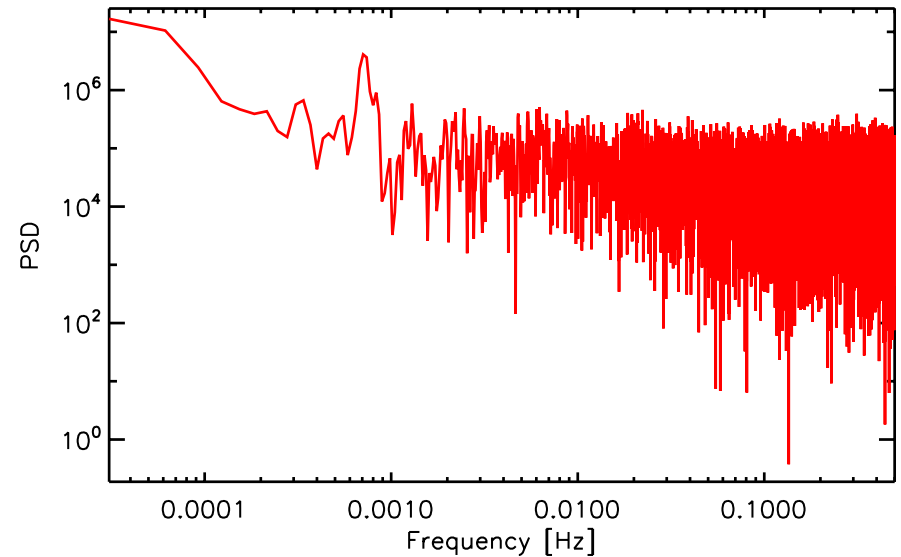
- Assumption 1: background bias constant between 3 dither positions

One example



Uncorrected background bias

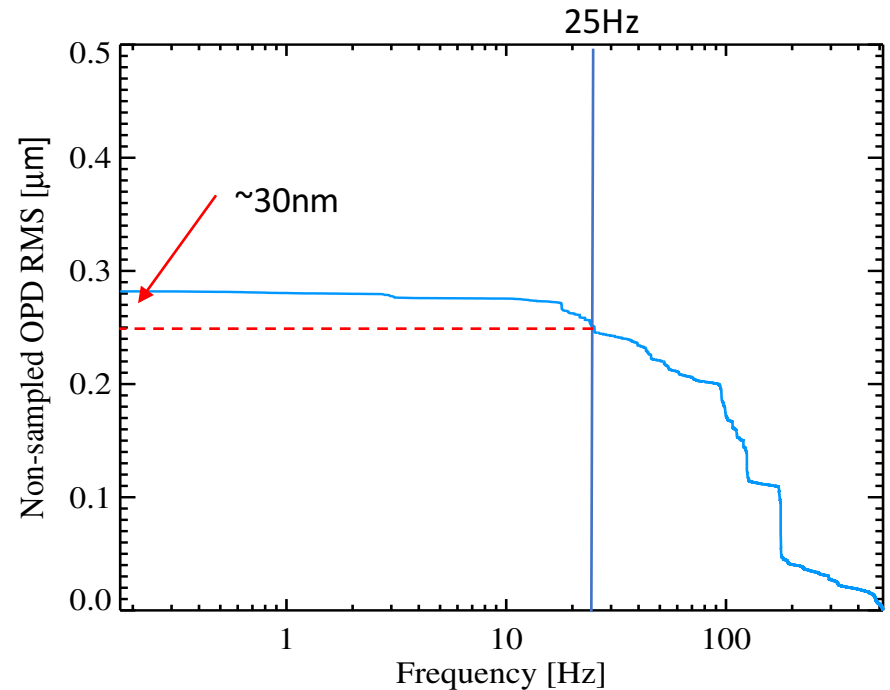
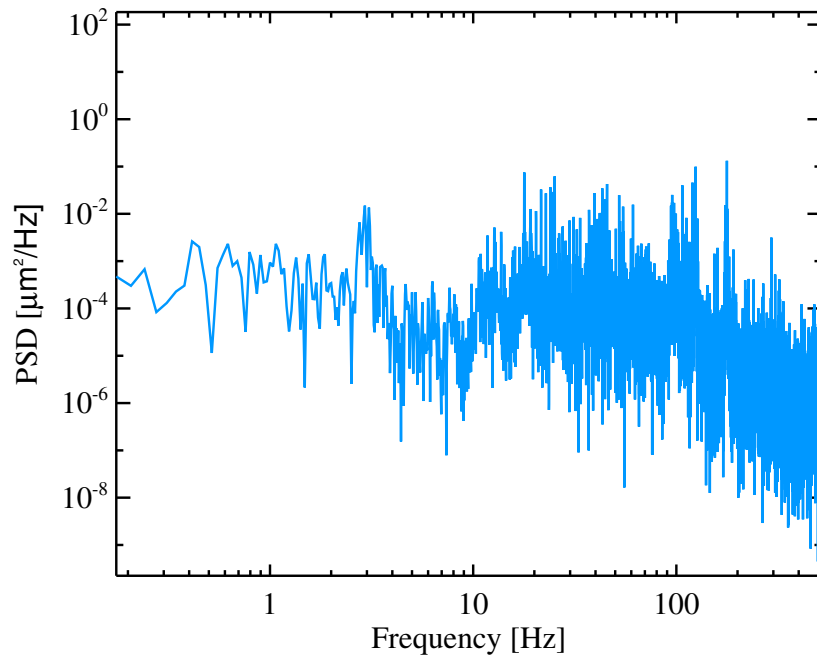
Mostly low frequency





# Fast dithering principle

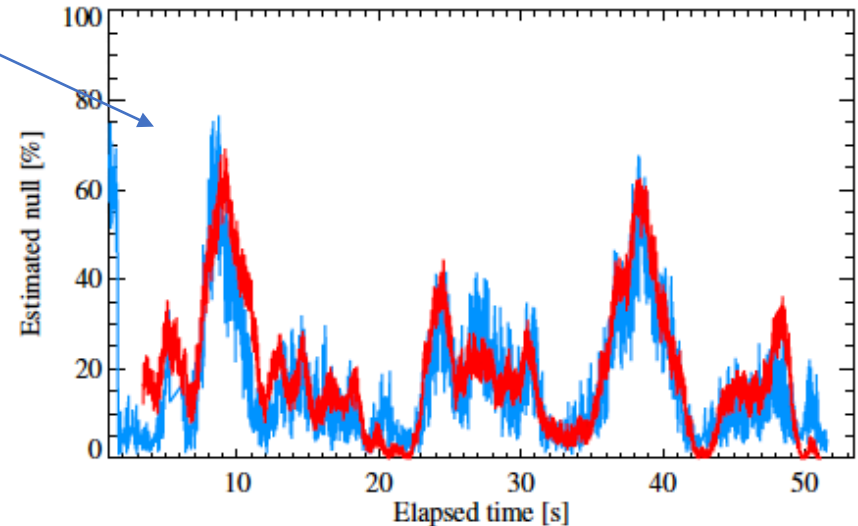
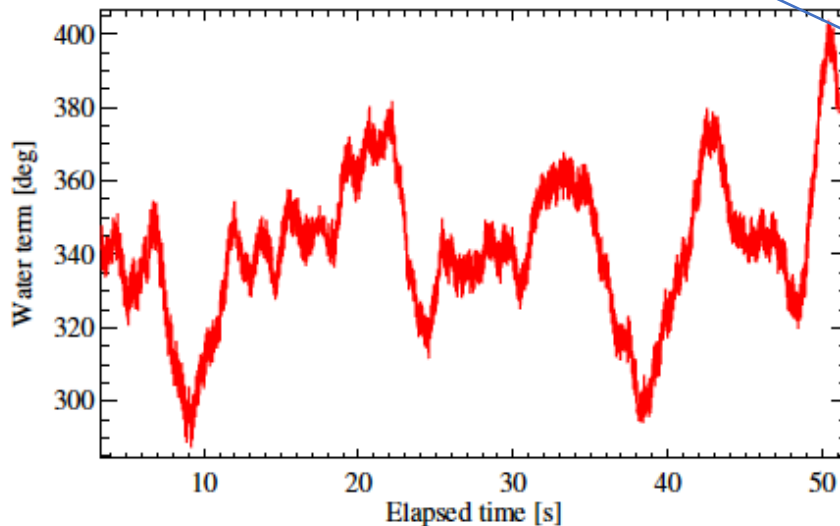
- Assumption 2: Phase setpoint constant between 3 dither positions
- Phase drift between measurements  $< 30\text{nm}$  or  $0.02\text{rad}$  or  $\Delta N \sim 100\text{ppm}$





# Fast dithering principle

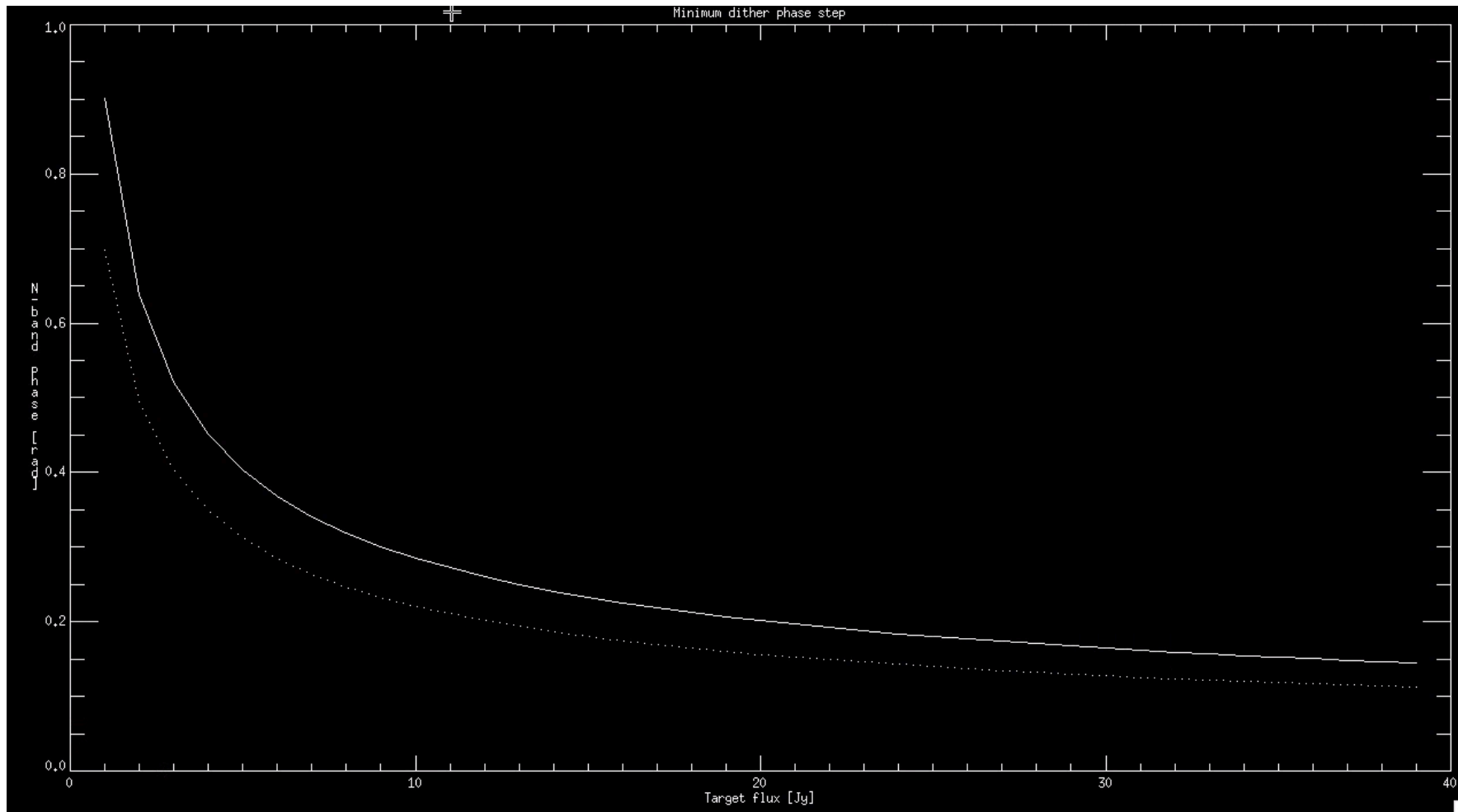
- Assumption 2: Phase setpoint constant between 3 dither positions
  - What about PWV?
  - Null can vary by 70% in 3sec...This is  $\sim 1\%$  in 40ms!! => must be taken into account in post-processing for high PWV nights (can we rely on H-K phase?) or can still use th NSC in case of problem.





# Dithering amplitude matters

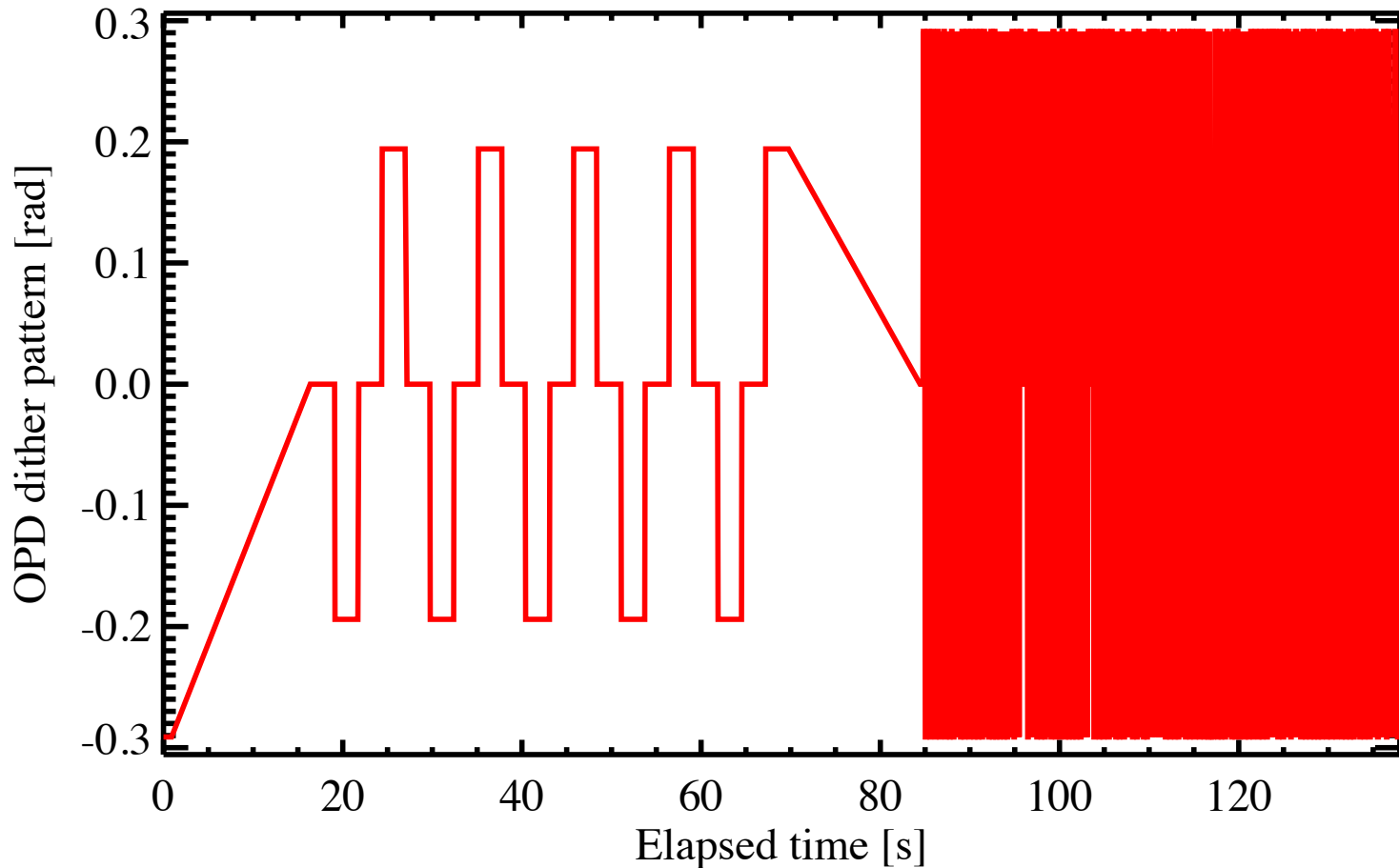
- Minimum N-band phase steps as a function of target flux (3 and 5-sigma > background RMS) :





# Results of fast dither approach

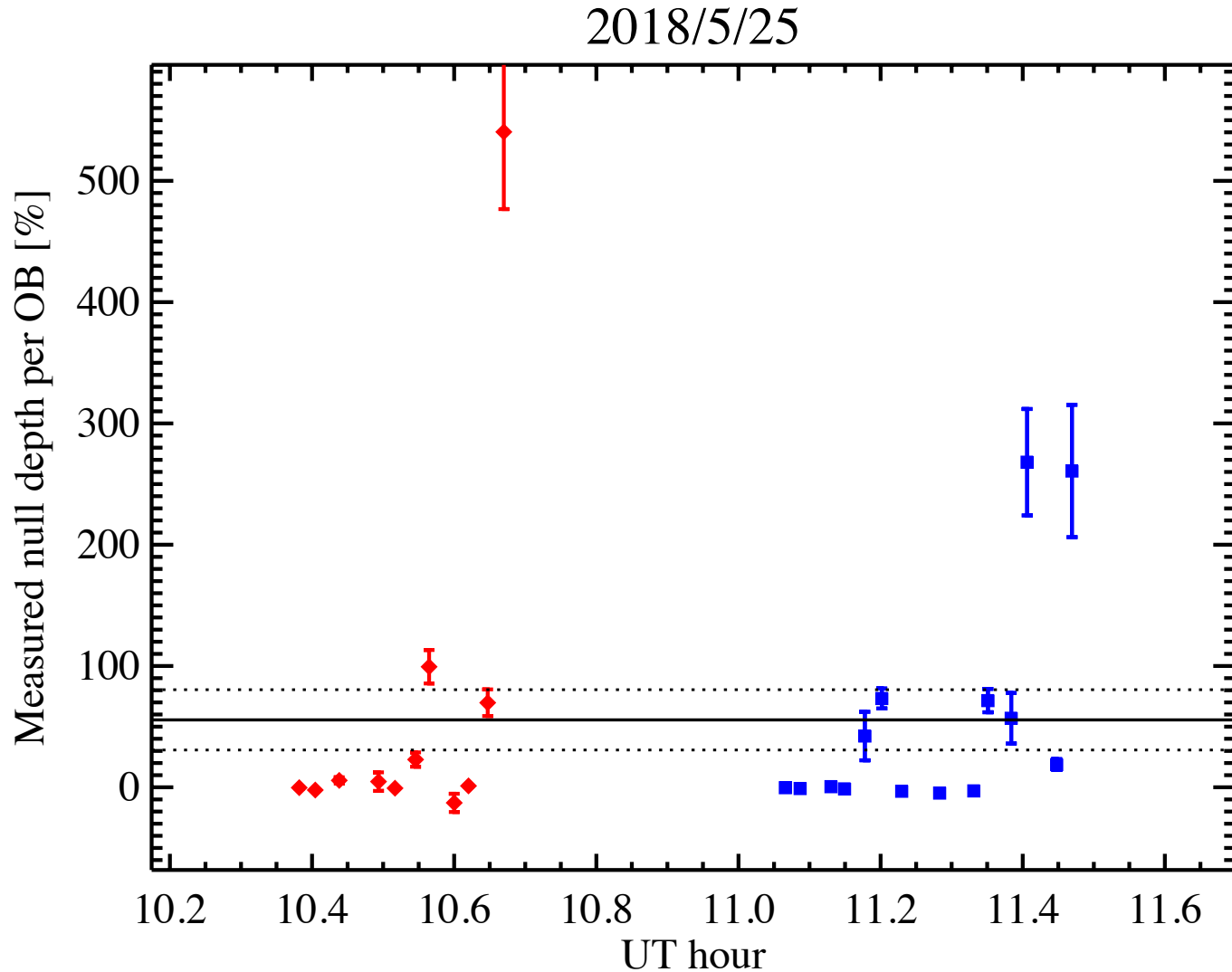
- Data obtained on May 25, 2018 on 61 Cyg A (4 Jy) and calibrator
- Each OB divided in one slow and one fast dither sequence:





# Results of fast dither approach

- Method doesn't work (so far)

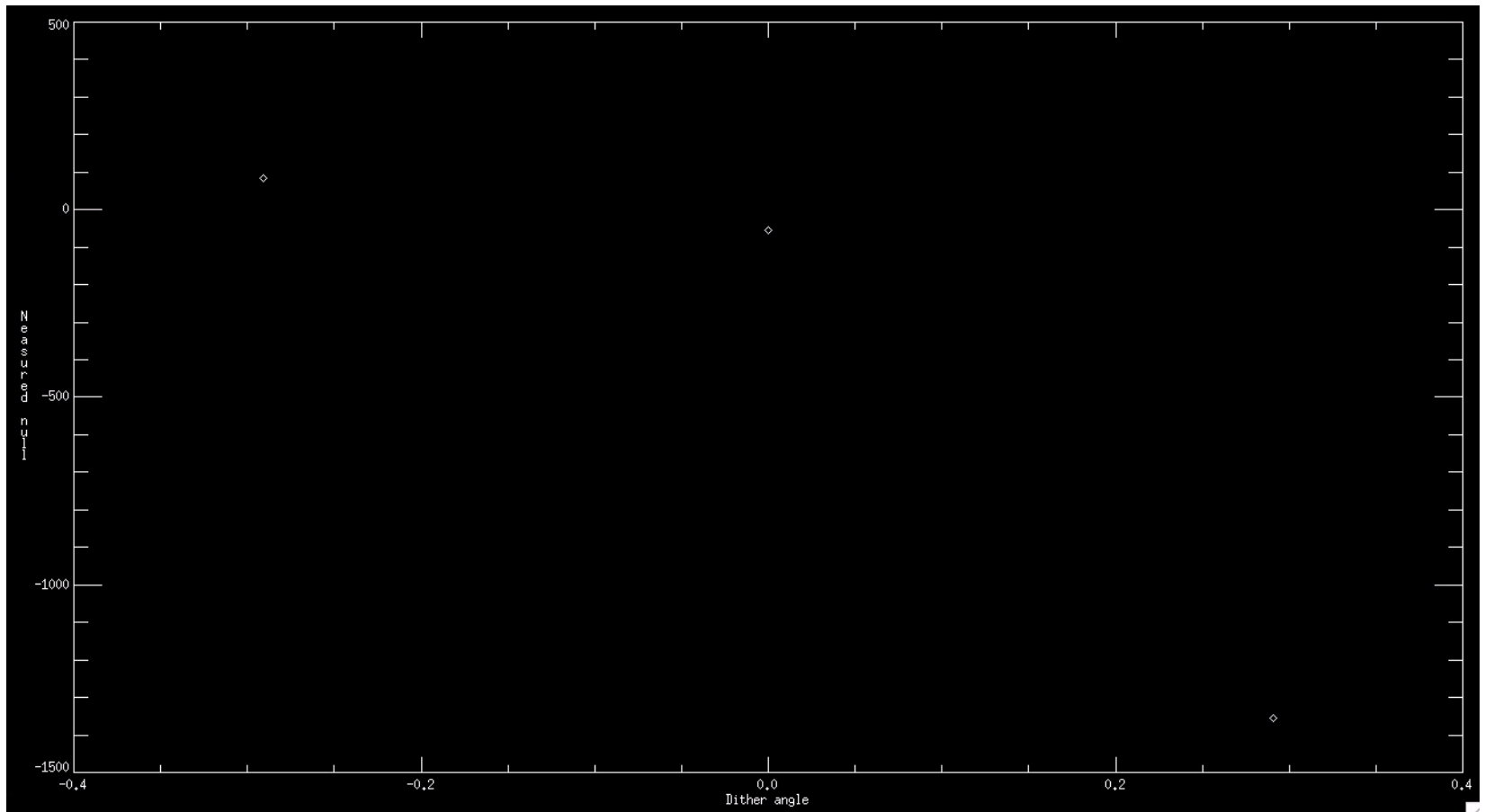




# Results of fast dither approach

---

- Dither pattern not apparent in the null measurements??





# Results of fast dither approach

- Using default NSC for both, fast-dither data show smaller error bars

**MEAN ERROR PER OB**

0.18%

**CALIBRATED NULL**

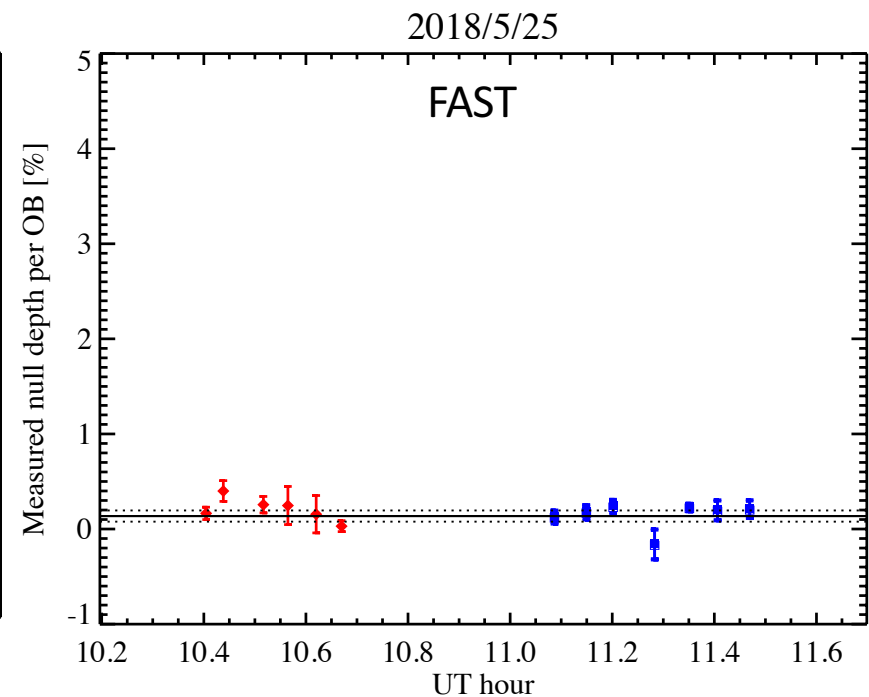
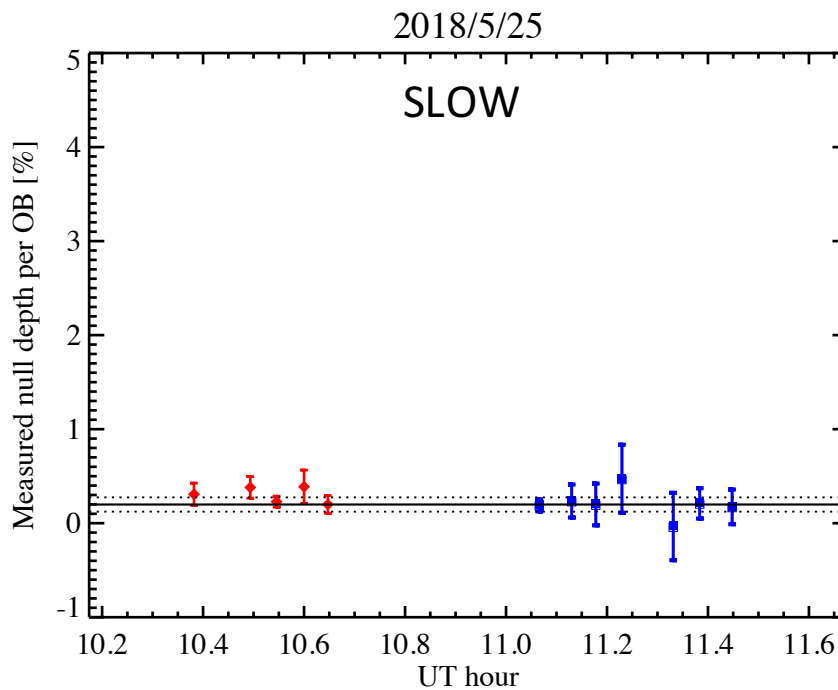
0.094% +/- 0.098%

**MEAN ERROR PER OB**

0.10%

**CALIBRATED NULL**

0.065% +/- 0.081%





# Summary and conclusions

---

## IMMEDIATE ACTION

- Using a larger dither amplitude will improve the null uncertainty (at least 0.3 rad or more, to be tested)

## ANALYSIS NEEDS

- Test more advanced background subtraction or flat fielding strategies on existing data (pipeline still uses very basic, but fine tuned, approach)
- Test null calibration using images rather than fluxes

## PIPELINE DEVELOPMENTS

- Replace brute-force computer-intensive NSC approach by MCMC
- Asymmetric error bars not propagated (only the maximum of the 2)